2016

A New Mouse Model Of Metastatic Gastric Cancer And E-Cadherin Primary Tumor Suppression

Jacob Edward Till
University of Pennsylvania, JacobETill@gmail.com

A New Mouse Model Of Metastatic Gastric Cancer And E-Cadherin Primary Tumor Suppression

Abstract
Gastric cancer is the fifth most common cancer and the third leading cause of cancer death worldwide. The majority of patients with gastric cancer are diagnosed with disseminated disease and even patients diagnosed with early stage disease have high rates

of recurrence. The utility of current mouse models of gastric cancer is limited by slow development of gastric tumors and lack of metastasis. Here I describe a new mouse model of gastric cancer driven by p53 loss, Cdh1 loss, and oncogenic Kras expression in

gastric parietal cells (referred to as ACKPY mice). I generated these mice to investigate the contribution of oncogenic Kras to the progression of gastric cancer given the high rate of mutation and amplification of the RTK/Ras pathway identified in gastric cancer

patients. These mice develop mixed-type gastric adenocarcinomas with metastases to lymph nodes, lung, and liver. Oncogenic Kras and loss of Trp53 is sufficient to drive rapid carcinogenesis in a variety of models. Therefore, I tested if loss of E-cadherin was

necessary for the onset of gastric adenocarcinoma in gastric parietal cells by generating ACKPY mice with one or two alleles of wild-type Cdh1 (E-cadherin). E-cadherin expression significantly increased survival and the limited number of mice with gastric

tumors have tumors that were focal in nature, suggesting an additional event was necessary for gastric tumorigenesis. Loss of E-cadherin expression was observed in some of these tumors, suggesting that its loss may be necessary for gastric tumorigenesis in this model. I show that loss of E-cadherin in our model increases β-catenin signaling and that inhibition of β-catenin signaling prolonged survival of ACKPY mice. Microarray data comparing gene expression in stomachs harvested from Cdh1fl/fl and Cdh1fl/+ mice showed a correlation between E-cadherin loss and upregulation of oncogenic Kras signaling. Gene sets regulated by each of the main Kras effector pathways were overrepresented in our microarray data. Examination of ERK phosphorylation revealed that

E-cadherin likely does not regulate MAPK activity in our model. The upregulation of oncogenic Kras target genes that result from the loss of E-cadherin may alternatively be explained by E-cadherin regulation of other Kras effector pathways.

Degree Type
Dissertation

Degree Name
Doctor of Philosophy (PhD)

Graduate Group
Cell & Molecular Biology

A NEW MOUSE MODEL OF METASTATIC GASTRIC CANCER AND E-CADHERIN PRIMARY TUMOR SUPPRESSION

Jacob Till

A DISSERTATION

in

Cell and Molecular Biology

Presented to the Faculties of the University of Pennsylvania

in

Partial Fulfillment of the Requirements for the

Degree of Doctor of Philosophy

2017

Supervisor of Dissertation

_____

Sandra Ryeom

Associate Professor of Cancer Biology

Graduate Group Chairperson

_____

Daniel S. Kessler

Associate Professor of Cell and Developmental Biology

Dissertation Committee

Ellen Puré, Ph.D., Grace Lansing Lambert Professor of Biomedical Science

M. Celeste Simon, Ph.D., Arthur H. Rubenstein, MBBCh Professor

Constantinos (Costas) Koumenis, Ph.D., Professor of Radiation Oncology

David M. Feldser, Ph.D., Assistant Professor of Cancer Biology

A NEW MOUSE MODEL OF METASTATIC GASTRIC CANCER AND E-CADHERIN PRIMARY TUMOR SUPPRESSION

DEDICATION

To the strongest person I know, my Mom.

My strength got me here, but not without her.

She beat cancer, twice.

ACKNOWLEDGEMENTS

There are so many people to thank and words are not nearly adequate to express my gratitude to everyone who has helped me to reach this point. First and foremost, I have to thank my mentor Sandra Ryeom. From my first interactions with her during an independent study in medical school, I knew I wanted to learn to be the type of rigorous scientist she is. Though her scientific guidance and education has been exemplary, it is the personal mentorship that has meant the most. This has not been an easy road and I have struggled through some very difficult times over the past 5 years. Through it all, Sandra has been a steadfast support, never wavering in her belief and encouragement that I could make it through. Many lesser individuals might have lost faith or patience, she did not, and for that I will be eternally grateful.

The disappointments of science are innumerable and the truly great moments rare. I certainly could not have survived the lows without a community of kind and caring individuals to soften the blows and celebrate the highs. I have been fortunate to share my time in lab with some wonderful individuals who have truly enriched my life and my science. I have learned so much from and appreciate the compassion of all the Ryeom Laboratory members past and present. I would, however, be remiss if I didn't thank specifically Keri Schadler. Your friendship and support meant more than I can ever thank or repay. Through some of the hardest times in my life you were there for me, always loving and always supportive. I also have to specifically thank Allyson Lieberman. I feel so fortunate to have shared both friendship and science with you for the past several years.

Truly excellent scientific mentors are few and far between, the proper balance of advocacy, advice, and brilliance is rare. I am lucky to have had that opportunity to be mentored by a committee of outstanding mentors. Thank you Professors David Feldser, Costas Koumenis, Ellen Puré, and Celeste Simon. Your guidance and support have been immensely valuable in helping me reach this point. I also have to thank Skip Brass and Maggie Krall for their guidance and support through the rocky journey that has let to my PhD. You have taken care of me and helped me find my way to success against a truly daunting foe.

I have been so fortunate to have great friends through this process, friends that have stood by me and helped me in the darkest of times. Friends to share the ups and downs and everything in between, I couldn't have done it without you.

Finally, I have to thank the greatest supports in my life, my family. Dad, your past struggles and your stability for the past 8 years have been a blessing and an inspiration. Aunt Nancy, Aunt Karen, Sandy, Ellen, and Uncle Jeff, your love and support is a beautiful gift I can never repay. David, I am so grateful that you've been there for me and especially for my mom through so much. Jeanie and Andy, no one has ever had more enthusiastic cheerleaders. Above all the others, Mom, I wouldn't be here without you. From applying to programs to coming to Philadelphia under less than ideal circumstances, you have always supported me and loved me and I cannot thank you enough.

ABSTRACT

A NEW MOUSE MODEL OF METASTATIC GASTRIC CANCER AND E-CADHERIN PRIMARY TUMOR SUPPRESSION

Jacob Till

Sandra Ryeom

Gastric cancer is the fifth most common cancer and the third leading cause of cancer death worldwide. The majority of patients with gastric cancer are diagnosed with disseminated disease and even patients diagnosed with early stage disease have high rates of recurrence. The utility of current mouse models of gastric cancer is limited by slow development of gastric tumors and lack of metastasis. Here I describe a new mouse model of gastric cancer driven by *p53* loss, *Cdh1* loss, and oncogenic *Kras* expression in gastric parietal cells (referred to as ACKPY mice). I generated these mice to investigate the contribution of oncogenic Kras to the progression of gastric cancer given the high rate of mutation and amplification of the RTK/Ras pathway identified in gastric cancer patients. These mice develop mixed-type gastric adenocarcinomas with metastases to lymph nodes, lung, and liver. Oncogenic *Kras* and loss of *Trp53* is sufficient to drive rapid carcinogenesis in a variety of models. Therefore, I tested if loss of E-cadherin was necessary for the onset of gastric adenocarcinoma in gastric parietal cells by generating ACKPY mice with one or two alleles of wild-type *Cdh1* (E-cadherin). E-cadherin expression significantly increased survival and the limited number of mice with gastric tumors have tumors that were focal in nature, suggesting an additional event was necessary for gastric tumorigenesis. Loss of E-cadherin expression was observed in some

of these tumors, suggesting that its loss may be necessary for gastric tumorigenesis in this model. I show that loss of E-cadherin in our model increases β-catenin signaling and that inhibition of β-catenin signaling prolonged survival of ACKPY mice. Microarray data comparing gene expression in stomachs harvested from $Cdh1^{fl/fl}$ and $Cdh1^{fl/+}$ mice showed a correlation between E-cadherin loss and upregulation of oncogenic Kras signaling. Gene sets regulated by each of the main Kras effector pathways were over-represented in our microarray data. Examination of ERK phosphorylation revealed that E-cadherin likely does not regulate MAPK activity in our model. The upregulation of oncogenic Kras target genes that result from the loss of E-cadherin may alternatively be explained by E-cadherin regulation of other Kras effector pathways.

TABLE OF CONTENTS

LIST OF TABLES

LIST OF FIGURES

CHAPTER 1 INTRODUCTION

i. Abstract

The term gastric cancer generally refers to adenocarcinoma of the stomach, as approximately 95% of all gastric cancers are adenocarcinomas. Gastric cancer is the fifth most common cancer worldwide and the third leading cause of cancer death (Jacques Ferlay et al. 2015; J Ferlay et al. 2013). The majority of gastric cancers are diagnosed after they have progressed to disseminated disease (Surveillance Research Program, n.d.) and even patients diagnosed with early stage gastric cancer have relatively poor survival due to high rates of recurrence (Washington 2010). Since 1965, gastric adenocarcinoma has been commonly been divided into two main subcategories: intestinal-type and diffuse-type (Lauren 1965). The progression to intestinal-type gastric cancer follows a well-described sequence known as the Correa Pathway: inflammation leads to atrophy, followed by metaplasia, then dysplasia, and finally carcinoma (Correa 1992; Fox and Wang 2007). While little is known about the histologic and pathologic changes that occur during the progression to diffuse-type gastric cancer, both sporadic and hereditary forms are associated with loss of expression of E-cadherin (Graziano, Humar, and Guilford 2003). The mouse has long been used as a model of gastric cancer; initially chemically induced models and Helicobacter infection models were used, which was followed by the development of genetically engineered mouse models (Poh et al. 2016; Hayakawa et al. 2013; Yu, Yang, and Nam 2014; Giraud and Judd 2009).

ii. Gastric Cancer Epidemiology

Gastric cancer is the fifth most common cancer worldwide (fourth among men) with almost 1 million new cases in 2012 (Table 1-1). The 952,000 new cases diagnosed in 2012 (6.8% of all malignancies) put it behind only cancers of the lung, breast, colorectum, and prostate. Greater than 70% of gastric cancer cases occur in the developing world (677,000 cases in 2012) with more than half in Eastern Asia (549,000 cases in 2012). Incidence rates among men (631,000 cases in 2012) are about twice as high as those among women (320,000 cases in 2012). Though it ranks as the fifth most common cancer, with 723,000 deaths (8.8% of all cancer deaths) in 2012 (Table 1-1), it is the second most deadly among the top 5 cancers, behind lung cancer (Jacques Ferlay et al. 2015; J Ferlay et al. 2013).

Cancer	Incidence	Mortality
Lung	1824701	1589925
Breast	1671149	521907
Colorectum	1360602	693933
Prostate	1094916	307481
Stomach	951594	723073
Liver	782451	745533
Cervix uteri	527624	265672
Oesophagus	455784	400169
Bladder	429793	165084
Non-Hodgkin lymphoma	385741	199670
Leukaemia	351965	265471
Pancreas	337872	330391
Kidney	337860	143406
Corpus uteri	319605	76160
Lip, oral cavity	300373	145353
Thyroid	298102	39771
Brain, nervous system	256213	189382
Ovary	238719	151917
Melanoma of skin	232130	55488
Gallbladder	178101	142823
Larynx	156877	83376
Other pharynx	142387	96105
Multiple myeloma	114251	80019
Nasopharynx	86691	50831
Hodgkin lymphoma	65950	25469
Testis	55266	10351
Kaposi sarcoma	44247	26974

Table 1-1. Global cancer incidence and mortality by cancer type (2012).
(J Ferlay et al. 2013)

The incidence of gastric cancer worldwide has declined significantly since 1975 (the first time such statistics were compiled) when it was the most common malignancy (J Ferlay et al. 2013). In the US, this decline can be observed in the decrease in gastric cancer mortality since the 1930s (Siegel, Naishadham, and Jemal 2012). Many studies have shown that this decline is due specifically to a decrease in intestinal-type gastric cancer, which has been hypothesized to be highly associated with environmental risks. This decline predates the discovery and treatment of the specific pathogen *H. pylori* (which I will discuss later). One hypothesis explaining the decreased incidence in gastric cancer is the rise in popularity of refrigeration technology (Howson, Hiyama, and Wynder 1986; La Vecchia et al. 1990). This improved food storage, reduced salt-based preservation, prevented bacterial and fungal contamination, and allowed greater incorporation of fresh food and vegetables into the diet.

iii. Gastric Cancer in the Clinic

The signs and symptoms of gastric cancer, if present at all, tend to be vague and nonspecific in nature. Patients may experience weight loss, anorexia, fatigue, epigastric discomfort, pain, postprandial fullness, heartburn, indigestion, nausea, or vomiting. None of these signs and symptoms unequivocally indicates gastric cancer and more commonly indicate other benign disease. As a result, many patients are diagnosed at late stage. Signs and symptoms of incurable disease include ascites, jaundice, palpable mass, intestinal obstruction, ovarian mass (Krukenber's tumor), peritoneal implant in the pelvis (Blumer's shelf), and nodal metastasis around the umbilicus (Sister Mary Joseph's Node), to a supraclavicular lymph node (Vichow's node) or an axillary node (Irish node)

(Avital et al. 2015). Data from the Surveillance, Epidemiology, and End Results (SEER) Program of the National Cancer Institute (NCI) compiled from 2004-2013 show that at least 60% of patients present with at least regionally invasive disease (Surveillance Research Program, n.d.).

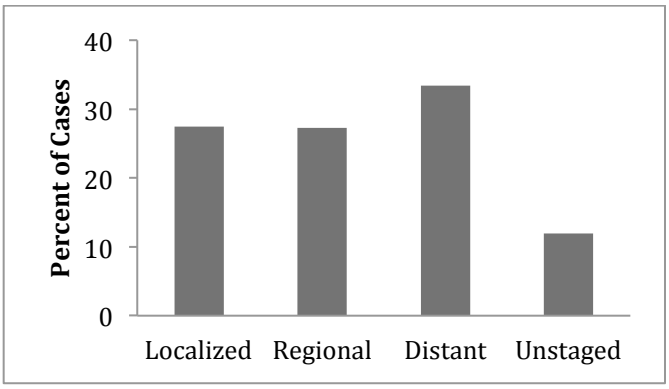

Figure 1-1. Stage distribution of Surveillance, Epidemiology, and End Results (SEER) data on gastric cancer from 2004-2013.
(Surveillance Research Program, n.d.)

There are a number of known risk factors for gastric cancer ranging from environmental to genetic factors. Nutritional risk factors include high salt and nitrate diets, low dietary vitamin A and C, poor food preparation (smoking, curing), lack of refrigeration, and poor drinking water (well water). Rubber and coal workers are at increased risk due to their occupational exposures. Other environmental factors include *H. pylori* infection, cigarette smoking, Epstein-Barr virus, radiation exposure, benign gastric ulcers, and prior treatment for MALT lymphoma. Type A blood, pernicious anemia, family history (without known genetic factors), Hereditary Nonpolyposis Colon Cancer, Familial Adenomatous Polyposis, Li-Fraumeni Syndrome, BRCA1/2 mutation, and Hereditary Diffuse Gastric Cancer are all genetic risk factors for gastric cancer.

Finally, several precursor lesions increase the risk of progression to gastric cancer including adenomatous gastric polyps, dysplasia, chronic gastritis, intestinal metaplasia, and Menetrier disease (Avital et al. 2015).

In the US, staging follows the traditional TNM staging as defined by the American Joint Committee on Cancer (AJCC). Increasing stage correlates with increased mortality. Staging is determined through the use of multiple modalities including physical exam, endoscopy, biopsy, imaging, and surgery. Notably, stage 1A patients, considered "curable," have only a 71% 5-year survival rate (Washington 2010). Recommended therapy for patients with stage 1 disease is total or sub-total gastrectomy with lymphadenoectomy. Postoperative chemoradiation is recommended for patients with stage 1B disease. For all other patients, a combination of palliation, neoadjuvant chemoradiation, surgery, and adjuvant chemoradiation is recommended based on stage and medical fitness (Waddell et al. 2013).

iv. Human Gastric Histology

To understand the biology of gastric cancer, it is important to understand the anatomy and histology of the stomach. The stomach is a large, saccular organ with a volume of 1.2-1.5 liters and a capacity of more than 3 liters. Food enters the stomach from the esophagus passing through the gastro-esophageal junction and exits the stomach via the pyloric sphincter where it enters the duodenum. The stomach is subdivided into 5 regions: the cardia, the fundus, the corpus (body), the antrum, and the pyloruos (Figure 1-2A). The gastric wall (from inner to outer) is composed of the mucosa, submucosa, muscularis propria, and serosa. The mucosa and submucosa are thrown into folds called

rugae. The inner surface of the mucosa is perforated by millions of foveollae or gastric pits that lead to the gastric glands. The mucosa is composed of the surface epithelium, lamina propria, and muscularis mucosa. Gastric adenocarcinoma arises from this surface epithelium (Figure 1-2B).

The more superficial compartment of the gastric mucosa is called the foveolar compartment. It is primarily composed of columnar mucous cells and is relatively uniform through the stomach. The foveolar layer consists of the more superficial mucous cells, which secrete mucins and the deeper, less mucinous, mucous neck cells, which are thought to give rise to both the foveolar and the deeper glandular compartments (Figure 1-2C).

The deeper glandular compartment is composed of gastric glands. The glands vary in their composition of four main cell types depending on the region of the stomach. The four main cell types are mucous cells, parietal cells, chief cells, and endocrine cells. Parietal cells are the acid producing cells, pumping hydrogen ions out into the lumen in exchange for potassium ions. Parietal cells are also important for their production of secreted signals that regulate the differentiation and maintenance of gastric progenitors. They are typically located in the superficial half of the glandular layer, appearing large and pale pink on hematoxylin & eosin (H&E) staining. Chief cells produce and secrete pepsinogens (proteolytic proenzymes). They are typically located in the lower half of the glandular layer, appearing smaller and dark purple on H&E stain. Endocrine cells are scattered throughout the gastric glands and appear triangular shaped with brightly pink granules on H&E stain. They are characterized by the hormones they secrete; some of the

most common endocrine cells are gastrin-producing G cells, somatostatin-producing D cells, and endothelin-producing X cells (Adler, Farraye, and Crawford 2015) (Figure 1-2C).

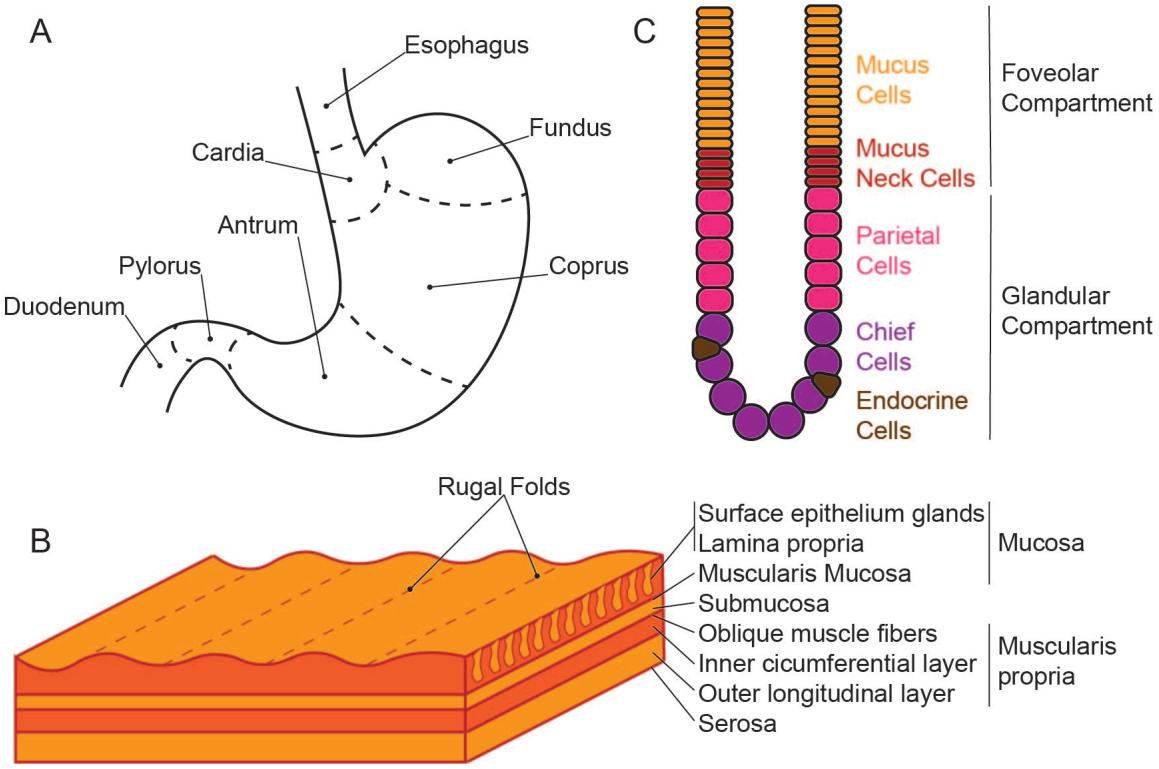

Figure 1-2 Normal gastric histology.
(A) Schematic view of human stomach regions
(B) Schematic diagram of stomach wall
(C) Schematic diagram of a gastric pit/gland

v. Mouse Gastric Histology

The mouse stomach has some notable differences from the human stomach that must be kept in mind when discussing mouse models of gastric cancer. Whereas the human stomach is relatively uniform in its histology, the mouse stomach is subdivided into two sections. The proximal third comprises the non-glandular forestomach that is squamous and esophageal in morphology. The distal two-thirds is referred to as the

glandular stomach and is analogous to the human stomach. A projecting fold, called the limiting ridge, demarcates these two regions. The glandular stomach is analogous to the human stomach and is similarly divided into anatomic regions that differ in their glandular cellular content: cardia, corpus, pyloric antrum (Scudamore 2013) (Figure 1-3).

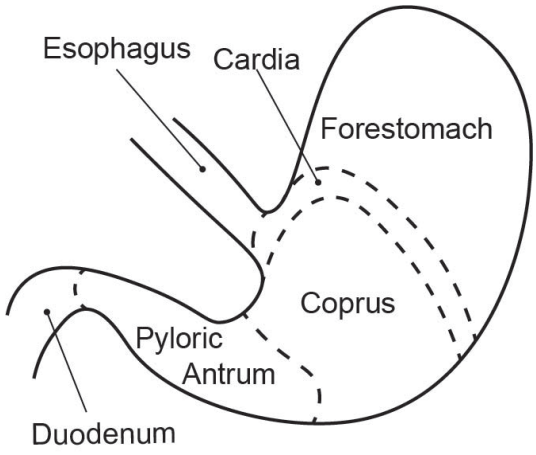

Figure 1-3. Schematic view of mouse stomach regions

vi. Gastric Cancer Histologic Classification

The term gastric cancer refers to adenocarcinoma of the stomach, as approximately 95% of all gastric cancers are adenocarcinomas. Since 1965 gastric adenocarcinoma has been commonly divided into two main subcategories: intestinal-type and diffuse-type (Lauren 1965). The World Health Organization (WHO) subdivides these categories further and adds other subtypes. The intestinal-type is characterized by the formation of glands or tubules. WHO tubular and papillary adenocarcinoma fall into this category. The diffuse-type is characterized by single cells or small clusters of cells that are poorly cohesive and do not form glands. Signet ring cells, so called for the large mucin droplet that displaces and flattens the nucleus to one side, are pathognomonic of diffuse-type gastric cancer. WHO poorly cohesive carcinoma and mucinous

adenocarcinoma fall into this category. More recently, a third category referred to as "mixed-type" has been added to the Lauren classification to include neoplasms with both intestinal- and diffuse-type characteristics (Lauwers 2015).

Intestinal-type gastric cancer is found more commonly in areas of the world with a higher incidence of gastric cancer and is the subtype that has declined the most rapidly in the past few decades. Additionally, it is more common among older individuals and men. Diffuse-type gastric cancer rates are more homogenous across the world, the incidence has declined more slowly, and it occurs with similar frequency between the sexes and throughout all age groups. These data suggest that the intestinal-type is more highly associated with environmental factors, whereas the diffuse-type is less environmentally associated (Muñoz and Asvall 1971).

Though both types are associated with *H. pylori* infection, little else is known about the histologic and pathologic changes that occur during the progression to diffuse-type gastric cancer. The progression to intestinal-type gastric cancer follows a well-described sequence known as the Correa Pathway (Figure 1-4) (Correa 1992; Fox and Wang 2007). This progression begins with chronic inflammation (gastritis) often due to the specific pathogen *H. pylori*. The inflammation leads to epithelial defects including gland dilation and mineralization in addition to the infiltration of lymphocytes. It is followed by an atrophic gastritis that is characterized by loss of parietal cells and focal fibrosis. The definitions of atrophic gastritis and intestinal metaplasia often overlap; however, the loss of parietal cells in atrophic gastritis is considered mechanistically important. Loss of acid production (achlorhydria) leads to bacterial overgrowth and loss

of secreted signals dysregulates growth and differentiation of progenitors. This is followed by intestinal and/or pseudopyloric/spasmolytic polypeptide-expressing metaplasia (SPEM). Intestinal metaplasia is characterized by a transition from normal cell architecture to an elongated intestinal phenotype with mucous droplets and occasionally the formation of goblet cells. SPEM has recently been recognized as more closely associated with progression to gastric cancer and it has been suggested to be the true precursor lesion. It is a type of mucous metaplasia that, as the name suggests, is characterized by expression of spasmolytic polypeptide. This is followed by dysplasia with irregular glandular architecture characterized by infolding and branching as well as cellular and nuclear atypia. The final stage is frank carcinoma with invasion (Fox and Wang 2007) (Figure 1-4).

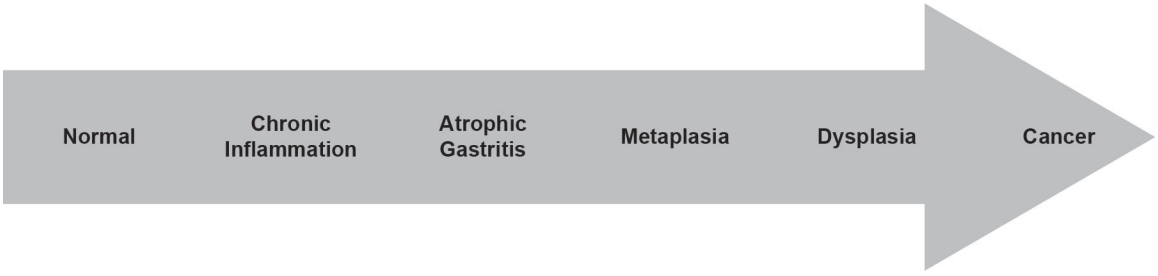

Figure 1-4. Correa pathway (Fox and Wang 2007).

vii. Hereditary Diffuse Gastric Cancer

Genetically engineered mouse models are generated utilizing common or hereditary genetic lesions to induce cancer; this has been the case with gastric cancer as well. In 1964, Jones reported on the case of a 21-year-old Maori male with an inoperable carcinoma of the stomach. This was particularly interesting because of the man's young age and the high incidence of the disease in close relatives (five with proven gastric cancer and several others suspected) (Jones 1964). This kindred was updated in 1998 by

Guilford *et al* to include an additional 25 cases of gastric cancer that had occurred since the initial report (Guilford et al. 1998). Jones termed this phenomenon "early onset familial gastric cancer," but it would come to be known as "Hereditary Diffuse Gastric Cancer" (HDGC). The inheritance pattern observed in the Maori kindred was one of dominant inheritance with incomplete penetrance (Guilford et al. 1998), consistent with a susceptibility gene as observed in other hereditary cancer syndromes (Nagy, Sweet, and Eng 2004).

Using classical genetic mapping techniques, Guilford and colleagues mapped the genetic locus to chromosome 16q22.1, which contains the candidate gene for E-cadherin (*CDH1*). E-cadherin is a calcium dependent cell-cell adhesion protein important for establishing cellular polarity and maintaining normal tissue morphology. Loss of expression of E-cadherin is found in many cancers and correlates with infiltrative and metastatic ability; therefore, it has been termed an "invasion suppressor gene" (A. O. O. Chan 2006). Single-stranded conformational polymorphism screening of coding exons revealed a band shift in exon 7 in two affected and 4 obligate carriers that was not present in 150 unrelated chromosomes. Upon direct sequencing, the first causal mutation (G1008T) was identified. This mutation, in the final nucleotide of an exon, removes the splice site. Guilford *et al* identified an additional frame shift mutation and premature stop codon in two additional families with HDGC. The disease appears to follow a classic two-hit sequence as expression of E-cadherin is lost in HDGC tumors. However, unlike many other inherited cancer syndromes, this loss is frequently due to promoter hypermethylation rather than loss of heterozygosity. Further, *CDH1* hypermethylation

and loss of expression is found in the majority of sporadic cases of diffuse-type gastric cancer (Graziano, Humar, and Guilford 2003). Interestingly, *H. pylori* infection has been shown to modulate promoter methylation of *CDH1* (Liu et al. 2014).

The risk of gastric cancer in patients with HDGC-associated mutations has been estimated at approximately 70% (67% in men and 83% in women) with an additional risk of lobular breast adenocarcinoma in women of 52% (Guilford, Humar, and Blair 2010; Kaurah et al. 2007). Over 100 different *CDH1* mutations have been identified with no characteristic mutational types or hotspots. HDGC patients typically present with diffuse-type gastric adenocarcinoma with signet ring cells and linitis plastica (at late stage) that is indistinguishable from sporadic forms of diffuse-type gastric cancer. The only option for patients with known HDGC to prevent cancer is prophylactic total gastrectomy. However, this option comes with significant morbidity including alteration of eating habits, dumping syndrome, diarrhea, and weight loss. Surveillance endoscopy is a poorly favored option as even advanced diffuse-type gastric cancer can be missed due to its often-subtle appearance. Current recommendations are for prophylactic total gastrectomy prior to 20 years of age when mortality risk from surgery and mortality risk from HDGC are about equal at <1% (Guilford, Humar, and Blair 2010).

While E-cadherin has been identified as the genetic hit in HDGC, the exact mechanism by which a mutation leads to gastric cancer is still not known. Several mechanisms have been proposed to explain E-cadherin's tumor suppressor activity including sequestration of β-catenin, regulation of Rho GTPases, interaction with EGFR, and inhibition NF-κB. E-cadherin sequesters β-catenin at the adherens junction in the

cadherin-catenin complex that links the adherens junction to the cytoskeleton. Loss of E-cadherin may lead to increased free β-catenin, which can translocate to the nucleus, bind its transcription factor partners and transcribe classical WNT pathway target genes. Further, E-cadherin regulates Rho GTPases involved in cell motility and migration. E-cadherin has also been shown to interact with EGFR and act in a context-dependent manner to activate or inhibit its signaling. Finally, E-cadherin can inhibit the activity of NF-κB likely through binding and sequestering its p65 subunit (Liu et al. 2014).

viii. Gastric Cancer Molecular Classification

Two recent studies have attempted to molecularly classify gastric adenocarcinomas using high-throughput genomic technologies. The Cancer Genome Atlas Research Network (TCGA) analyzed a panel of 295 treatment-naïve gastric adenocarcinoma samples for: copy number variation, whole-exome sequencing, methylation profiling, RNA sequencing, microRNA sequencing, and reverse-phase protein array, and microsatellite instability (MSI). Integration of the results of unsupervised clustering on each platform classified the samples into four groups (Bass et al. 2014). The first TCGA group was associated with high Epstein-Bar virus (EBV) burden and promoter hypermethylation. The second group had high MSI, mutation rates, and promoter hypermethylation. The remaining samples were divided into two groups based on the degree of copy number variation. Further analysis defined four similar sub-types based on EBV positivity (9%), high MSI (22%), genomic stability (GS, 20%), or chromosomal instability (CIN, 50%). Each sub-type was further characterized by its associated mutational spectrum, notable pathway/gene activation or inactivation, and

histologic type. The GS sub-type contained 73% of the diffuse-type gastric cancer samples and was associated with *CDH1* and *RHOA* mutations. The CIN group was associated with intestinal morphology, *TP53* mutation, and receptor tyrosine kinase (RTK)-RAS activation (Figure 1-5) (Bass et al. 2014).

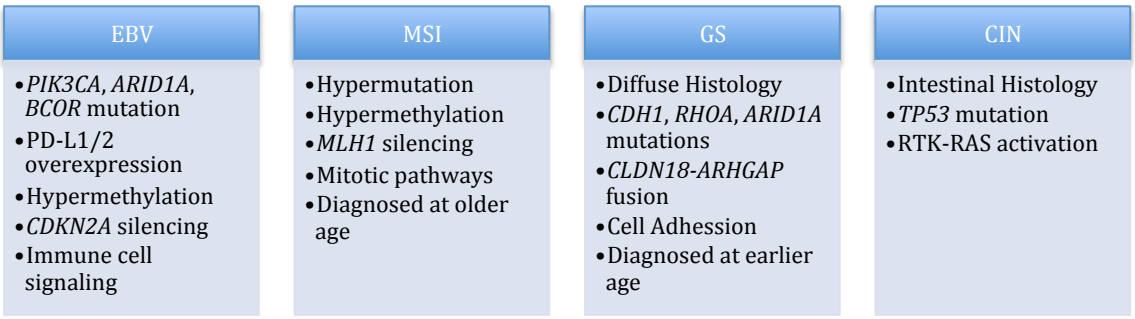

Figure 1-5. Summary of The Cancer Genome Atlas (TCGA) gastric cancer subtypes (Poh et al. 2016; Bass et al. 2014).

The Asian Cancer Research Group (ACRG) analyzed a panel of 291 primary gastric tumors for: expression profiling, copy number variation, and targeted gene sequencing. For this classification, principal components analysis separated the samples into three clusters. The first was positively correlated with an epithelial-to-mesenchymal transition (EMT) signature and negatively correlated with a cell proliferation signature. The second correlated with MSI, cytokine signaling, cell proliferation, and methylation signatures. The remaining cluster of samples were subdivided based on their *TP53* activation status, resulting in four subtypes: MSI, microsatellite stable (MSS)/EMT, MSS/*TP53*$^{+}$, and MSS/*TP53*$^{-}$. Each sub-type had distinct genomic alterations, survival outcomes, and recurrence rates. The authors note that the MSS/EMT subtype was predominantly (80%) diffuse-type. However, it only contained 27% of the diffuse-type samples and the highest rate of *CDH1* mutation was in the MSI group. The highest

percentage of *EGFR* and *ERBB2 (HER2)* amplifications were found in the MSS/*TP53*$^{-}$ group, but the highest rate of *KRAS* mutation was in the MSI group (Figure 1-6) (Cristescu et al. 2015).

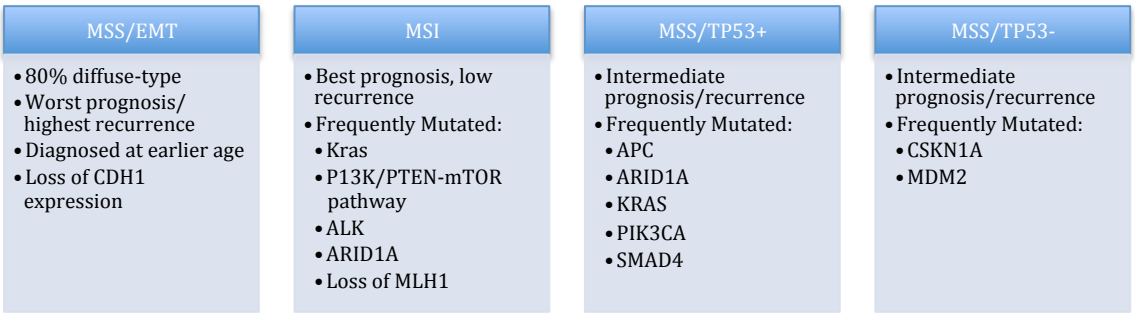

Figure 1-6. Summary of Asian Cancer Research Group (ACRG) gastric cancer subtypes (Poh et al. 2016; Cristescu et al. 2015).

ix. Animal Models of Gastric Cancer

To advance our understanding of the cellular and molecular mechanisms underlying gastric cancer progression and to develop new treatments, there is a need for a mouse model that better replicates advanced human disease. Three types of mouse models have traditionally been used: chemically induced models, helicobacter induced models, and genetically engineered models. These models have also been combined into hybrid models to study their interactions and to accelerate or advance disease progression. However, current animal models of gastric cancer do not adequately recapitulate advanced disease because of long latency periods and the lack of metastatic disease or the presence of metastasis only to regional nodes (Hayakawa et al. 2013; Giraud and Judd 2009; Poh et al. 2016; Yu, Yang, and Nam 2014).

The earliest mouse model of gastric cancer is the N-methyl-N-nitrosourea (MNU) induced model (Tatematsu et al. 1992). However, most mice died due to squamous cell carcinomas (SCC) of the forestomach prior to adenocarcinoma development in the

glandular stomach. Reducing the dose of MNU in the drinking water produced adenocarcinomas without the confounding forestomach SCCs (Tatematsu et al. 1993; Yamachika et al. 1998). The MNU model has been utilized in combination with genetically engineered mice to investigate many signaling pathways involved in gastric cancer, including p53 (Yamamoto et al. 2000), E-cadherin (Humar et al. 2009), β-catenin (Takasu et al. 2008), and NF-κB (Sakamoto et al. 2010) (Table 1-2). More recently, two chemically induced models of precancerous change have come into use: the parietal cell specific protonophore DMP-777 and the structurally related L-635 (Hayakawa et al. 2013). DMP-777 was first used in rats (Goldenring et al. 2000), but in both rats and mice it causes acute oxyntic atrophy, mucous cell hyperplasia, and SPEM (Goldenring et al. 2000; Nomura et al. 2005). In contrast, treatment with L-635 is more rapid and has the additional feature of a prominent inflammatory infiltration (Nam et al. 2010).

Other mouse models of gastric cancer attempted to utilize the specific pathogen *H. pylori* as it is known to contribute to gastric carcinogenesis in humans. In the late 1980s it was shown that mice are resistant to infection with the human pathogen *H. pylori* (Ehlers, Warrelmann, and Hahn 1988; Cantorna and Balish 1990), so the feline isolate *H. felis* (A Lee et al. 1990) or *H. pylori* mutant strains have been used instead (Adrian Lee et al. 1997). *H. felis* infection produces gastritis and atrophy with some strain dependence (A Lee et al. 1990; A Lee et al. 1993; Sakagami et al. 1996). Prolonged infection leads to hyperplasia, metaplasia, and dysplasia leading to adenocarcinoma (Fox et al. 2002). Results of infection with the commonly used Sydney strain of *H. pylori* (SS1) are strain specific, it causes gastritis and atrophy but no carcinoma at 23 months in C57BL/6 and

Balb/cA mice (Xin Wang et al. 2003) but causes intra-mucosal cancer at 15 months in B6.129 mice (Rogers et al. 2005). Infection with *H. felis* or *H. pylori* strains have also been used in conjunction with MNU (Tomita et al. 2011; Han et al. 2002) and genetic models of gastric cancer (T. C. Wang et al. 2000; Fox et al. 2002).

Genetic Model	Finding	Ref
Trp53$^{+/+}$ vs. $^{+/-}$ vs. $^{-/-}$	Higher incidence of tumors in *Trp53*$^{-/-}$ mice. No Trp53 mutations in the tumors of any group	(Yamamoto et al. 2000)
Cdh1$^{+/+}$ vs. Cdh1$^{+/-}$	Equal incidence of intestinal-type adenoCA. Diffuse-type was 11x more common in *Cdh1*$^{+/-}$.	(Humar et al. 2009)
K19-C2mE Tg ± *H. pylori* SS1	β-catenin accumulation in pyloric but not fundic tumor cell cytoplasm and nuclei. β-catenin mutations were more common in *H. pylori* associated tumors.	(Takasu et al. 2008)
Ikkβ$^{fl/fl}$ vs. *Ikkβ*$^{\Delta Foxa3}$	Decreased tumorigenesis with KO of *Ikkβ*. Increased apoptotic cell death in *Ikkβ* KO. Apoptosis was dependent on decreased IL1α.	(Sakamoto et al. 2010)

Table 1-2. Relevant compound MNU-induced/genetically engineered models.

The age of transgenic mouse models has seen a plethora of genetically engineered mouse models (GEMMs) of gastric cancer. There are 24 models that result in at least intra-mucosal gastric cancer and more that model pre-neoplastic changes (Poh et al. 2016; Hayakawa et al. 2013; Yu, Yang, and Nam 2014; Giraud and Judd 2009). The long latency and lack of metastasis in the majority of these models limit their utility. Relevant to our studies are the models that utilize deletion of *Cdh1* and activate oncogenic *Kras* as well as the more recent models that attempt to define the cell of origin of gastric cancer.

As described earlier, germline mutations in the *Cdh1* gene (encoding E-cadherin) are responsible for HDGC. In 2011, Mimata *et al* attempted to model HDGC using the *Cdh1* conditional allele and a gastric parietal specific Cre, *Atp-4b-Cre*. The *Atp4b* promoter was first used in 1995 to drive SV40 T antigen expression to study pre-parietal

cell biology (Q. Li, Karam, and Gordon 1995). Similar experiments generated neuroendocrine tumors when expression of a conditional SV40 T antigen allele was driven by *Atp-4b-Cre* expression (Syder et al. 2004).

The *Cdh1* conditional deletion resulted in hyperplasia that progressed from 3 months on but no invasive cancer by two years. However, they did observe signet ring cells (pathognomonic of diffuse gastric cancer) at 12 months (Mimata et al. 2011). In 2012, Shimada *et al.* added conditional deletion of the tumor suppressor *Trp53* and found that these double-conditional knockout mice developed intra-mucosal tumors at 6 months and invasive tumors at 9 months with a median survival of one year. At this one-year time point, 40% of mice had local lymph node metastasis (Shimada et al. 2012).

Early studies of the role of oncogenic Kras in gastric cancer utilized the Keratin 19 (C*K19)* promoter to drive expression throughout the gastrointestinal tract. One report described parietal cell atrophy and mucous neck cell hyperplasia at 3-6 months of age (Brembeck et al. 2003). At 16 months, invasive intestinal-type adenocarcinomas were observed (Okumura et al. 2010). Another group bred the conditional $Kras^{LSL\text{-}G12D}$ to a $CK19\text{-}Cre^{ERT}$ transgene to produce tamoxifen-inducible oncogenic Kras expression. This study observed only hyperplasia, metaplasia, and adenomas of the stomach, however the lack of frank carcinomas may have been due to the increased mortality seen in these mice. Over half the mice had to be euthanized prior to the 6 month endpoint due to weight loss correlated with oral tumors (Ray et al. 2011). Expression of oncogenic $Kras^{LSL\text{-}G12D}$ under the control of the ubiquitous promoter $UBC9\text{-}Cre^{ERT}$ drove severe

inflammation, hyperplasia, metaplasia, and carcinogenesis in the stomach, but other organs were devoid of neoplastic changes (Matkar et al. 2011).

Several groups have recently argued that Mist1^{+} or Lgr5^{+} stem cells are the cell of origin of both intestinal-type and/or diffuse-type gastric cancer. The evidence they cite is their ability to drive tumorigenesis by specific genetic manipulation of these cell types using cre/lox technology (Hayakawa et al. 2015; X. Li et al. 2016). However, at least in the case of diffuse-type gastric cancer, similar manipulations of gastric parietal cells using Atp-4b-Cre results in tumor formation (Shimada et al. 2012). This suggests that several cells of origin exist, that this is not the right criterion on which to identify tumor-initiating cells, or that some overlap may exist between these cell populations.

x. Conclusion

Though a plethora of mouse models of gastric cancer exist, none adequately recapitulates the advanced disease as is seen in the majority of human patients. These models have long latencies, lack metastasis, or metastasize only to regional nodes. To advance our understanding of the cellular and molecular mechanisms underlying gastric cancer progression and to develop new treatments for gastric cancer, there is a need for a mouse model that better recapitulates advanced human disease.

Model	Incidence	Duration	Location	Type	Inv	Met	(Ref)
CEA/SV40	100%	50 d	Antrum	Intestinal	Y	N	(Thompson et al. 2000)
MMTV/Ad12	82%(M) 17%(F)	3–4 m	SCJ	Intestinal Adenosquamous	Y	N	(Koike et al. 1989)
HPV-16	100%	246 d(F) 352 d(M)	Antrum	Carcinoid	Y	Y	(Searle et al. 1994)
CA-AhR	100%	12 m	Corpus	Intestinal	Y	N	(Andersson et al. 2002)
Atp-4b/SV40	100%	12 m	Corpus/Antrum	Neuroendocrine	Y	Y	(Syder et al. 2004)
Atp-4b/Cdx2	100%	100 w	Corpus	Intestinal	Y	N	(Mutoh et al. 2004)
INS-GAS	75%	20 m	Corpus	Intestinal	Y	N	(T. C. Wang et al. 2000)
ACT-GAS	100%	20 m	Corpus	Intestinal	N	N	(Konda et al. 1999)
$GAS^{-/-}$	60%	12 m	Antrum	Intestinal	N	N	(Zavros et al. 2005)
$MTH1^{-/-}$	13%	18 m	Antrum	Intestinal	N	N	(Tsuzuki et al. 2001)
$TFF1^{-/-}$	30%	5 m	Antrum	Intestinal	Y	N	(Lefebvre et al. 1996)
$Smad4^{+/-}$	100%	18 m	Corpus/Antrum	Intestinal	Y	N	(Xu et al. 2000)
$Smad3^{-/-}$	100%	10 m	SCJ	Intestinal	Y	N	(Nam et al. 2012)
$Gp130^{Y757F/Y757F}$	100%	3 m	Antrum	Adenoma	N	N	(Tebbutt et al. 2002)
$K19/Kras^{G12V}$	38%	16 m	Corpus	Intestinal	Y	N	(Okumura et al. 2010)
K19/Wnt1 *K19/C2me*	100%	20 w	SCJ	Intestinal	Y	N	(H. Oshima et al. 2006)
Atp4b-Cre $Cdh1^{fl/fl}$ $p53^{fl/fl}$	100%	12 m	Corpus	Diffuse	Y	Y	(Shimada et al. 2012)
Villin-Cre $KLF4^{fl/fl}$	29%	20 m	Antrum	Intestinal	N	N	(Qiang Li et al. 2012)
$Elf^{+/-}$ $Smad4^{+/-}$	1/6	7 mo	Antrum	ND	Y	N	2005(Redman et al. 2005)
$Mist1\text{-}Cre^{ERT2}$ $Kras^{LSL\text{-}G12D}$ $Apc^{fl/fl}$	ND	4 mo	Corpus	Intestinal	N	N	(Hayakawa et al. 2015)
$Mist1\text{-}Cre^{ERT2}$ $Cdh1^{fl/fl}$ *H. felis*	78%	18 m	ND	Diffuse	N	N	(Hayakawa et al. 2015)
$Mist1\text{-}Cre^{ERT2}$ $Cdh1^{fl/fl}$ $LSL\text{-}p53^{R172H}$ *H. felis*	ND	9 m	ND	Diffuse	Y	N	(Hayakawa et al. 2015)
$Lgr5\text{-}Cre^{ERT2}$ $Smad4^{fl/fl}$ $PTEN^{fl/fl}$	40%	3 m	Corpus	Intestinal	Y	N	(X. Li et al. 2016)
$Gp130^{Y757F/Y757F}$ $Tff1\text{-}Cre^{ERT2}$ $Kras^{LSL\text{-}G12D}$	ND	3 m	Corpus/Antrum	Intestinal	Y	N	(Thiem et al. 2016)

Table 1-3. Genetically Engineered Mouse Models (GEMMs) of gastric adenocarcinoma.

CHAPTER 2 ACKPY METASTATIC MODEL OF GASTRIC CANCER

i. Abstract

The utility of current mouse models of gastric cancer is limited by slow development and lack of metastasis (Poh et al. 2016; Hayakawa et al. 2013; Yu, Yang, and Nam 2014; Giraud and Judd 2009). Here I describe a new mouse model of gastric cancer driven by *p53* loss, *Cdh1* loss, and oncogenic *Kras* expression in gastric parietal cells. I generated these mice to investigate the contribution of oncogenic Kras to the progression of gastric cancer given the high rate of mutation and amplification of the receptor tyrosine kinase (RTK)/Ras pathway in gastric cancer. These mice develop invasive diffuse and intestinal type gastric adenocarcinomas as early as 6 weeks of age and die with metastases to the lymph nodes, lung, and liver by 3 months. The rapid disease progression allows for timely analysis of tumor biology, diagnostics, and therapeutics while the metastatic phenotype makes it highly relevant to human disease.

ii. Introduction

The utility of current mouse models of gastric cancer is limited due to the long latency periods for tumor development, the lack of metastasis in these models or metastasis only to regional nodes in a few models (Poh et al. 2016; Hayakawa et al. 2013; Yu, Yang, and Nam 2014; Giraud and Judd 2009). To date, there are six mouse models of metastatic gastric cancer (Table 2-1). However, only one has clinical relevance. Two utilize the SV40 transgene that plays no role in human cancer (Thompson et al. 2000; Q. Li, Karam, and Gordon 1995; Syder et al. 2004). One utilizes human papilloma virus (HPV)-16 (Searle et al. 1994) that is not associated with gastric cancer in humans

(Kamangar et al. 2006). A fourth utilized adenovirus 12 (Koike et al. 1989) and a fifth utilized a constitutively active dioxin/aryl hydrocarbon receptor (Andersson et al. 2002), neither of which has ever been shown to be involved in the development of gastric cancer. Further, the lesions found in the adenovirus 12 model were adenosquamous lesions of the forestomach, which is consistent with esophageal disease and not adenocarcinoma of the stomach (Koike et al. 1989). The only model that contains genetic lesions identified in human disease is the double conditional deletion of the *Cdh1* and *Trp53* genes, but only 40% of mice have local nodal metastasis. A mouse model that better replicates advanced human disease would advance our understanding of the cellular and molecular mechanisms underlying gastric cancer progression.

Model	Incidence	Duration	Phenotype	Metastasis	Reference
CEA/SV40	100%	50 d	Intestinal	Invasion to the duodenum	(Thompson et al. 2000)
ATP-4b/SV40		12 months	Neuroendocrine	LN Liver	(Q. Li, Karam, and Gordon 1995; Syder et al. 2004)
HPV-16	100%	246–352 d	Carcinoid	LN Liver	(Searle et al. 1994)
MMTV-Ad12	56%	4 months	Adenosquamous	LN Lungs	(Koike et al. 1989)
CA-AhR	100%	12 m	Intestinal	Invasion of local organs	(Andersson et al. 2002)
CDH1/p53	100%	12 m	Diffuse	LN (40%)	(Shimada et al. 2012)

Table 2-1. Metastatic mouse models of gastric cancer (LN = Lymph Node).

The H^+/K^+ ATPase pump, found only in gastric parietal cells and pre-parietal cells is responsible for the acidification of the stomach. The *Atp4b* gene encodes the beta subunit and has been used to alter expression of various genes in this cell population (Syder et al. 2004). One such model is the conditional deletion of the *Cdh1* gene in gastric parietal cells by use of the *Atp4b-Cre* allele in $Cdh1^{fl/fl}$ mice. These mice

developed signet ring-like cells at 12 months of age but no invasive cancer even at 24 months (Mimata et al. 2011). Shimada *et al* added a conditional deletion of *Trp53* resulting in invasive diffuse-type gastric cancer by 9 months, with 40% of mice developing metastasis to regional lymph nodes at one year (Shimada et al. 2012). We have attempted to overcome the limitations of this model by adding a third genetic hit.

In the TCGA cohort, the RTK/Ras signaling axis is altered in the majority of gastric cancer samples. EGFR family members (*EGFR*, *ERBB2*, *ERBB3* and *ERBB4*) are amplified or mutated in 44% (126/287) of cases. The Ras family is genetically modified in 18% (46) of cases and, of those, 14% (36) are specifically *KRAS* alterations. In fact, *KRAS* is mutated in 9% (23) of all cases and the vast majority (20) of these mutations are known oncogenic mutations (18 in codons 12/13, 2 in codon 61). Additionally, *RASA1*, a negative regulator of Ras, is mutated or deleted in 9% (24) of cases. Finally, the Raf family is modified in 14% of cases (Figure 2-1) (Bass et al. 2014; Cerami et al. 2012). Activation of this pathway has been modeled in several studies. Oncogenic Kras activation has been shown to produce precancerous or cancerous lesions in the mouse stomach in a promoter-dependent manner (Ray et al. 2011; Okumura et al. 2010; Matkar et al. 2011).

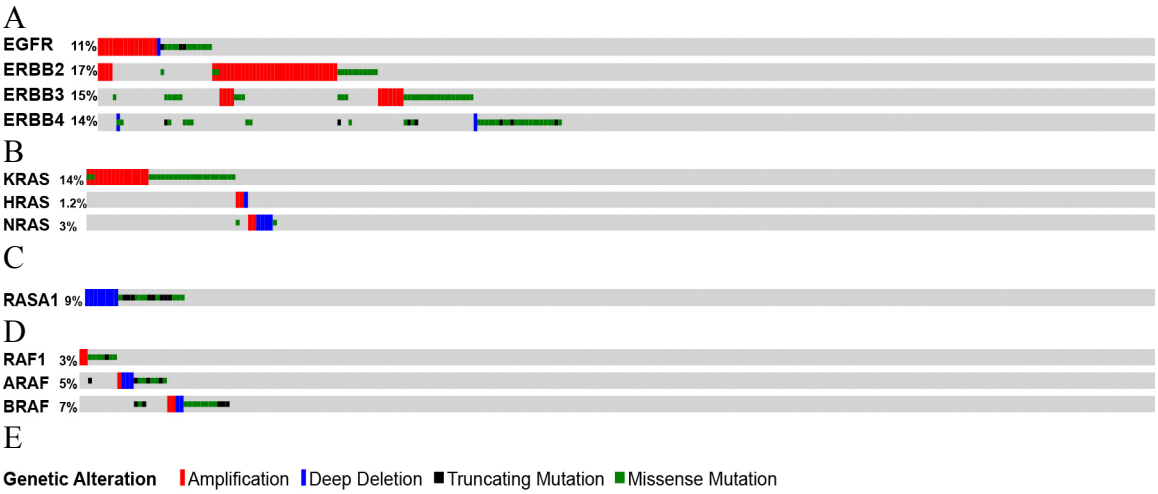

Figure 2-1. Genetic alterations of the RTK/Ras/Raf axis in gastric cancer. (Bass et al. 2014; Cerami et al. 2012) (A) EGFR family, (B) Ras family, (C) RASA1, (D) Raf family, (E) Symbol key.

Based on these data, we investigated the contribution of oncogenic Kras towards the progression of gastric cancer. I generated a mouse model of gastric cancer driven by gastric parietal cell-specific (*Atp-4b-Cre*) loss of E-cadherin (*Cdh1*$^{fl/fl}$), loss of *p53* (*Trp53*$^{fl/fl}$), and expression of oncogenic *Kras* (*Kras*$^{LSL\text{-}G12D/+}$). Additionally, I included a yellow fluorescent protein (YFP) reporter allele (*Rosa26*$^{LSL\text{-}YFP}$). These mice will hereafter be referred to as ACKPY mice (Figure 2-2).

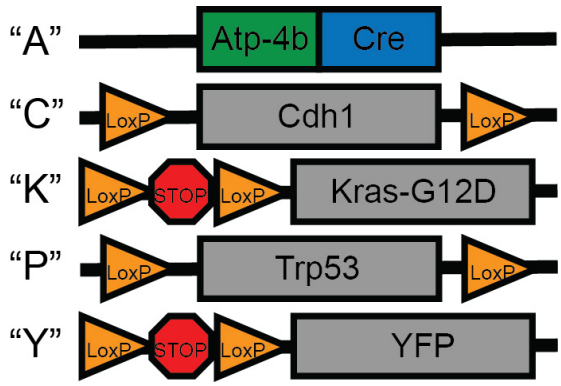

Figure 2-2. Schematic of ACKPY mouse model genetics.

iii. Results

Addition of oncogenic *Kras* to *Cdh1/Trp53* deletion model decreases survival four-fold

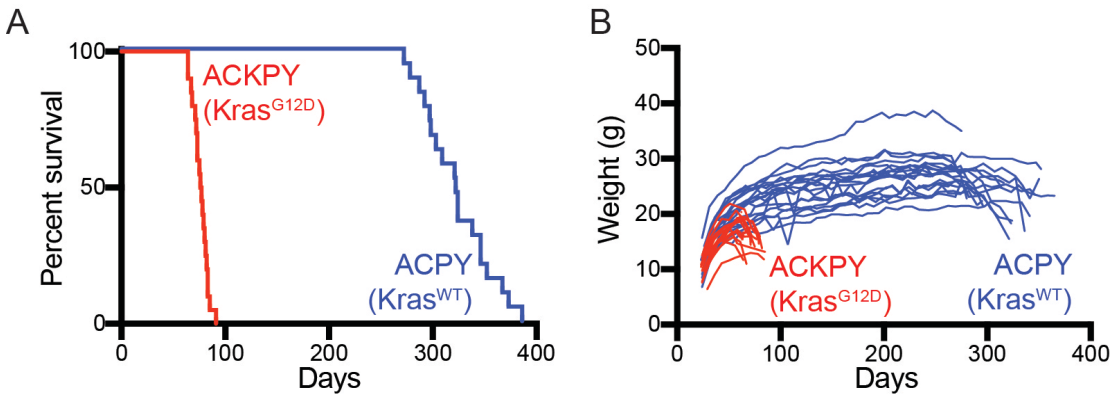

Figure 2-3. Survival and weight phenotypes of ACKPY (Kras$^{G12D/+}$) mice compared to ACPY (Kras$^{+/+}$) mice.
(A) Kaplan-Meier survival curve of ACKPY (n=20) and ACPY (n=19) mice (B) Weight graph of corresponding mice over time.

Characterization of the ACKPY mouse model revealed a rapid course of disease. The mice had a median survival of 76.5 days (range 64-91 days, SD 7.2). This was over four times faster than the ACPY controls (wild-type *Kras, Cdh1* loss and *Trp53*), which had a 322-day median survival (range 272-386 days, SD 32.8, Figure 2-3A). ACKPY mice began to lose weight around 60 days of age and disease progression correlated with weight loss (Figure 2-3B).

ACKPY mice rapidly develop mixed-type gastric cancer with *linitis plastica*

At necropsy, stomachs were dramatically enlarged with normal stomach replaced by tumor. They displayed classic *linitis plastica* (i.e. leather bottle stomach) with thickened, rigid, and whitened gastric walls (Figure 2-4A). Histologically, the gastric cancers that developed in these mice were mixed-type, with regions consistent with both diffuse- and intestinal-type morphology (Figure 2-4B). In one human cohort, mixed-type

gastric cancer accounted for 15% of cases (with 54% intestinal- and 32% diffuse-type) (Polkowski et al. 2016).

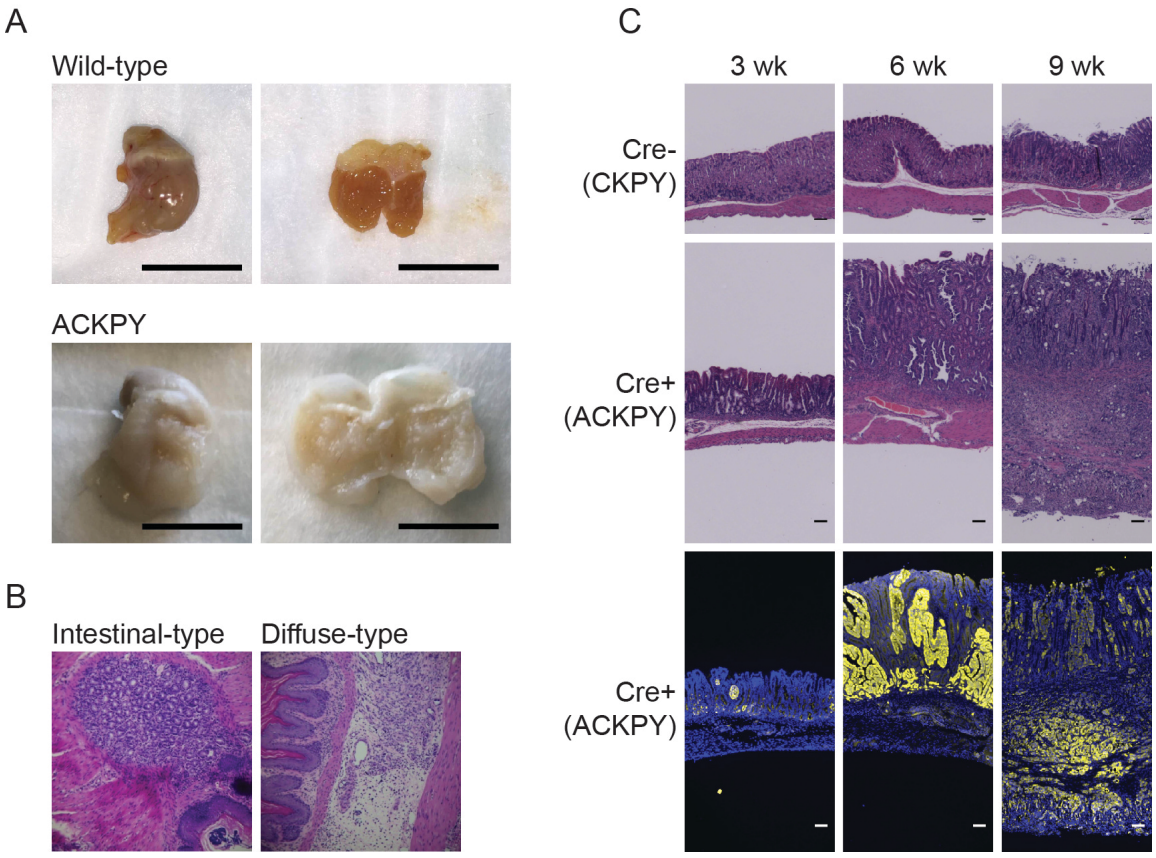

Figure 2-4. Gross and histologic phenotype of ACKPY tumors.
(A) Representative gross images of wild-type and ACKPY stomachs (scale bar: 1 cm).
(B) Representative images of intestinal- and diffuse-type lesions found in ACKPY mice.
(C) Representative H&E and immunofluorescent (blue: DAPI, yellow: YFP) images of ACKPY and Cre- control stomachs harvested from mice at 3, 6, and 9 weeks of age (scale bar: 1 mm).

We examined the kinetics of disease progression in this model by analyzing stomachs of ACKPY mice and Cre^- (CKPY) controls at 3, 6, and 9 weeks of age. As expected, Cre^- control stomachs displayed normal architecture at all time points (Figure 2-4C). ACKPY mice had few or no identifiable gastric parietal cells by 3 weeks of age

and 100% of mice demonstrated high-grade dysplastic lesions and/or intra-mucosal carcinomas. At this time point, immunofluorescence microscopy for YFP^+ recombined cells revealed clusters of transformed cells. By 6 weeks of age, there was a dramatic increase of these lesions with invasion in 40% of mice. By 9 weeks of age all mice had invasive carcinomas (Figure 2-4C).

Metastatic disease in ACKPY mice

Ten mice were sacrificed at 64-83 days of age and analyzed for metastasis to local lymph nodes, liver, and lungs. Upon gross examination of the abdomen under a fluorescent dissecting microscope (Figure 2-5A), the stomach was enlarged and YFP^+ nodules were apparent within the perigastric fat in all mice. Histologic evaluation of the perigastric fat identified these nodules as perigastric lymph node metastases (Figure 2-5C). Though no gross lesions were observed in the liver, immunofluorescent histologic analysis of tissue specimens identified micro-metastatic lesions in 20% of mice (Figure 2-5D).

Gross examination of the thoracic cavity identified YFP^+ lesions in the mediastinum adjacent to the trachea in 50% of mice examined (Figure 2-5B). Histologically these were confirmed as mediastinal lymph node metastases (Figure 2-5E). YFP^+ lung metastases were identified in all mice (Figure 2-5F). In 50% of mice these lung metastases could be observed grossly, while the remaining 50% harbored micro-metastases only identifiable by immunofluorescent microscopy.

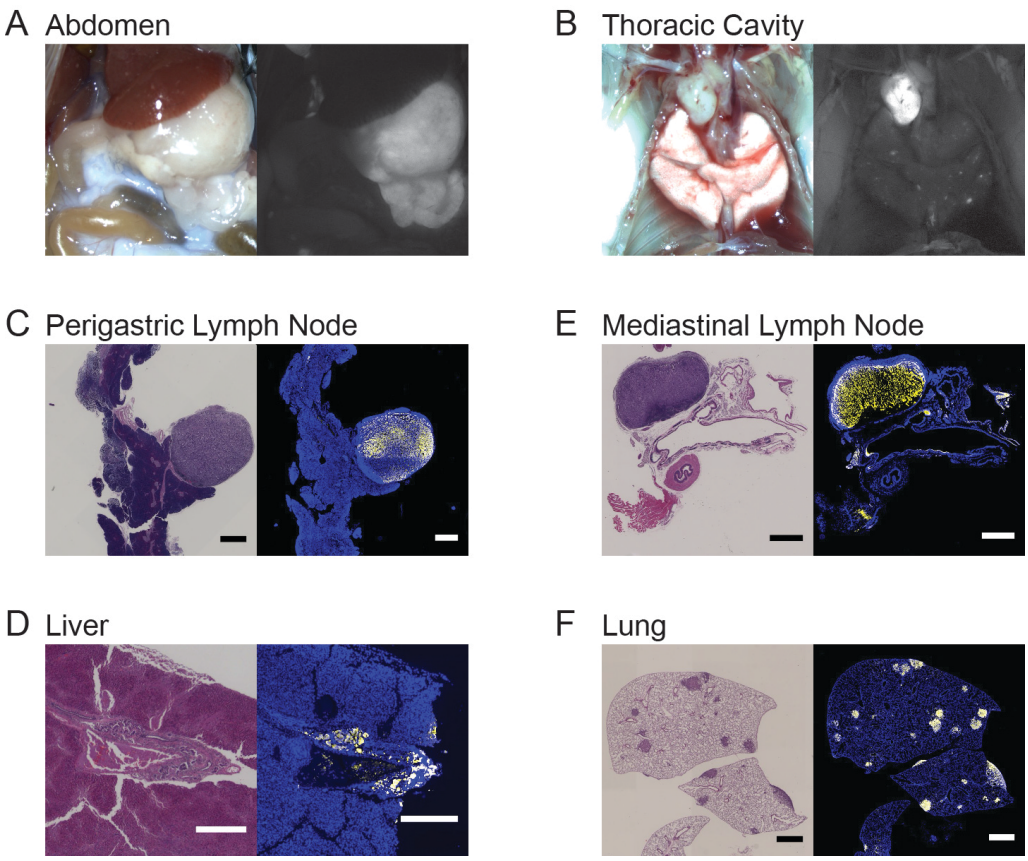

Figure 2-5. Metastatic phenotype of ACKPY mice.
(A&B) Representative gross and fluorescent images of the abdomen or thoracic cavity, (C,D,E,F) H&E and immunofluorescent (blue: DAPI, yellow: YFP) images of metastatic lesions in ACKPY mice. Scale bars are all 1 mm except for the liver that is 0.5 mm.

I successfully isolated four independent cell lines from four different primary gastric tumors and one from a local lymph node metastasis. All cell lines tested formed flank tumors in wild-type C57BL/6 mice (Figure 2-6A), experimental validation of the neoplastic nature of these lesions. One of the two gastric cancer-derived cell lines tested metastasized to the lung in an experimental model of spontaneous metastases (Figure 2-6B).

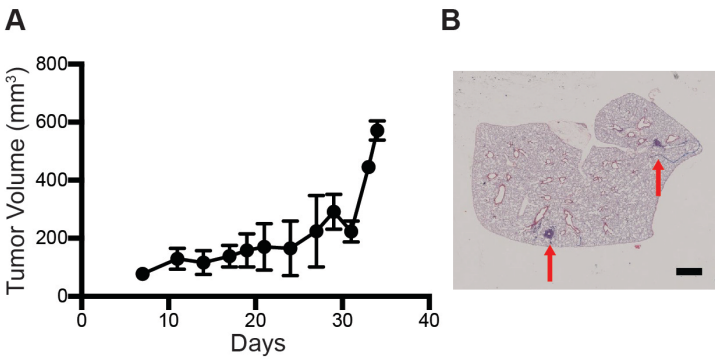

Figure 2-6. Metastatic ACKPY cell line.
(A) Growth curve of primary tumor cell line injected subcutaneously into the flank of naïve mice ($5x10^6$ cells/mouse, n=4). Data are presented as the mean tumor volume ± SD. (B) H&E image of lung metastases (red arrows) derived from an ACKPY gastric cancer flank tumor.

ACKPY model depends on MAPK activity downstream of oncogenic *Kras*

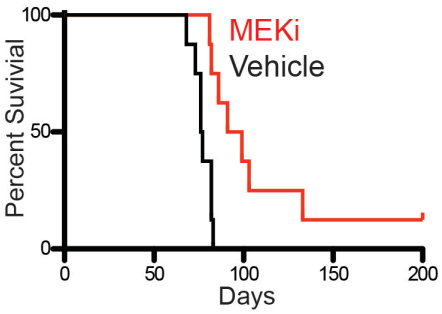

Figure 2-7. Kaplan-Meier survival curve of ACKPY mice treated with MEK inhibitor. Mice were treated beginning at 4 weeks of age with MEK inhibitor PD0325901 administered ad libitum in the mouse chow at 7 mg/kg of diet.

To test the dependence of our model on oncogenic *Kras* signaling through the MAPK pathway, I treated mice with an inhibitor to the downstream kinase MEK (PD0324901). These mice had an increase in median survival of 18.5 days over vehicle (p=0.001, n=8). Of note, one mouse survived over 200 days on treatment (Figure 2-7). These data support the utility of the ACKPY model for testing preclinical compounds in the treatment of gastric cancer.

iv. Discussion

This newly generated ACKPY mouse model of gastric cancer represents a highly tractable and clinically relevant mouse model for the field of gastric cancer research. More recently, several additional groups have used specific promoters to drive oncogenic Kras expression in the stomach (Table 2-2). Of the four studies that expressed oncogenic Kras alone, three of them demonstrated precancerous changes (Ray et al. 2011; Matkar et al. 2011; Thiem et al. 2016). One group examined mice at 16 months (Okumura et al. 2010) and found gastric cancer in less than 40% of mice. Two recent genetic models utilize oncogenic Kras and an additional genetic lesion (*Apc* deletion or *Gp130* activation) to drive cancer development (Hayakawa et al. 2015; Thiem et al. 2016). However, one does not invade (Hayakawa et al. 2015) and neither metastasizes (Hayakawa et al. 2015; Thiem et al. 2016). Our ACKPY model is clinically relevant, invasive, and metastasizes widely.

Model	Incidence	Duration	Location	Type	Inv	Met	(Ref)
CK19-Cre^{ERT} Kras$^{LSL-G12D}$	ND	6 m	ND	Adenoma	N	N	(Ray et al. 2011)
UBC9-Cre^{ERT} Kras$^{LSL-G12D}$	ND	13-18 d	Fore/Glandular Stomach Junction	Mucus Gland Metaplasia	N	N	(Matkar et al. 2011)
Tff1-Cre^{ERT2} Kras$^{LSL-G12D}$	ND	9 m	Corpus/Antrum	Adenoma	N	N	(Thiem et al. 2016)
K19/Kras^{G12V}	38%	16 m	Corpus	Intestinal	Y	N	(Okumura et al. 2010; Brembeck et al. 2003)
Mist1-Cre^{ERT2} Kras$^{LSL-G12D}$ Apc$^{fl/fl}$	ND	4 mo	Corpus	Intestinal	N	N	(Hayakawa et al. 2015)
Gp130$^{Y757F/Y757F}$ Tff1-Cre^{ERT2} Kras$^{LSL-G12D}$	ND	3 m	Corpus/Antrum	Intestinal	Y	N	(Thiem et al. 2016)

Table 2-2. Oncogenic *Kras* driven mouse models of precancerous and cancerous gastric disease.

Both the increased rate of tumor formation and the increased metastasis observed in the ACKPY model over the ACPY model is genetically attributable to the inclusion of an oncogenic *Kras* allele. To test the dependence of our model on oncogenic *Kras* signaling through the MAPK pathway, I treated mice with an inhibitor to the downstream kinase MEK. While this treatment significantly increased survival (median survival of 95 days compared to 76.5 days for untreated) it did not do so to the level of genetic exclusion of the oncogenic *Kras* allele as seen in ACPY mice (median survival of 1 year).

This discrepancy may be due to one or more of several explanations. First and foremost, inhibitor treatment was initiated at 4 weeks of age, a time at which small tumors are already present. Thus, the context of MAPK inhibition is completely different than MAPK activity resulting from lifelong germline wild-type *Kras* activity. For example, drug resistance could evolve quickly within already established tumors to overcome the MEK inhibition. Second, there is no reason to think the level of MEK/MAPK activity in the *Kras* wild-type context (ACPY) would be equivalent to the level of inhibited activity in the oncogenic *Kras* context (ACKPY+inhibitor). Inhibition is not perfect and the dosage may have been too low; allowing for a degree of MAPK signaling to still be present in the inhibited ACKPY tumors that is higher than the level of MAPK signaling in the ACPY stomachs. Finally, as will be discussed in future chapters, the MAPK pathway is not the only pathway downstream of oncogenic KRAS. Simple inhibition of one downstream pathway in the context of oncogenic *Kras* would not be expected to be equivalent to the genetic inhibition of all downstream pathways in the context of wild-type *Kras* (as is the case in ACPY mice).

Our findings also have implications for the gastric cancer cell of origin debate. Hayakawa *et al* (2015) showed that activation of oncogenic *Kras* and loss of *Apc* in Mist1^{+} stem cells was sufficient to drive intestinal-type gastric cancer, indicating that this population may be the cell or origin for intestinal-type gastric cancer. Further, because they were able to drive tumorigenesis by loss of *Cdh1* and *H. felis* infection in this cell population, they argued that Mist1^{+} stem cells are the cell of origin of diffuse-type gastric cancer. However, Li et al (2016) found that Lgr5^{+} stem cells are the cell of origin of intestinal-type gastric cancer by showing that deletion of *Smad4* and *PTEN* in this population led to tumor formation. By these criteria, our data driving mixed-type gastric cancer in pre-parietal cells or parietal cells (those that express *Atp4b*) (Q. Li, Karam, and Gordon 1995) suggests that they are also a cell of origin for both intestinal-type and diffuse-type gastric cancer.

These conflicting data may be resolved by further investigation of the overlap between these lineages and their progeny. Lgr5^{+} stem cells (Barker et al. 2010) and Mist1^{+}/Troy^{+} stem cells (Stange et al. 2013) have been shown to generate all cell types in the gastric glands, including parietal cells. Perhaps it is not the Lgr5^{+} or Mist1^{+} stem cells that are being transformed, but their parietal cell or pre-parietal cell differentiated daughter cells. Further experimentation is necessary to test this hypothesis.

As proof of principle of the model's utility, we have begun to investigate the role of the microbiome in our model. As has been shown in many cancers, but particularly those of the alimentary tract, the microbiome plays an important role in the development

of disease (Ohtani 2015). We treated our ACKPY model with a commonly utilized quadruple antibiotic cocktail to deplete the microbiota. Microbiome depletion was confirmed by qPCR for the bacterial 16S ribosomal subunit in stomach and cecal contents at necropsy (Figure 2-8B). Though the results are preliminary, microbiome depletion resulted in a 7.5-day increase in median survival (p=0.04, n=6) over vehicle (n=5) (Figure 2-8A). While the specific pathogen *H. pylori* is known to contribute to pathogenesis of gastric cancer, these data implicate the normal microbiota in gastric cancer development.

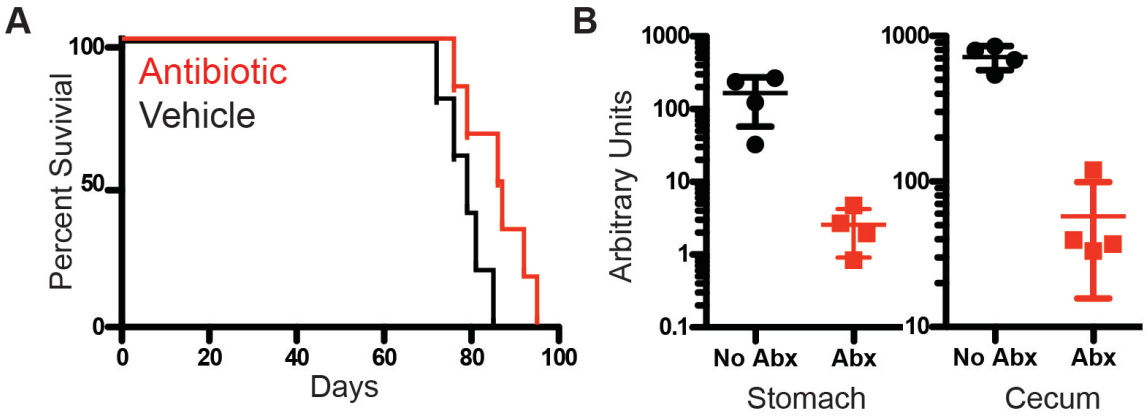

Figure 2-8. Antibiotic depletion of microbiome increases ACKPY survival. (A) Kaplan-Meier curve showing 7.5-day increase in median survival (p=0.04,) for antibiotic treated mice (red, n=6) over vehicle (black, n=5). (B) Microbiome depletion as measured by qPCR for the bacterial 16S ribosomal subunit (normalized to total DNA content) in stomach (p=0.02) and cecal (p<0.0001) contents at necropsy. Antibiotics were administered via the drinking water *ad libitum* at 1 g/L ampicillin, 1 g/L neomycin, 1 g/L metronidazole, 0.5 g/L vancomycin, and 4 g/L sucralose.

Given the metastatic phenotype of the ACKPY model, we wished to determine if we could detect circulating tumor cells (CTCs) and if their presence would correlate with any of the metastatic phenotypes. We used flow cytometry to measure CTCs in cardiac

blood by counting the number of YFP^+ cells present (CTCs defined as DAPI-, CD45-, YFP+). These data are preliminary but promising; mice with many CTCs (>90 per 100 µl blood) were found to have macro-metastatic disease of the lung, whereas mice with few CTCs (<15 per 100 µl blood) did not (Table 2-3). These data indicate a promising avenue of future research and the utility of the model in the burgeoning field of CTCs.

Animal	CTCs per 100 µl blood	Macroscopic Lung Metastases
1	338	Yes
2	111	Yes
3	95	Yes
4	13	No
5	11	No
6	11	No
7	2	No

Table 2-3. Number of circulating tumor cells (CTCs) correlates with lung metastasis phenotype.
CTCs defined as DAPI-, CD45-, YFP^+ cells per 100 µl blood.

This model offers the potential to investigate the molecular mechanisms driving gastric cancer via both the E-cadherin pathways and the RTK/Ras signaling axis, and may also serve as a useful model for testing new therapies targeting both primary gastric cancer and metastatic lesions. Both the rapid progression of gastric cancer and widespread metastases set it apart from other available mouse models of gastric cancer.

CHAPTER 3 E-CADHERIN AS GATEKEEPER TO MUTANT KRAS AND P53 LOSS-DRIVEN GASTRIC CANCER

i. Abstract

Expression of oncogenic *Kras* and loss of *Trp53* is sufficient to drive rapid development of lung cancer (Jackson et al. 2005), pancreatic ductal adenocarcinoma (Bardeesy et al. 2006), squamous cell carcinoma (Caulin et al. 2007), acute myeloid leukemia (Z. Zhao et al. 2010), and undifferentiated pleomorphic sarcoma (Kirsch et al. 2007; Mito et al. 2009) in the mouse. To determine if loss of E-cadherin was necessary for the onset of gastric adenocarcinoma or if oncogenic *Kras* and loss of *Trp53* in gastric parietal cells were sufficient to drive tumorigenesis I generated ACKPY mice with either one or two alleles of wild-type *Cdh1* (E-cadherin). E-cadherin expression significantly increased survival and the gastric tumors that did arise were more focal in nature compared to $Cdh1^{fl/fl}$ mice, suggesting an additional event is necessary for gastric tumorigenesis. Loss of E-cadherin expression was observed in some of these tumors, suggesting that its loss may be necessary for gastric tumorigenesis in this model.

ii. Introduction

Conditional expression of oncogenic *Kras* and *Trp53* deletion have been used to model many types of cancer in the mouse. Expression of oncogenic *Kras* in the pancreas is sufficient to drive carcinogenesis (Hingorani et al. 2003). In the mouse lung, oncogenic *Kras* alone drives adenoma formation that rarely progresses to adenocarcinomas (Johnson

et al. 2001). Addition of *Trp53* loss or mutation accelerates these processes (Jackson et al. 2001; Jackson et al. 2005; Hingorani et al. 2005; Bardeesy et al. 2006). Expression of oncogenic *Kras* alone in the mouse skin (Caulin et al. 2007) and hematopoietic system (I. T. Chan et al. 2004; Braun et al. 2004) results in the development of precancerous lesions, while addition of *Trp53* loss or mutation results in carcinoma and leukemia, respectively (Caulin et al. 2007; Z. Zhao et al. 2010). Finally, expression of oncogenic *Kras* and loss of *Trp53* can also drive a mouse model of undifferentiated pleomorphic sarcoma (Kirsch et al. 2007; Mito et al. 2009) (Table 3-1). Given the sufficiency of oncogenic *Kras* and deletion of *Trp53* to drive tumorigenesis in multiple cell types, I investigated whether *Cdh1* loss was necessary in our ACKPY model to drive carcinogenesis in gastric parietal cells or if expression of oncogenic *Kras* and deletion of *Trp53* were sufficient for the development of gastric adenocarcinoma.

There is evidence in other *Kras/Raf1* mouse models of cancer that loss of *Cdh1* is either required for high penetrance tumorigenesis or that its loss enhances tumorigenesis. Oncogenic *Kras* and *Cdh1* deletion in combination have been shown to increase tumor formation in a liver tumorigenesis model. Though both oncogenic *Kras* and loss of *Cdh1* individually were sufficient to drive tumor formation in a minority of mice, the combination of both lesions resulted in 100% incidence of tumors, higher-grade disease, increased invasiveness, and intrahepatic metastasis (Table 3-2). The authors argued that loss of E-cadherin leads to an epithelial-mesenchymal transition phenotype, up-regulation of stem cell marks, and an increased ERK activation (Nakagawa et al. 2014). In a mutant Raf-driven model of non-small cell lung cancer (NSCLC) the additional loss of E-

cadherin resulted in the progression of adenomas to adenocarcinomas with increased vascularity, invasiveness, and micro-metastasis to local lymph nodes (Table 3-2). They identified β-catenin signaling resulting in increased vascular endothelial growth factor (VEGF) expression as the key mediator of this phenotype (Ceteci et al. 2007).

Model	Genetics	Phenotype	Reference
Lung	*Kras*$^{G12D\text{-}LA}$	Adenoma, Adenocarcinoma	(Johnson et al. 2001)
	Kras$^{G12D\text{-}LA}$ *Trp53*$^{+/-,\ -/-}$	Accelerated progression	
	Adeno-Cre (intra-nasal) *Kras*$^{LSL\text{-}G12D}$	Adenoma, Adenocarcinoma	(Jackson et al. 2001)
	Adeno-Cre (intra-nasal) *Kras*$^{LSL\text{-}G12D}$ *Trp53*$^{fl/+,fl/fl,R172H/+.R172H/fl,R270H/+,R270H/fl}$	Accelerated progression	(Jackson et al. 2005)
Pancreas	*Pdx1-Cre* *Kras*$^{LSL\text{-}G12D}$	PanIN PDAC	(Hingorani et al. 2003)
	Pdx1-Cre *Kras*$^{LSL\text{-}G12D}$ *Trp53*$^{LSL\text{-}R172H/+}$	Accelerated progression	(Hingorani et al. 2005)
	Pdx1-Cre *Kras*$^{LSL\text{-}G12D}$ *Trp53*$^{fl/+,fl/fl}$	Accelerated progression	(Bardeesy et al. 2006)
Skin	*K5.Cre* *Kras*$^{LSL\text{-}G12D}$ *TPA*	Benign Papilloma	(Caulin et al. 2007)
	K5.Cre *Kras*$^{LSL\text{-}G12D}$ *Trp53*$^{LSL\text{-}R172H/+}$ *TPA*	Spindle Cell Carcinoma	
	K5.Cre *Kras*$^{LSL\text{-}G12D}$ *Trp53*$^{fl/fl}$ *TPA*	Squamous Cell Carcinoma	
Blood	*Mx1-Cre* *Kras*$^{LSL\text{-}G12D}$	Myeloproliferative Disorder	(I. T. Chan et al. 2004; Braun et al. 2004)
	LGshp53CreER *Kras*$^{LSL\text{-}G12D}$	Acute Myeloid Leukemia	(Z. Zhao et al. 2010)
Sarcoma	*Adeno-Cre* (intra-muscular) *Kras*$^{LSL\text{-}G12D}$ *Trp53*$^{fl/fl}$	Undifferentiated Pleomorphic Sarcoma	(Kirsch et al. 2007; Mito et al. 2009)

Table 3-1. Oncogenic *Kras* and *Kras/Trp53* driven mouse models of cancer.

Model	Genetic	Phenotype	(Reference)
Liver Hepatocellular Carcinoma (HCC)	*Alb-Cre* $Kras^{LSL-G12D}$	-4/10 with tumors @ 8 mo -dysplastic nodules or well-differentiation HCC	(Nakagawa et al. 2014)
	Alb-Cre $Cdh1^{fl/fl}$	-2/12 with tumors @ 11 mo -HCC (α-fetoprotein^{+})	
	Alb-Cre $Kras^{LSL-G12D}$ $Cdh1^{fl/fl}$	10/10 with tumor @ 8 mo -HCC (α-fetoprotein^{+}) -typical trabecular type type to poorly differentiated type	
Liver Intra-hepatic cholangiocarcinoma (IHCC)	*Alb-Cre* $Kras^{LSL-G12D}$	-1/8 died of IHCC by 75 wks -Died at 36 wks	(O'Dell et al. 2012)
	Alb-Cre $Kras^{LSL-G12D}$ $Trp53^{fl/+}$	-75% died of IHCC by 75 wks -Median Survival 52 wks	
	Alb-Cre $Kras^{LSL-G12D}$ $Trp53^{fl/fl}$	-100% died of IHCC by 30 wks -Median Survival 19 wks	
Lung Non Small Cell Lung Cancer (NSCLC)	*SP-C C-RAF BXB*	-Adenomas by 6 weeks	(Ceteci et al. 2007)
	SP-C-rtTA *Tet-O-Cre* $Cdh1^{fl/fl}$	-No tumors @ 10 mo -Diffuse hyperplasia -Enlarged alveolar spaces -No inflammation	
	SP-C C-RAF BXB *SP-C-rtTA* *Tet-O-Cre* $Cdh1^{fl/fl}$	-Increased tumor volume -Increased vascularity -Increased invasiveness -Micro-metastases	

Table 3-2. *Kras/Raf* and *Cdh1* driven models of cancer.

iii. Results

$Cdh1^{fl/+}$ and $Cdh1^{+/+}$ mice live significantly longer than $Cdh1^{fl/fl}$ mice

The presence of one or two *Cdh1* wild-type alleles dramatically increases survival ($p<0.0001$, Figure 3-1) in comparison to $Cdh1^{fl/fl}$ (ACKPY) mice. Of 37 $Cdh1^{fl/+}$ mice, only 7 died naturally between 67 and 123 days. Similarly, out of 36 $Cdh1^{+/+}$ mice, only 6 died naturally between 72 and 133 days. In comparison, a cohort of 20 $Cdh1^{fl/fl}$ mice survived to endpoint between 64 and 91 days of age. However, theses data are confounded by cutaneous tumors in the remaining 30 $Cdh1^{fl/+}$ mice and 30 $Cdh1^{+/+}$ mice. These large tumors required euthanasia of the mice prior to gastric cancer endpoints.

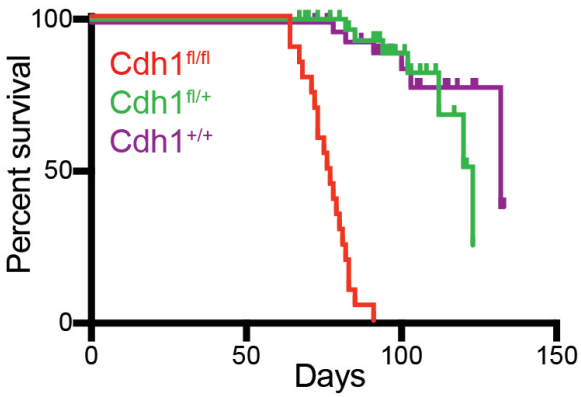

Figure 3-1. Kaplan-Meier curve showing increased survival of *Cdh1*$^{fl/+}$ and *Cdh1*$^{+/+}$ as compared to *Cdh1*$^{fl/fl}$ mice. Mice euthanized for cutaneous tumor are displayed as censored events.

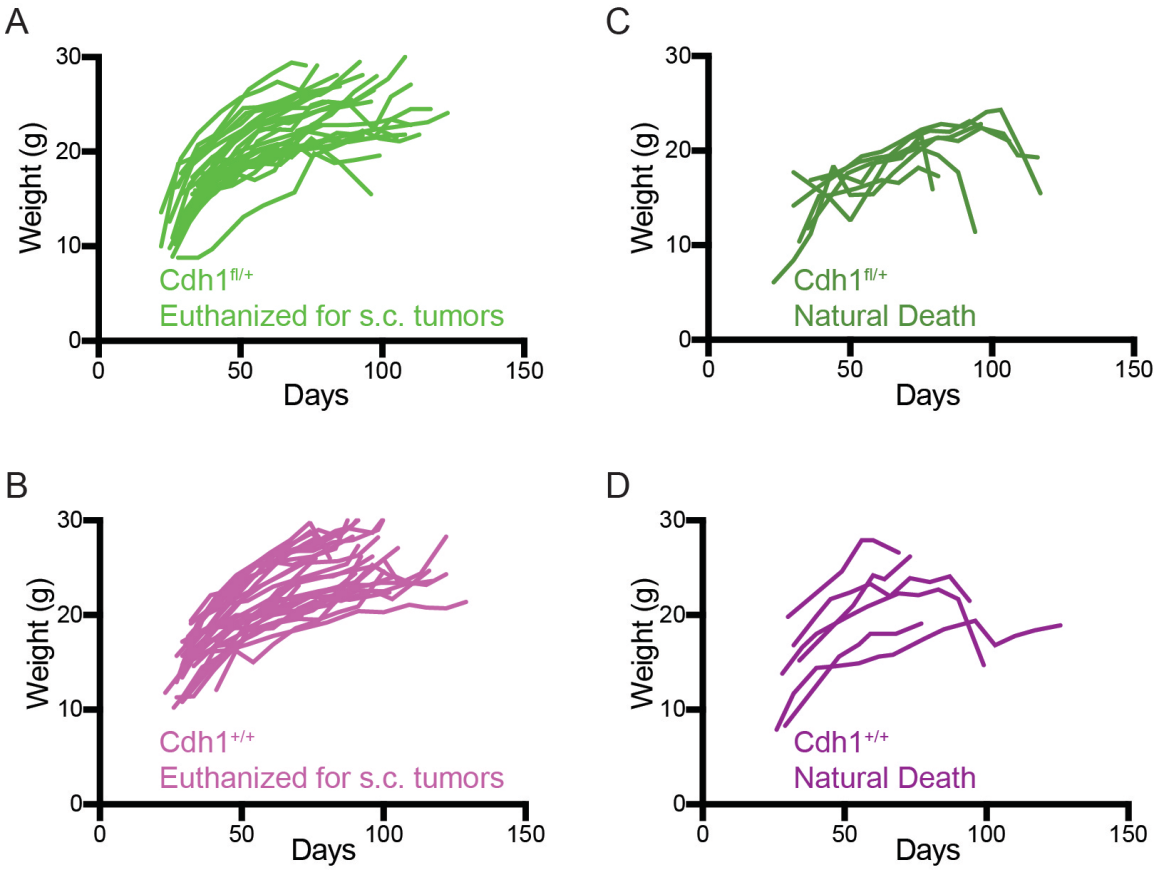

Figure 3-2. Weights of *Cdh1*$^{fl/fl}$, *Cdh1*$^{fl/+}$, and *Cdh1*$^{+/+}$ mice.
(A,B) *Cdh1*$^{fl/+}$ and *Cdh1*$^{+/+}$ mice euthanized for cutaneous tumors, (C,D) *Cdh1*$^{fl/+}$ and *Cdh1*$^{+/+}$ mice that died naturally.

The majority of *Cdh1*$^{fl/+}$ (Figure 3-2A) and *Cdh1*$^{+/+}$ (Figure 3-2B) mice do not undergo the significant weight loss that was observed in gastric cancer-bearing mice on a *Cdh1*$^{fl/fl}$ background. Upon histologic analysis, only 2 of 11 *Cdh1*$^{fl/+}$ mice and 1 of 15 *Cdh1*$^{+/+}$ mice with subcutaneous tumors had histologically detectable stomach tumors. The 7 *Cdh1*$^{fl/+}$ mice and 6 *Cdh1*$^{+/+}$ that died naturally lost weight prior to their death, suggesting that they had developed gastric cancer (Figure 3-2C,D).

Cdh1$^{fl/+}$ and *Cdh1*$^{+/+}$ mice develop subcutaneous tumors

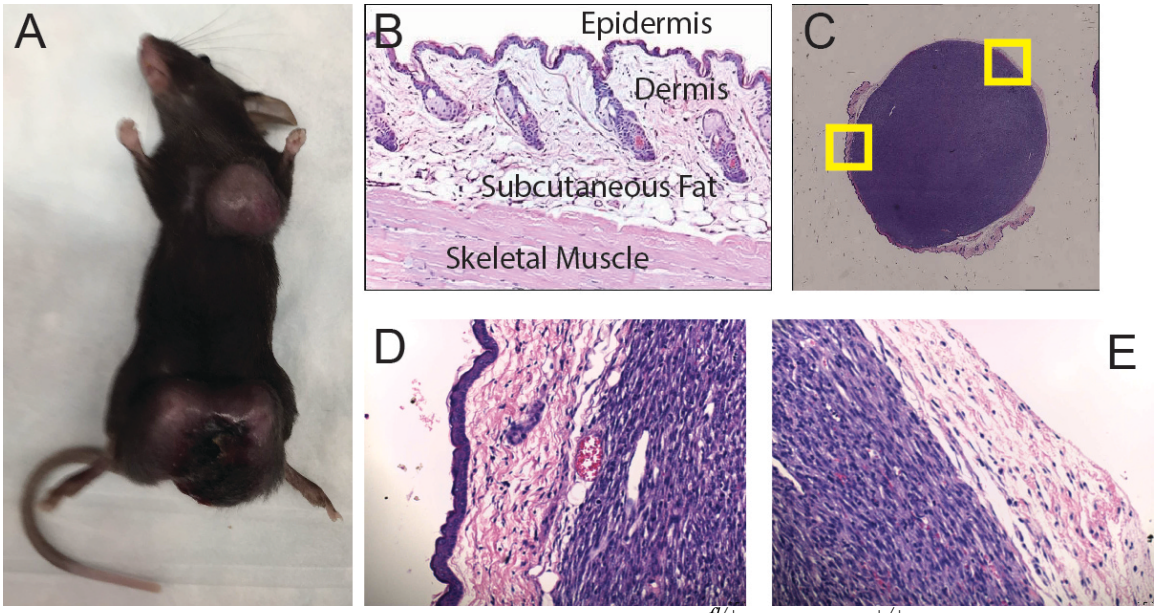

Figure 3-3. Subcutaneous tumors in *Cdh1*$^{fl/+}$ and *Cdh1*$^{+/+}$ mice.
(A) Gross image of a mouse with large tumors on its chest and pelvis, (B) Normal mouse skin histology (http://ctrgenpath.net/), (C) 5x microscopic image of a subcutaneous tumor, (D) 20x detail of compressed epidermis and dermis overlaying the subcutaneous tumor, (E) 20x detail of thinned skeletal muscle underlying the subcutaneous tumor.

ACKPY mice with one (*Cdh1*$^{fl/+}$) or two (*Cdh1*$^{+/+}$) copies of wild-type *Cdh1* developed cutaneous tumors throughout their bodies that necessitated euthanasia of the animals prior to gastric cancer defined endpoints due to the inability of the mice to ambulate (Figure 3-3A). Analysis of more *Cdh1*$^{fl/fl}$ mice revealed the occurrence of these

tumors at a rate of approximately one in twenty. These cutaneous tumors arise in the subcutaneous fat; they (Figure 3-3BC) were covered by epidermis and dermis (Figure 3-3D) and overlaid skeletal muscle (Figure 3-3E). Initial characterization revealed sarcomatoid histology.

Cdh1$^{fl/+}$ stomach tumors are more focal and display sarcomatoid features

Although stomachs isolated from *Cdh1*$^{fl/+}$ and *Cdh1*$^{+/+}$ mice are enlarged and hyperplastic (Figure 3-4C and A), the majority do not harbor tumors. When these mice develop gastric tumors, they are more focal in nature (Figure 3-4D), unlike the widespread tumors identified in *Cdh1*$^{fl/fl}$ stomachs (Figure 3-4B). This suggests that a secondary event is occurring that is necessary for tumorigenesis to occur at these sites. This event could be genetic, epigenetic, pathway upregulation, or other biological processes that lead to carcinogenesis. Histologically, *Cdh1*$^{fl/+}$ tumors are mixed-type gastric cancer with sarcomatoid features.

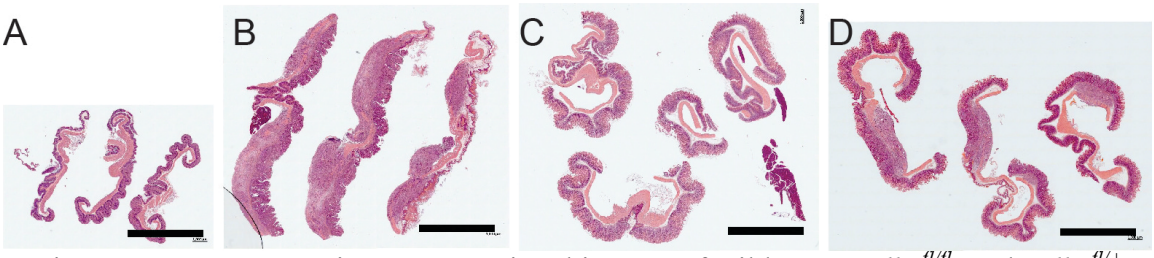

Figure 3-4. Representative cross-sectional images of wild-type, *Cdh1*$^{fl/fl}$, and *Cdh1*$^{fl/+}$ stomachs.
(A) wild-type, (B) *Cdh1*$^{fl/fl}$, (C) *Cdh1*$^{fl/+}$ without tumor, and (D) *Cdh1*$^{fl/+}$ with tumor (scale bars = 5 mm).

Loss of E-cadherin Expression in *Cdh1*$^{fl/+}$ Stomach Tumors

We hypothesized that the event occurring in these rare, focal, *Cdh1*$^{fl/+}$ stomach tumors might be loss of E-cadherin. E-cadherin expression was examined by

immunofluorescent (IF) staining. E-cadherin is present in wild-type gastric epithelium (Figure 3-5A). Similarly, E-cadherin expression is preserved in gastric tissue from *Cdh1*$^{fl/+}$ stomachs that lack tumors (Figure 3-5C) and in normal tissue of tumor bearing *Cdh1*$^{fl/+}$ mice (Figure 3-5D). However, in tumors of *Cdh1*$^{fl/+}$ mice, E-cadherin expression is absent or variable (Figure 3-5E). As expected, E-cadherin is absent in recombined cells (YFP^{+}) in *Cdh1*$^{fl/fl}$ stomachs, but present in adjacent normal (YFP^{-}) tissue (Figure 3-5B).

Two primary cell lines were derived from independent *Cdh1*$^{fl/fl}$ stomachs and two lines were derived from independent *Cdh1*$^{fl/+}$ stomachs. Neither of the cell lines derived from *Cdh1*$^{fl/fl}$ stomachs expressed E-cadherin by Western blot. However, only one of the two *Cdh1*$^{fl/+}$ gastric cancer cell lines expressed E-cadherin by Western blot (data not shown). These data suggest that the hypothetical secondary event leading to tumor formation in *Cdh1*$^{fl/+}$ mice may be the loss of E-cadherin in some cases.

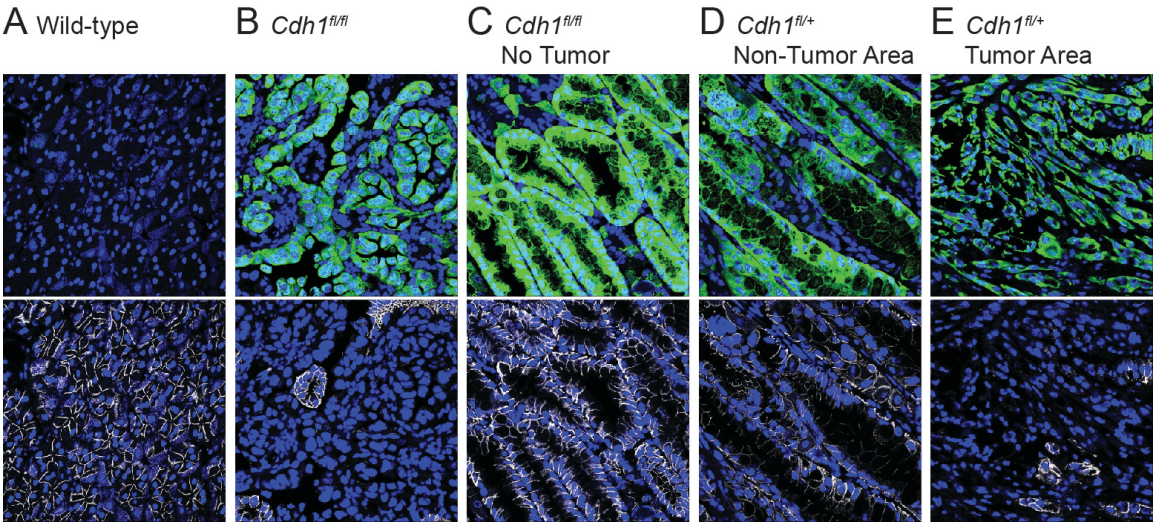

Figure 3-5. Representative immunofluorescent images of E-cadherin expression (white) counter-stained with DAPI (blue) and for YFP (green).

Cdh1 loss in a model of lung adenocarcinoma suppresses tumorigenesis

To determine whether E-cadherin loss accelerates tumorigenesis in all tissues, I examined whether *Cdh1* loss is necessary for lung cancer development. We administered adenoviral Cre intratracheally to Cre negative $Cdh1^{fl/fl}$ (CKPY) and $Cdh1^{fl/+}$ mice to trigger oncogenic *Kras* activation, *Trp53* loss with and without loss of *Cdh1* in the lungs (Johnson et al. 2001; Jackson et al. 2001; Jackson et al. 2005). Examination of lungs 12 weeks post infection demonstrated a decrease in overall tumor burden in $Cdh1^{fl/fl}$ mice compared to $Cdh1^{fl/+}$ mice (Figure 3-6, p=0.02). This is in marked contrast to the dramatic increase in tumor burden observed in the stomach.

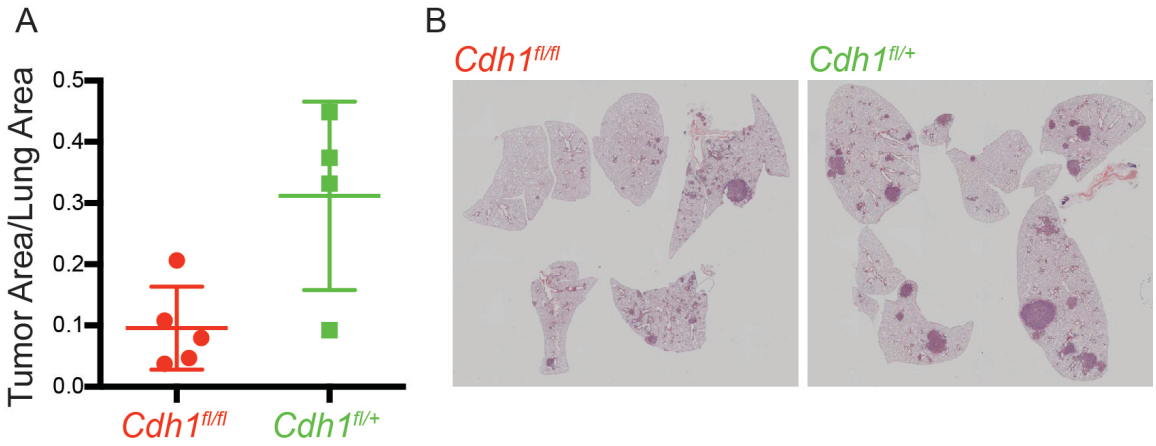

Figure 3-6. $Cdh1^{fl/fl}$ vs $Cdh1^{fl/+}$ lung adenocarcinoma.
(A) Tumor to lung ratio for $Cdh1^{fl/fl}$ (n=5) vs $Cdh1^{fl/+}$ (n=4), error bars represent standard deviation. (B) Representative images of $Cdh1^{fl/fl}$ and $Cdh1^{fl/+}$ lungs.

Subcutaneous tumors are more similar to sarcomas than gastric cancers

I wished to determine if these sarcomatoid subcutaneous tumors arising in $Cdh1^{fl/+}$ and $Cdh1^{+/+}$ mice were primary sarcomas of the skin or metastatic lesions from the stomach. Though most of the mice in which subcutaneous tumors arose lacked detectable gastric tumors one could not rule out the possibility of small, unidentified

gastric tumors that metastasized to the subcutaneous space. One could also not rule out the possibility that these lesions were the result of off target Cre activation in the subcutaneous space resulting in sarcoma formation. Microarray expression data from glandular stomach tissue and subcutaneous metastasis tissue from four independent *Cdh1*$^{fl/+}$ mice was examined.

Initially, I analyzed the expression of the top 10 stomach enriched genes as annotated by The Human Protein Atlas (Uhlén et al. 2015). Though only *Gkn1* and *Muc5ac* expression were statistically significant in their differential expression, there is a clear trend toward lower expression of stomach specific genes in the subcutaneous tumors.

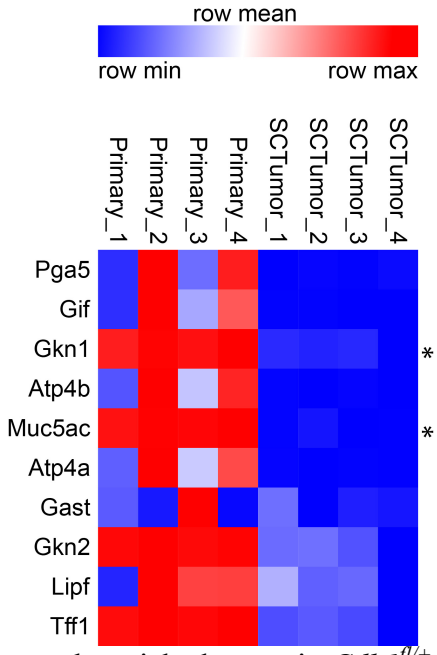

Figure 3-7. Expression of stomach enriched genes in *Cdh1*$^{fl/+}$ stomachs and subcutaneous tumors.

Next, I compared two publically available microarray expression data sets from the Gene Expression Omnibus (Edgar, Domrachev, and Lash 2002): GSE15459, 200

primary gastric tumors from the Singapore patient cohort (Ooi et al. 2009), and GSE21050, 310 soft tissue sarcomas from the French Sarcoma Group (Chibon et al. 2010). By comparing these data sets, I selected the top 25 genes that were more highly expressed in the gastric cancers and the top 25 genes that were more highly expressed in the sarcomas.

Using this set of 50 genes that differentiates between sarcomas and gastric cancers, I performed hierarchical clustering analysis on the expression data from our $Cdh1^{fl/+}$ stomach and subcutaneous tumor microarrays. I found that the stomach samples and the subcutaneous tumor samples formed distinct clusters. Further, the 25 genes more highly expressed in gastric cancers were more highly expressed in the stomach samples and the 25 genes more highly expressed in sarcomas were, for the most part, more highly expressed in the subcutaneous tumors (Figure 3-8, Figure 3-9).

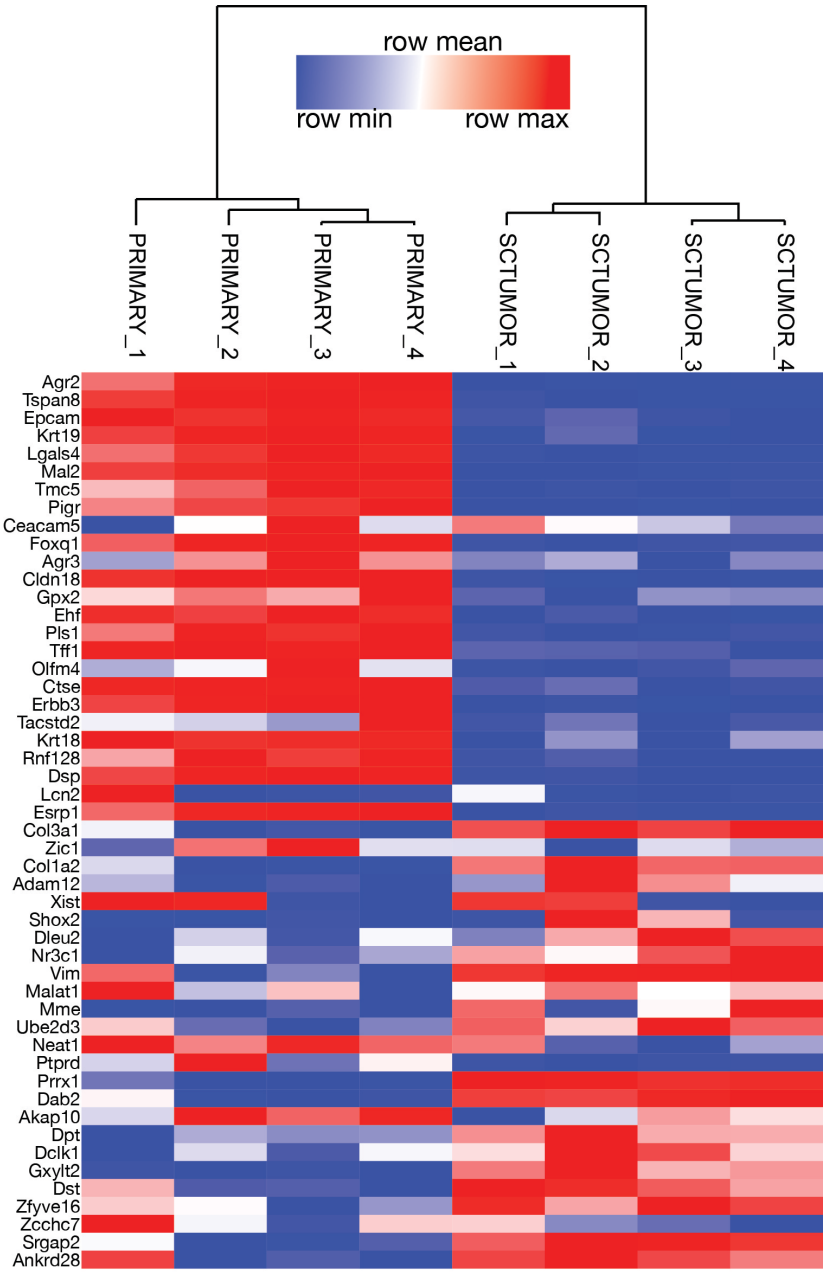

Figure 3-8. Hierarchical clustering of *Cdh1*$^{fl/+}$ stomach and subcutaneous tumor samples based on 50 genes that differentiate between gastric cancer and sarcomas.

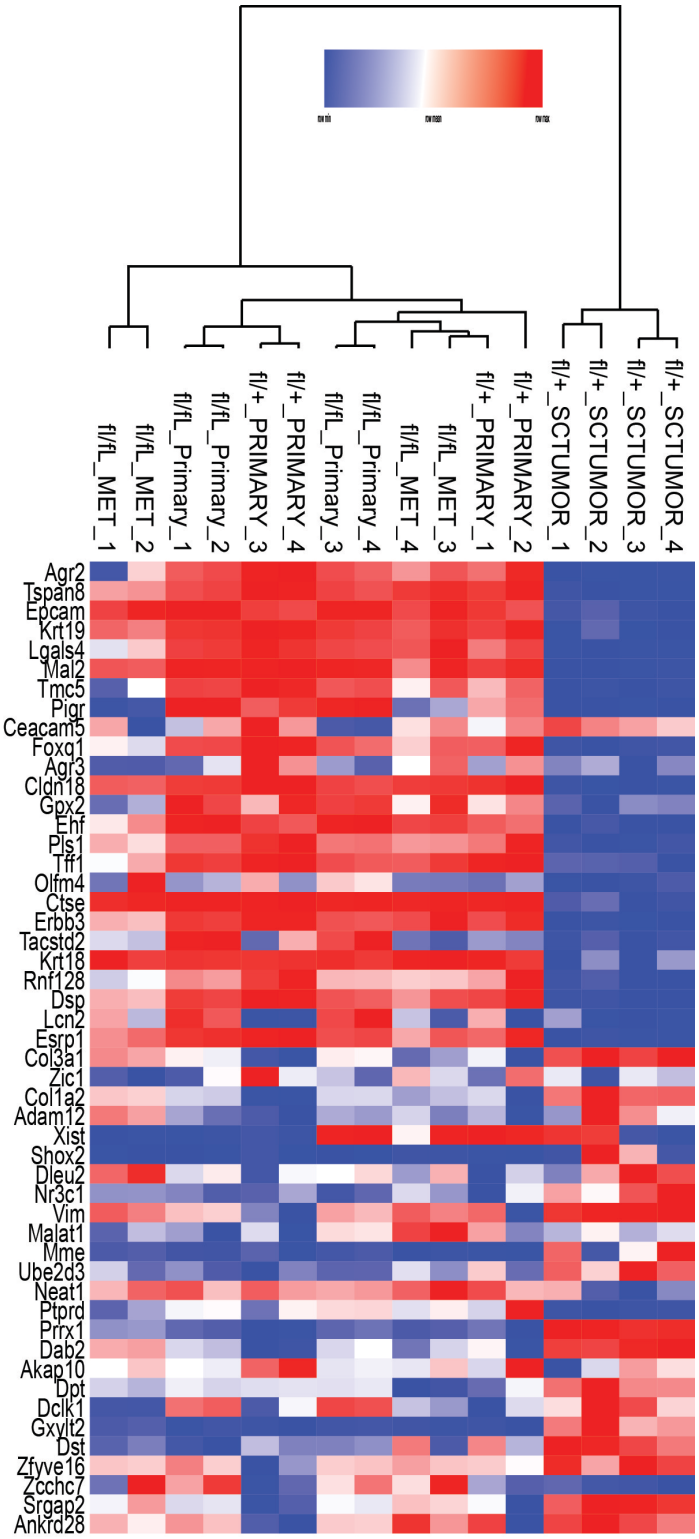

Figure 3-9. Hierarchical clustering, for 50 genes that differentiate between gastric cancer and sarcomas, of *Cdh1*$^{fl/+}$ stomachs and subcutaneous tumors as well as *Cdh1*$^{fl/fl}$ stomachs and metastases.

iv. Discussion

E-cadherin as the gatekeeper to mutant *Kras* and *Trp53* loss-driven gastric cancer

Though E-cadherin is well known in cancer biology as an "invasion suppressor gene" (Birchmeier, Hülsken, and Behrens 1995; Pećina-Slaus 2003), here we demonstrate its role as a suppressor of primary tumorigenesis. In gastric parietal cells, despite the strong oncogenic stimulus of mutant *Kras* and *Trp53* loss, E-cadherin expression dramatically decreases tumorigenesis. From these data we can definitively say that *Cdh1* loss cooperates with oncogenic *Kras* expression and loss of *Trp53* to promote primary tumor formation. The observed loss of E-cadherin expression in the tumors that arise in $Cdh1^{fl/+}$ mice suggests that E-cadherin is a gatekeeper to tumorigenesis in gastric parietal cells.

This function, however, appears to be somewhat specific to gastric parietal cells. In our model of lung adenocarcinoma, loss of E-cadherin reduced primary tumor formation. Of note, this is in contrast to the mutant *C-raf* driven model of lung cancer where *Cdh1* loss accelerated tumorigenesis (Table 3-2). However, this is a poor comparison for two reasons: (1) the *C-raf* model had wild-type *Trp53* and (2) oncogenic *C-raf* only models activation of one of the many pathways downstream of *Kras* (as I will discuss in Chapter 5). As discussed, the oncogenic Kras liver cancer model also displays synergy between oncogenic *Kras* and loss of *Cdh1* (Nakagawa et al. 2014). However, loss of *Trp53* paired with oncogenic Kras in the liver also accelerates tumor formation and is not dependent on *Cdh1* loss as we see here (O'Dell et al. 2012).

This gatekeeper function of a tumor suppressor gene in the face of mutant *Kras* and *Trp53* loss is not without precedent. Recently, a similar phenomenon has been observed with the adenomatous polyposis coli (*Apc*) tumor suppressor in colorectal cancer (Dow et al. 2015). They showed that *Apc* knock-down in $Lgr5^{+}$ colon cells led to adenoma formation that was reversible with *Apc* restoration. They could drive adenocarcinoma development with the addition of oncogenic *Kras* expression and *Trp53* loss. However, even these adenocarcinomas regressed with restoration of *Apc*.

APC is an important member of the canonical Wnt pathway; though not directly involved in the enzymatic modification of β-catenin, it is crucial in facilitating its destruction and regulation through a variety of mechanisms (Mohammed et al. 2016). Similarly, E-cadherin binds and sequesters β-catenin at adherens junctions. Presumably, loss of either would lead to increased β-catenin signaling which may be crucial for mutant *Kras* and *Trp53* loss-driven oncogenesis in both gastric parietal cells and $Lgr5^{+}$ colon stem cells.

Off target Cre activation results in subcutaneous sarcomas

The presence of subcutaneous tumors in the majority of $Cdh1^{fl/+}$ and $Cdh1^{+/+}$ mice as well as rarely in $Cdh1^{fl/fl}$ mice raises the question: are they independent tumors arising in the subcutaneous space or metastases derived from gastric cancers arising in these mice? These sarcomatoid lesions could be arising independently as a result of off target Cre expression driving expression of oncogenic *Kras* and loss of *Trp53* in a rare skin cell population that expresses *Atp4b* for unknown reasons. It is well described that oncogenic *Kras* and loss of *Trp53* is sufficient to drive sarcomagenesis in the mouse with

a latency of 56 to 117 days (median 79 days) (Kirsch et al. 2007). This latency is strikingly similar to the age at which the subcutaneous tumors appear in our mice.

The lack of detectable gastric cancer in the majority of the *Cdh1*$^{fl/+}$ and *Cdh1*$^{+/+}$ would suggest that the subcutaneous tumors arise independent of gastric tumorigenesis. However, we cannot rule out the possibility of small gastric lesions that we are not detecting that are metastasizing. Further, the reported specificity of the *Atp4b-Cre* to gastric parietal cells would argue against off-target activation. No specific data is available on Cre specificity in the Atp4b-Cre strain I used (Syder et al. 2004), however data is available on a similar strain produced by another group (Zengming Zhao et al. 2010). This group mated their strain to a conditional Smad4 allele and screened a panel of tissues including skin for recombination. They only detected recombination in the stomach. The Human Protein Atlas has immunohistochemical staining data of a variety of tissues using two independent antibodies to ATP4B. They only detected expression in gastric parietal cells and not the skin ("The Human Protein Atlas: ATP4B," n.d.; Uhlén et al. 2015).

However, this does not rule out a very rare cell population that was not represented in their samples, expresses ATP4B at a level bellow their level of detection, or a species-specific cell population in the skin of mice that expresses ATP4B. Further, a hypothetical cell population may have sufficient activity at the transgenic *Atp4b* promoter to drive *Cre* expression but insufficient activity at the endogenous *Atp4b* promoter (due to other regulatory elements) to express ATP4B.

Recent work has shown that the majority of stringently tested targeted Cre strains have unreported off-target activities (Heffner et al. 2012). In addition, the gene expression analysis I performed comparing the stomachs of *Cdh1*$^{fl/+}$ mice to their subcutaneous tumors strongly suggests these tumors have an expression profile more consistent with sarcomas than with gastric-derived metastases. The subcutaneous tumors can be differentiated from the stomachs based on genes specific to sarcomas versus gastric cancers (Figure 3-8) and stomach-enriched genes (Figure 3-7).

Finally, assuming the *Cdh1*$^{fl/+}$ sub-cutaneous tumors are sarcomas arising from rare Cre expression in a mesenchymal skin cell, one would expect these tumors to arise in *Cdh1*$^{fl/fl}$ mice as well given that they use the same Atp4b-Cre transgene. In fact, subcutaneous tumors are rarely observed in the *Cdh1*$^{fl/fl}$ mice at a rate of about 1 in 20. As the subcutaneous tumors typically arise at approximately 3 months of age in the *Cdh1*$^{fl/+}$ mice, one would only expect them to be seen in *Cdh1*$^{fl/fl}$ mice that live to this age. However, median survival of *Cdh1*$^{fl/fl}$ mice is 76.5 days, to young to see subcutaneous tumors arise in the majority of these mice.

CHAPTER 4 E-CADHERIN LOSS UPREGULATES B-CATENIN SIGNALING IN THE ACKPY MOUSE MODEL OF GASTRIC CANCER

i. Abstract

E-cadherin has been shown to bind and inhibit the oncogenic function of β-catenin (Gottardi, Wong, and Gumbiner 2001). Several groups have previously demonstrated that loss or mutation of E-cadherin alone does not increase β-catenin signaling in gastric and pancreatic cancer cells (Caca et al. 1999), breast cancer cells (van de Wetering et al. 2001) or β-cell tumors (Herzig et al. 2007) . However, in our model of gastric cancer, E-cadherin loss drives β-catenin activation and inhibition of β-catenin signaling prolonged survival of our ACKPY mice. Given these conflicting results, we must consider the context of this increase in β-catenin signaling in our model. Many studies have demonstrated cross-activation of canonical WNT signaling by the receptor tyrosine kinase (RTK)/Ras/mitogen-activated protein kinase (MAPK) pathway (Zeller et al. 2013). Taken together, these data suggest crosstalk between oncogenic Kras and loss of E-cadherin in our model, wherein oncogenic Kras primes the system by inactivating the β-catenin destruction machinery (Lemieux et al. 2015) and loss of E-cadherin releases β-catenin from sequestration.

ii. Introduction

Canonical WNT signaling, sometimes referred to as the "β-catenin dependent" pathway, results in β-catenin translocation to the nucleus and upregulation of target genes. The amount of free β-catenin is tightly regulated in the cell by phosphorylation, ubiquitination, and proteasomal degradation. In the absence of WNT ligands, free β-

catenin is bound and phosphorylated by a complex consisting of Axin, Adenomatous polyposis coli (APC), Casein kinase 1 alpha (CK1α), and glycogen synthase kinase 3β (GSK3β). Phosphorylated β-catenin is recognized and ubiquitinated by the E3 ligase β-transducin repeat-containing protein (β-TrCP) targeting β-catenin for proteasomal degradation (Figure 4-1A). When WNT ligands are present, they bind to the Frizzled(FZ)/Low-density lipoprotein receptor-related protein 5/6 (LRP5/6) receptor complex, leading to dissociation of the Axin/APC/CK1α/GSK3β destruction complex. This is achieved by the binding of Dishevelled (Dvl) to the ligand-bound Fz/LRP5/6 receptor complex, which leads to the phosphorylation of LRP5/6 and binding of Axin to the receptor complex. Dissociation of the destruction complex prevents phosphorylation of β-catenin, results in its accumulation, and subsequent translocation to the nucleus. In the nucleus, it binds the T-cell factor (TCF)/lymphoid enhancing factor (LEF) transcription factor complex, displacing negative regulator Groucho, and activating transcription of target genes (Figure 4-1B) (Chiurillo 2015).

Canonical WNT signaling has long been implicated in the development of gastric cancer. Many studies have shown increased expression or activating mutation of positive WNT regulators and decreased expression or inactivating mutation of WNT repressors in gastric cancer samples and cell lines (Chiurillo 2015). Several studies have demonstrated that *H. pylori* can also upregulate canonical WNT signaling (Song et al. 2015). Relevant to the model I present here, E-cadherin has long been known to bind cytoplasmic β-catenin and suppress its oncogenic activity by sequestering it in the cadherin-catenin complex (Gottardi, Wong, and Gumbiner 2001). It has been suggested, but not shown,

that reciprocal regulation occurs; that loss of E-cadherin can lead to increased oncogenic transformation through release of free β-catenin (Gottardi, Wong, and Gumbiner 2001; Liu et al. 2014; Chiurillo 2015). Here I present the first direct evidence demonstrating that loss of E-cadherin, at least in the context of oncogenic *Kras* and loss of *p53* in gastric parietal cells, is sufficient to increase β-catenin signaling.

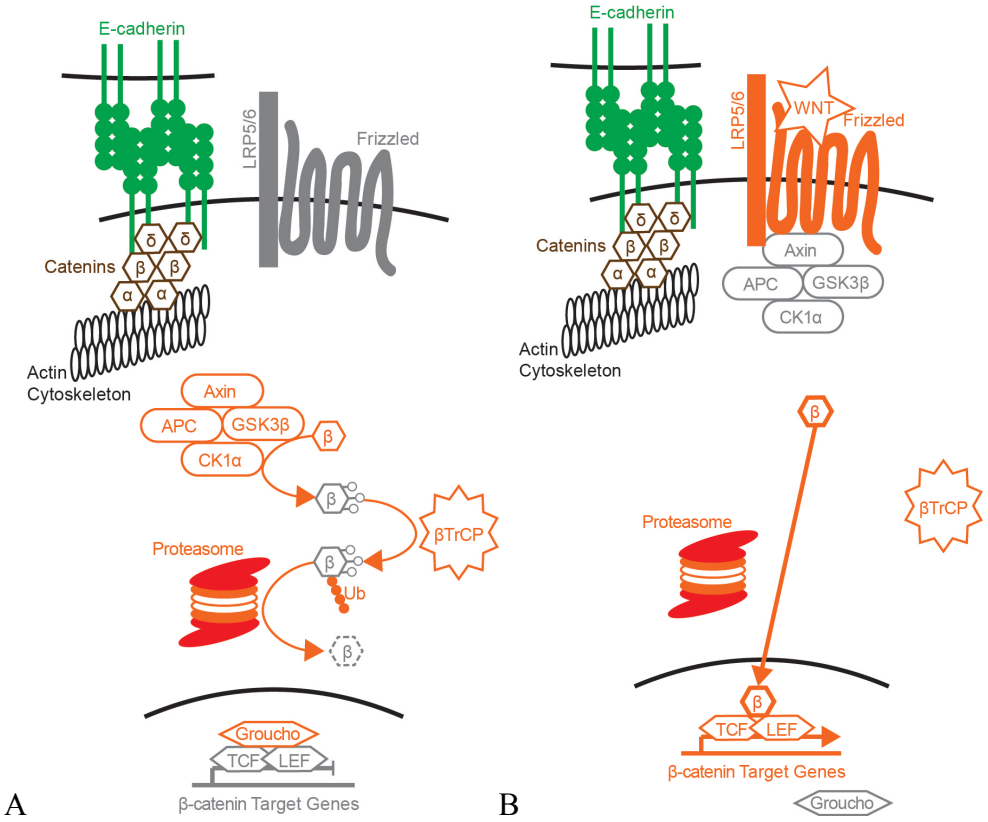

Figure 4-1. Canonical WNT pathway.
(A) WNT ligand absent. (B) WNT ligand present)

Results

Microarray reveals upregulation of TCF/LEF targets with E-cadherin loss

To identify differential gene expression in our model of gastric cancer, I performed a microarray on glandular stomach tissue from four independent $Cdh1^{fl/fl}$ and $Cdh1^{fl/+}$ mice. Principal components analysis revealed two clusters: one that contained 3

of the *Cdh1*$^{fl/+}$ stomachs and a second that contained all 4 of the *Cdh1*$^{fl/fl}$ stomachs. One of the *Cdh1*$^{fl/+}$ stomachs did not fall distinctly within either of these groups but was closer to the *Cdh1*$^{fl/fl}$ stomachs (Figure 4-2A). Unsupervised hierarchical clustering analysis indicates that the single outlier *Cdh1*$^{fl/+}$ stomach sample clustered more closely to *Cdh1*$^{fl/fl}$ stomachs rather than *Cdh1*$^{fl/+}$ stomachs (Figure 4-2B). One interpretation of these data suggests that this *Cdh1*$^{fl/+}$ outlier contained a rare *Cdh1*$^{fl/+}$ tumor and thus clusters closer to the *Cdh1*$^{fl/fl}$ tumor containing stomachs than the other, tumor free, *Cdh1*$^{fl/+}$ stomachs. This data correlates with the 1 in 4 frequency of stomach tumors observed in *Cdh1*$^{fl/+}$ mice. Microarray data from the *Cdh1*$^{fl/+}$ outlier was removed from future analysis due to the likely presence of a stomach tumor.

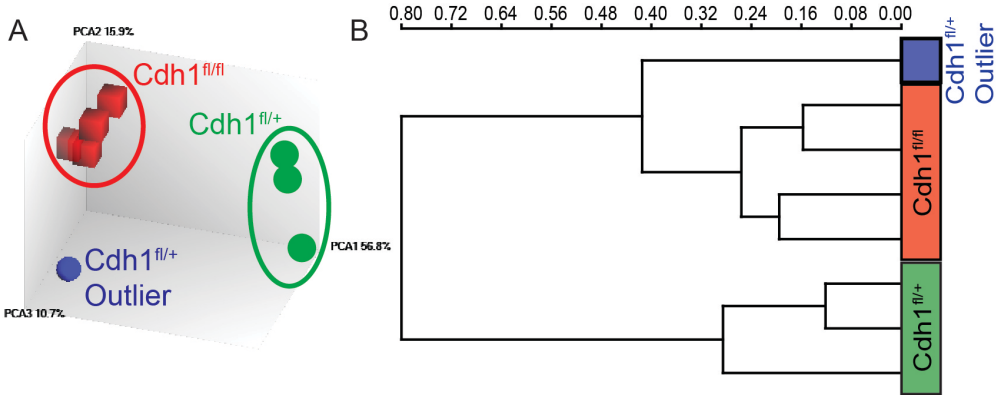

Figure 4-2. Principal component analysis and unsupervised hierarchical clustering analysis of microarray data from *Cdh1*$^{fl/fl}$ and *Cdh1*$^{fl/+}$ stomachs.

To determine which pathways were differentially regulated between the two genotypes, I performed gene set overlap analysis (Subramanian et al. 2005) on genes upregulated in the *Cdh1*$^{fl/fl}$ stomachs versus *Cdh1*$^{fl/+}$ stomachs and a publicly available data set of transcription factor target gene sets. The first hit was a set of genes containing a LEF1 binding site in their promoters, and the sixth was a set of genes containing the

TCF3 binding site (Table 4-1). Further, when genes upregulated in *Cdh1*$^{fl/fl}$ versus *Cdh1*$^{fl/+}$ stomachs were compared to oncogenic signature gene sets, the results contained several genes sets whose upregulation resulted from expression of LEF1, WNT1, and CTNNB1 (Table 4-1). All these data are consistent with an up-regulation of β-catenin target genes.

Name	Description	FDR q-value
	Transcription Factor Target Gene Sets	
CTTTGT_V$LEF1_Q2	Genes with promoter regions containing the LEF1 motif	3.27 e^{-87}
CAGGTG_V$E12_Q6	Genes with promoter regions containing the TCF3 motif	1.44 e^{-58}
	Oncogenic Signature Gene Sets	
LEF1_UP.V1_UP	Upregulated in DLD1 cells over-expressing LEF1	2.86 e^{-19}
WNT_UP.V1_UP	Upregulated in C57MG cells over-expressing WNT1	1.42 e^{-8}
BCAT.100_UP.V1_UP	Upregulated in HEK293 cells expressing active CTNNB1	3.83 e^{-8}

Table 4-1. Selected results from Gene Set Overlap Analysis comparing genes overexpressed in *Cdh1*$^{fl/fl}$ vs. *Cdh1*$^{fl/+}$ to transcription factor target gene sets and oncogenic signature gene sets.

Validation of β-catenin target gene regulation by E-cadherin

To validate the microarray data, I analyzed RNA isolated from stomachs of other *Cdh1*$^{fl/fl}$ and *Cdh1*$^{fl/+}$ mice for expression of several canonical WNT/β-catenin target genes: MYC (He et al. 1998), CCND1 (McCormick and Tetsu 1999; Shtutman et al. 1999), AXIN2 (Yan et al. 2001; Lustig et al. 2002; Jho et al. 2002), LEF1 (Hovanes et al. 2001; Filali et al. 2002; T. W.-H. Li et al. 2006), CD44 (Wielenga et al. 1999; Zeilstra et al. 2008), MMP7 (Crawford et al. 1999; Brabletz et al. 1999). All genes were significantly upregulated in *Cdh1*$^{fl/fl}$ compared to *Cdh1*$^{fl/+}$ stomach tissues.

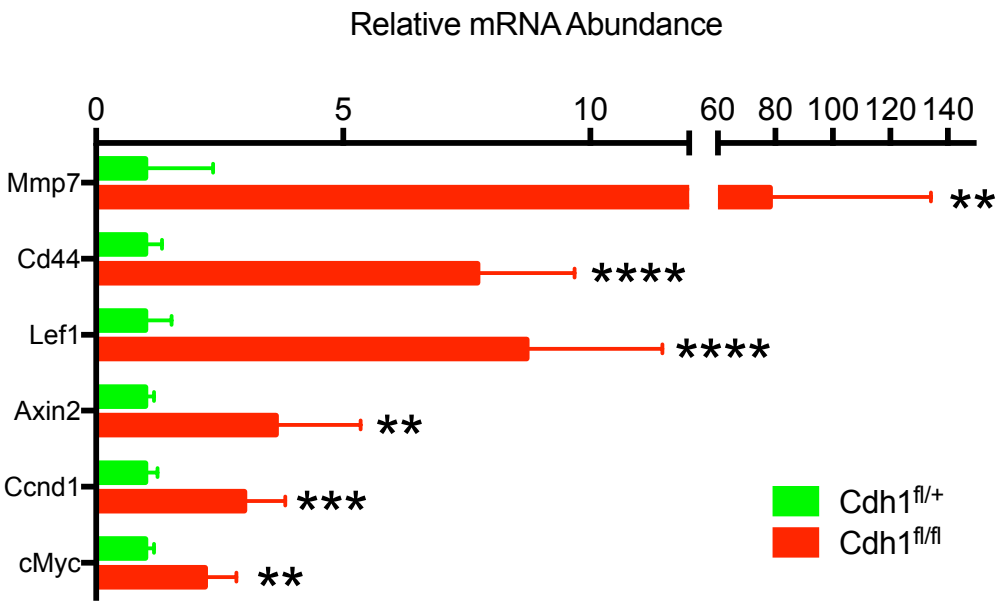

Figure 4-3. qPCR validated upregulation of WNT/β-catenin targets in *Cdh1*$^{fl/fl}$ over *Cdh1*$^{fl/+}$ stomachs.

Loss of membranous β-catenin in *Cdh1*$^{fl/fl}$ and *Cdh1*$^{fl/+}$ tumors mirrors loss of E-cadherin

β-catenin is normally sequestered at the plasma membrane by E-cadherin. To test if loss of E-cadherin alters the subcellular localization of β-catenin, I co-immunostained *Cdh1*$^{fl/fl}$ and *Cdh1*$^{fl/+}$ stomachs with and without tumors for E-cadherin, β-catenin, and YFP. As expected, a wild-type control stomach lacked YFP but expressed E-cadherin and β-catenin that were localized to the plasma membrane (Figure 4-4A, white arrows). Conversely, *Cdh1*$^{fl/fl}$ stomachs showed loss of expression of E-cadherin and β-catenin in YFP^{+} tumors (Figure 4-4B, yellow arrows), but expression patterns were normal in YFP^{-} areas (Figure 4-4B, white arrows).

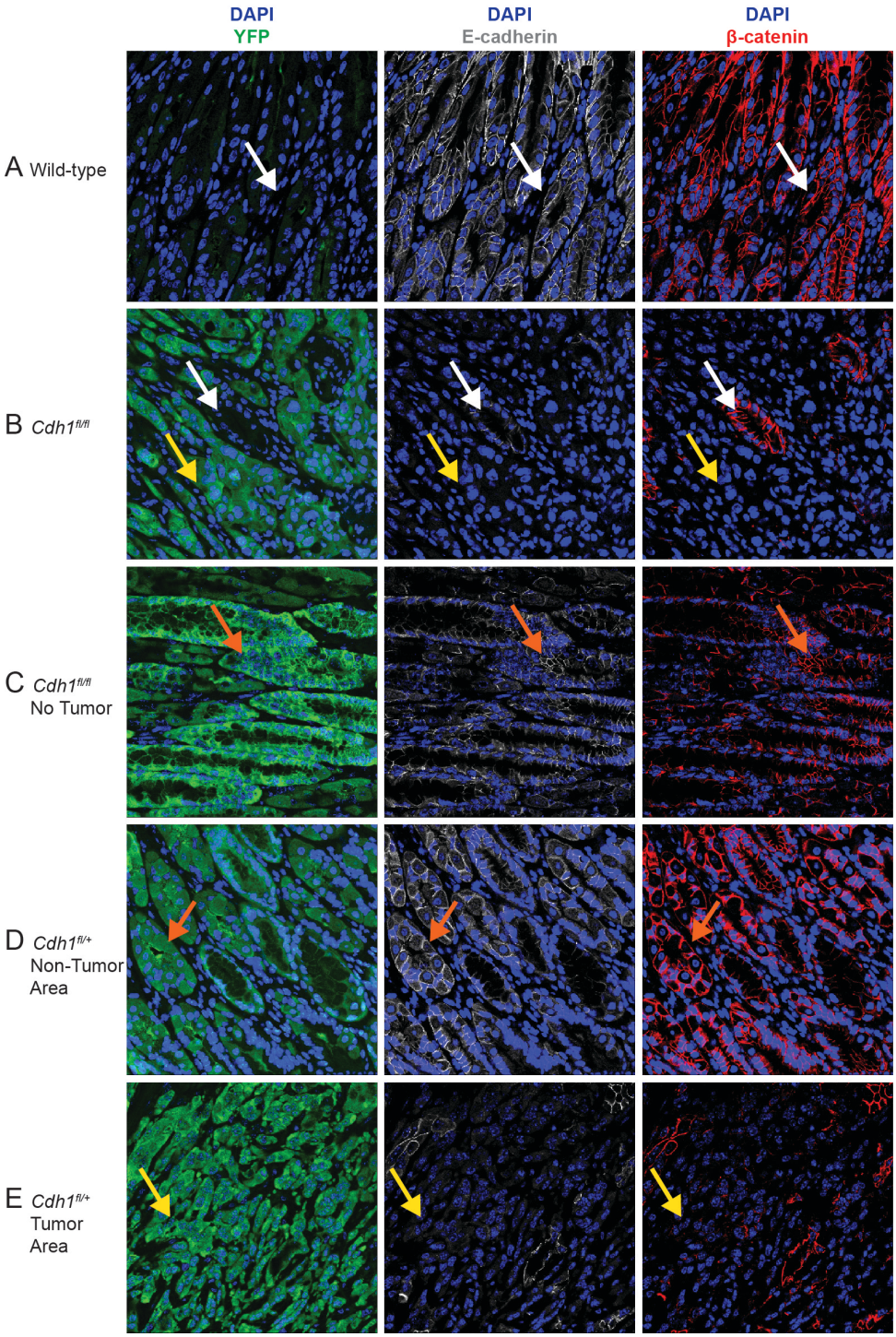

Figure 4-4. Representative images showing loss of membranous β-catenin in *Cdh1*$^{fl/fl}$ and *Cdh1*$^{fl/+}$ tumors.

(White arrows) Retained E-cadherin and β-catenin in YFP negative areas. (Yellow arrows) Lost E-cadherin and β-catenin in YFP positive tumor areas. (Orange arrows) Retained E-cadherin and β-catenin in YFP positive non-tumor areas.

The *Cdh1*$^{fl/+}$ stomach without a tumor (Figure 4-4C) and the normal area of a *Cdh1*$^{fl/+}$ stomach with a tumor (Figure 4-4D) retained expression of E-cadherin and β-catenin throughout (Figure 4-4, orange arrows). In contrast to the benign regions, the tumor area of the *Cdh1*$^{fl/+}$ stomach displayed loss of membranous expression of E-cadherin and β-catenin (Figure 4-4E, yellow arrows).

Inhibition of β-catenin/TCF signaling increases survival of ACKPY mice

To test the necessity of β-catenin signaling in our ACKPY gastric cancer mouse model, I treated mice with the β-catenin/TCF complex inhibitor PKF118-310. Though the effect size is small, mice treated with the inhibitor had a statistically significant (p=0.04) 6-day increase in median survival (78 days) over vehicle treated mice (72 days).

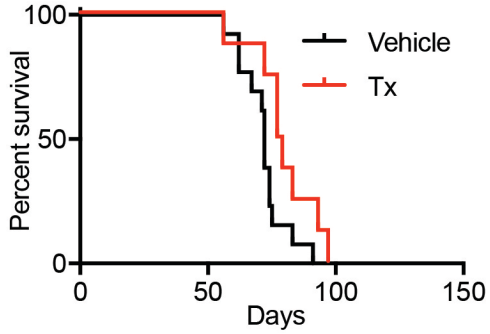

Figure 4-5. Kaplan-Meier curve showing increased survival with PKF118-310 treatment. Beginning at 4-weeks of age, mice were injected 3x per week with 1 mg/kg PKF118-310 (red, n=8) or a volumetrically equivalent does of 0.1% DMSO vehicle (black, n=13) intra-peritoneally.

Activation of β-catenin with LiCl did not promote tumorigenesis in *Cdh1*$^{fl/+}$ mice

To determine if β-catenin activation was sufficient to drive tumorigenesis in *Cdh1*$^{fl/+}$ mice, I treated them with the GSK3β inhibitor lithium chloride (LiCl). GSK3β is a key component of the degradation complex that phosphorylates β-catenin and targets it for ubiquitination and proteasomal degradation. Inhibition or loss of GSK3β leads to

increased free β-catenin that can translocate to the nucleus, bind TCF/LEF, and transcribe targets. My preliminary data suggest no difference in stomach tumor incidence between LiCl treated *Cdh1*$^{fl/+}$ mice and vehicle treated *Cdh1*$^{fl/+}$ mice (data not shown). However, interpretation of these data is limited as we were not able to confirm efficacy of the inhibition by assaying for destruction complex activity.

iii. Discussion

Though it has long been hypothesized that E-cadherin loss would lead to upregulation of β-catenin signaling, several studies have shown that this may not be the case. For example, cancer cell lines with deletion (Caca et al. 1999) or mutation (van de Wetering et al. 2001) of E-cadherin did not show constitutive β-catenin/TCF/LEF signaling. Further, in the Rip1Tag2 model of β-cell carcinogenesis, E-cadherin loss is rate-limiting. However, it has been shown that this loss does not upregulate β-catenin target genes and cannot be phenocopied by forced activation of TCF or β-catenin transcriptional activity (Herzig et al. 2007). Taken together, these data suggest that though loss of E-cadherin may release β-catenin from sequestration, the nuclear activity is still inhibited by a functional destruction complex (Jeanes, Gottardi, and Yap 2008).

Here we show that loss of E-cadherin is sufficient to drive increased β-catenin/TCF/LEF signaling in our model and that this signaling is important to the survival phenotype. However, the status of the β-catenin destruction complex is not known. Given the data suggesting E-cadherin loss alone is not sufficient to drive β-catenin signaling, we must consider the hypothesis that other manipulation in our model may be affecting the destruction complex.

In fact, many studies have shown significant crosstalk between the RTK/Ras/mitogen-activated protein kinase (MAPK) pathway and canonical WNT signaling (Zeller et al. 2013). For example, in intestinal tumor formation, APC and Kras mutation are synergistic not only in promoting tumor formation but also in the activation of WNT signaling (Janssen et al. 2006). One potential mechanism elucidated in colorectal cancer cell lines reveals that oncogenic Kras, functioning through the MAPK pathway, can activate canonical WNT signaling by phosphorylation of LRP6 (Lemieux et al. 2015). Additionally, in their investigation of the *Trp53/Cdh1* double conditional model, Shimada et al did not observe any expression of β-catenin in their tumors and concluded that β-catenin signaling was not involved in the development of diffuse gastric cancer in their model (2012).

Taken together, these data suggest that our β-catenin signaling phenotype is a synthetic phenotype resulting from both the loss of E-cadherin and expression of oncogenic Kras in our model: loss of E-cadherin releases β-catenin from sequestration and oncogenic Kras inhibiting the destruction complex. Further, it may suggest a reason why we do not see increased tumorigenesis in the LiCl treatment group. This treatment may be redundant in targeting the destruction complex that may already be impaired by oncogenic Kras.

CHAPTER 5 LOSS OF E-CADHERIN CORRELATES WITH UPREGULATION OF ONCOGENIC KRAS TARGET GENES IN THE ACKPY MOUSE MODEL OF GASTRIC CANCER

i. Abstract

Ras oncogenes directly regulate four core signaling pathways that influence nearly every hallmark of cancer (Hanahan and Weinberg 2000; Hanahan et al. 2011): the mitogen activated kinase (MAPK) pathway, the phosphatidylinositol-3-kinase (PI3K)/Akt/mammalian target of rapamycin (mTOR) pathway, the Ras-like GTPase guanine nucleotide exchange factor (Ral-GEFs) pathway, and the phospholipase C isoform ε (PLCε) pathway (Pylayeva-Gupta, Grabocka, and Bar-Sagi 2011). Microarray data comparing gene expression in stomachs harvested from $Cdh1^{fl/fl}$ vs. $Cdh1^{fl/+}$ mice correlates E-cadherin loss with the upregulation of oncogenic Kras signaling in our model. Gene sets regulated by MAPK activation were among those over-represented in our microarray analysis. However, examination of extracellular signal-related kinase (ERK) phosphorylation revealed that E-cadherin does not regulate MAPK activity in our model. The upregulation of oncogenic Kras target genes that result from the loss of E-cadherin may alternatively be explained by E-cadherin regulation of other Kras effector pathways. In fact, E-cadherin loss correlated with upregulation of gene sets driven by activation of each of the other effector pathways.

ii. Introduction

The Ras family of oncogenes has been extensively studied since its discovery in the early 1980s (Tsuchida et al. 2016). They have been implicated in the regulation of

nearly all of the hallmarks of cancer as outlined by Hanahan and Weinberg (Hanahan and Weinberg 2000; Hanahan et al. 2011; Pylayeva-Gupta, Grabocka, and Bar-Sagi 2011). The four core pathways they directly regulate have been known since the early 2000s (Downward 2003). While their reach seems endless, new downstream effectors are still being discovered (F. Zhang and Cheong 2016).

The first Ras effector discovered was the Raf/mitogen activated protein kinase (MAPK) pathway. Activated Ras binds and activates Raf, a kinase complex, which then activates MAPK/ERK Kinase (MEK) by phosphorylating it. MEK phosphorylates and activates the extracellular signal-related kinase (ERK), also known as MAPK. ERK phosphorylates a myriad of both cytoplasmic and nuclear targets, many of which are transcription factors (Mendoza, Er, and Blenis 2011).

Ras also activates the lipid kinase phosphatidylinositol-3-kinase (PI3K), generating the signaling molecule phosphatidyl inositol 3,4,5 tri-phosphate (PIP3). PIP3 recruits the kinase Akt to the plasma membrane where another target of PIP3, 3-phosphoinositide-dependent kinase 1 (PDK1), and the mammalian target of rapamycin (mTOR) complex 2 (mTORC2) activate it by phosphorylation. Akt has many targets that regulate a variety of pathways; most notable is its inhibition of the tuberous sclerosis complex genes (TSC1/2) that inhibit the GTPase Ras homolog enriched in brain (RHEB) that activates mTORC1. As such, Akt disinhibits RHEB via inhibition of TSC1/2 leading to activation of mTORC1, a master regulator of cell survival, division, and metabolism (Mendoza, Er, and Blenis 2011).

Ras also activates the Ras-like GTPases (Rals) via their guanine nucleotide exchange factors (GEFs). Like Ras proteins, the Rals interact with a variety of effectors to influence exocytosis, endocytosis, actin organization, second messenger production, and transcription factor activity. One such effector pathway results in NF-κB activation. RalB promotes the association of Sec5 with TANK-binding kinase (TBK1), which increases its activity as an inhibitor of κB (IκB) kinase (IKK), thereby relieving inhibition of NF-κB (Neel et al. 2011).

The fourth canonical target of Ras is phospholipase C (PLC) isoform ε, which increases its activity. PLC enzymes generate two important second messengers: diacylglycerol (DAG), which activates phosphokinase C (PKC), and inositol 1,4,5-trisphosphate (IP_3), which leads to an increase in intracellular calcium by release from intracellular stores and influx through cell membrane channels. Both of these pathways regulate a variety of pathways. As with the RalGEF pathway, the PLCε has also been shown to activate NF-κB (R.-Y. Zhang et al. 2016). Additionally, increased intracellular calcium activates calcineurin, which dephosphorylates the transcription factor nuclear factor of activated T cells (NFAT), exposing its nuclear localization signal and inducing translocation to the nucleus, thereby activating NFAT (Mognol et al. 2016).

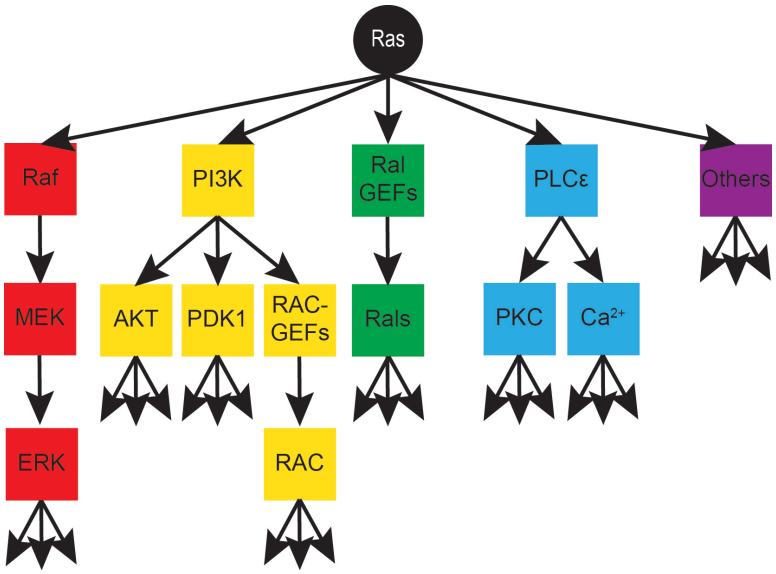

Figure 5-1. Main downstream effector pathways of the Ras family of oncogenes (Downward 2003; F. Zhang and Cheong 2016).

iii. Results

Microarray analysis correlates loss of E-cadherin with upregulation of oncogenic Kras signaling and increased expression of MAPK target genes

The microarray gene set overlap analysis (GSOA) data, described in Chapter 3, also revealed that RTK/Kras/MAPK driven gene sets were over-represented in our *Cdh1*$^{fl/fl}$ versus *Cdh1*$^{fl/+}$ stomach gene set. When comparing our gene set to the collection of cancer hallmark gene sets, the second most significant hit was one for "genes up-regulated by Kras activation." Further, significant overlap was found between our gene set and RTK/Kras/MAPK regulated gene sets (oncogenic signature gene sets), including 9 resulting from the over-expression of oncogenic *KRAS* and 4 from activation of RTK/MAPK components (Table 5-1). Given that both *Cdh1*$^{fl/fl}$ and *Cdh1*$^{fl/+}$ stomachs express oncogenic Kras, these data suggest that E-cadherin presence or loss may regulate the activity of oncogenic Kras in our model.

Name	Description	FDR q-value
Cancer Hallmark Gene Sets		
HALLMARK_KRAS_SIGNALING_UP	Genes up-regulated by KRAS activation.	3.36E-61
Oncogenic Signature		
EGFR_UP.V1_UP	Up-regulated in MCF-7 cells engineered to express ligand-activatable EGFR	7.54E-27
MEK_UP.V1_UP	Up-regulated in MCF-7 cells stably over-expressing constitutively active MAP2K1	1.30E-25
RAF_UP.V1_UP	Up-regulated in MCF-7 cells stably over-expressing constitutively active RAF1	1.30E-25
KRAS.600_UP.V1_UP	Up-regulated in four lineages of epithelial cell lines over-expressing oncogenic KRAS	1.47E-19
ERB2_UP.V1_UP	Up-regulated in MCF-7 cells engineered to express ligand-activatable ERBB2	9.62E-19
KRAS.DF.V1_UP	Up-regulated in epithelial lung cancer cell lines over-expressing oncogenic KRAS	9.39E-18
KRAS.600.LUNG.BREAST_UP.V1_UP	Up-regulated in epithelial lung and breast cancer cell lines over-expressing oncogenic KRAS	2.68E-17
KRAS.LUNG.BREAST_UP.V1_UP	Up-regulated in epithelial lung and breast cancer cell lines over-expressing oncogenic KRAS	2.55E-15
KRAS.BREAST_UP.V1_UP	Up-regulated in epithelial breast cancer cell lines over-expressing oncogenic KRAS	4.49E-11
KRAS.LUNG_UP.V1_UP	Up-regulated in epithelial lung cancer cell lines over-expressing oncogenic KRAS	1.34E-10
KRAS.300_UP.V1_UP	Up-regulated in four lineages of epithelial cell lines over-expressing oncogenic KRAS	8.06E-09
KRAS.PROSTATE_UP.V1_UP	Up-regulated in epithelial prostate cancer cell lines over-expressing oncogenic KRAS	2.75E-08
KRAS.50_UP.V1_UP	Up-regulated in four lineages of epithelial cell lines over-expressing oncogenic KRAS	2.78E-07

Table 5-1. Gene set overlap analysis comparing cancer hallmark gene sets and oncogenic signature gene sets to genes up-regulated in $Cdh1^{fl/fl}$ versus $Cdh1^{fl/+}$ stomachs.

E-cadherin does not attenuate MAPK activity

ERK, the downstream effector of the MAPK pathway, is activated by phosphorylation. To assess the effect of E-cadherin on the MAPK pathway activity downstream of oncogenic Kras, stomach tissue from $Cdh1^{fl/fl}$ and $Cdh1^{fl/+}$ mice was stained by immunofluorescence (IF) for phospho-ERK (pERK) and yellow fluorescence

protein (YFP) expression. Preliminary data comparing two stomach samples of each genotype suggested a considerable increase in pERK in the *Cdh1*$^{fl/fl}$ stomachs over the *Cdh1*$^{fl/+}$ stomachs (Figure 5-2A).

For quantitative analysis, I examined two larger cohorts of mice. One cohort, referred to as the terminal cohort, was composed of *Cdh1*$^{fl/fl}$ mice that had reached the humane survival endpoint (20% loss of body weight) and *Cdh1*$^{fl/+}$ mice that had reached the humane endpoint for their subcutaneous tumors ($\geq$ 2 cm^3). A second cohort was composed of age-matched *Cdh1*$^{fl/fl}$ and *Cdh1*$^{fl/+}$ mice euthanized between 9 and 10 weeks of age. IF staining of the terminal cohort revealed a trend towards increased pERK in *Cdh1*$^{fl/fl}$ stomachs over *Cdh1*$^{fl/+}$ stomachs, but this difference was not statistically significant ($p = 0.15$). However, IF staining of the age-matched cohort exhibited no such trend (Figure 5-2B).

To further analyze pERK expression in tissue sections, I performed immunohistochemical (IHC) staining on the same cohorts. In contrast to the IF staining, IHC staining of the terminal cohort indicated a trend toward increased expression of pERK in *Cdh1*$^{fl/+}$ stomachs over *Cdh1*$^{fl/fl}$ stomachs ($p=0.23$). In the age-matched cohort, this finding was a statistically significant increase ($p=0.01$). Additionally, analysis of the combination of these two cohorts revealed a statistically significant increase in pERK in *Cdh1*$^{fl/+}$ stomachs over *Cdh1*$^{fl/fl}$ stomachs ($p=0.01$, Figure 5-2C).

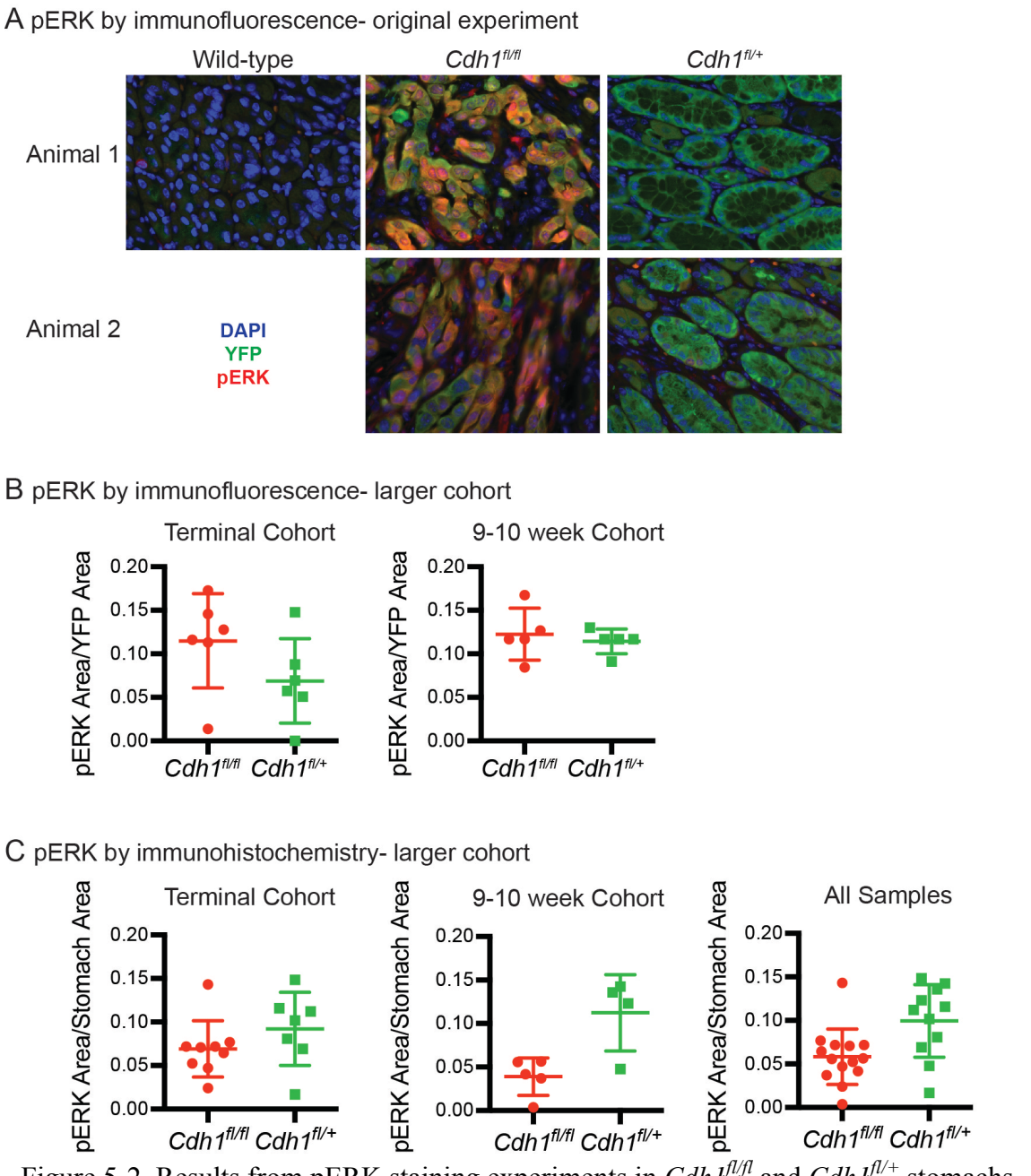

Figure 5-2. Results from pERK staining experiments in *Cdh1*$^{fl/fl}$ and *Cdh1*$^{fl/+}$ stomachs. (A) Initial immunofluorescence staining for pERK (red) and YFP (green) in *Cdh1*$^{fl/fl}$ and *Cdh1*$^{fl/+}$ stomachs. Counterstained with DAPI (blue), 63x. (B) Quantitative analysis of immunofluorescence staining for pERK^{+} and YFP^{+} overlap area (relative to total YFP^{+} area) in two *Cdh1*$^{fl/fl}$ vs. *Cdh1*$^{fl/+}$ stomach cohorts. (C) Quantitative analysis of immunohistochemical staining for pERK^{+} (relative to total stomach area) in two *Cdh1*$^{fl/fl}$ vs. *Cdh1*$^{fl/+}$ stomach cohorts, separate and combined.

Microarray analysis correlates loss of E-cadherin with upregulation of oncogenic Kras MAPK-independent effector pathways

Name	Description	FDR q-value
PI3K/AKT/mTOR Gene Sets		
HALLMARK_MTORC1_SIGNALING	Up-regulated through activation of mTORC1 complex.	1.76E-08
HALLMARK_PI3K_AKT_MTOR_SIGNALING	Up-regulated by activation of the PI3K/AKT/mTOR pathway.	4.54E-02
MTOR_UP.V1_DN	Down-regulated by everolimus (mTOR inhibitor) in prostate tissue.	1.31E-12
PTEN_DN.V2_UP	Up-regulated in HCT116 cells upon knockdown of PTEN	2.98E-11
AKT_UP_MTOR_DN.V1_DN	Down-regulated by everolimus (mTOR inhibitor) in mouse prostate tissue transgenically expressing human AKT1	1.76E-10
NF-κB Gene Sets		
HALLMARK_TNFA_SIGNALING_VIA_NFKB	Regulated by NF-kB in response to TNF	5.52E-45
V$NFKAPPAB_01	Genes with promoter regions containing the NFKB binding site	1.57E-17
V$NFKAPPAB65_01	Genes with promoter regions containing the RELA binding site	1.42E-14
HINATA_NFKB_IMMU_INF	Immune or inflammatory genes induced by NF-KB in primary keratinocytes and fibroblasts.	6.26E-07
RELA_DN.V1_DN	Genes down-regulated in HEK293 cells upon knockdown of RELA	2.21E-06
NFAT Gene Sets		
TGGAAA_V$NFAT_Q4_01	Genes with promoter regions containing the NFAT binding site	1.47E-69
V$NFAT_Q6	Genes with promoter regions containing the NFAT binding site	1.17E-18

Table 5-2. Gene set overlap analysis results for downstream *KRAS* pathways that are MAPK-independent.

Further review of the microarray GSOA revealed MAPK-independent gene sets downstream of oncogenic *KRAS* also overlapped with our $Cdh1^{fl/fl}$ over $Cdh1^{fl/+}$ stomach gene set. Using GSOA, our gene set overlapped with two publicly available cancer hallmarks gene sets upregulated by activation of the PI3K/AKT/mTOR pathway. Comparison of our gene sets to oncogenic signature gene sets demonstrated overlap with three sets of genes also upregulated by activation of the PI3K/AKT/mTOR pathway (Table 5-2, white). Gene sets upregulated by NF-κB were also over-represented in

comparison to cancer hallmarks gene sets (1 gene set), transcription factor target gene sets (2 gene sets), and oncogenic signature gene sets (2 gene sets) (Table 5-2, light gray). There was also overlap with two transcription factor target gene sets for NFAT (Table 5-2, dark gray).

iv. Discussion

Investigating E-cadherin regulation of MAPK

The suggestion that E-cadherin might negatively regulate the MAPK pathway downstream of oncogenic Kras in our model was intriguing. While crosstalk between E-cadherin and receptor tyrosine kinases (RTKs) has been suggested (Andl and Rustgi 2005) only two papers demonstrate E-cadherin-dependent down-regulation of MAPK (Laprise et al. 2004; Soto et al. 2008). Crosstalk between the canonical WNT and RTK/KRAS/MAPK pathways is well-described (Zeller et al. 2013), but only one study has implicated β-catenin signaling in the regulation of the pathway downstream of RTKs (Zeller et al. 2012). Prior to our semi-quantitative pERK staining data that suggest that this initial observation may not be true, we began to consider several pathways that could have potentially been at play.

First, E-cadherin has been shown to bind and activate the PI3K-p85 regulatory subunit, resulting in activation of Akt (De Santis et al. 2009). This E-cadherin regulation of the PI3K/Akt pathway has been shown to inhibit MEK/ERK activity (Laprise et al. 2004). We hypothesized that E-cadherin in $Cdh1^{fl/+}$ stomachs might lead to increased AKT activity that might explain the inhibition of pERK in these mice. As such, I examined $Cdh1^{fl/fl}$ and $Cdh1^{fl/+}$ stomach tissue for the active form of AKT (pAKT-

Ser473) by IF. In a pilot experiment, I did not observe pAKT expression in either cohort (data not shown).

Second, E-cadherin and β-catenin have been shown to influence the expression of several negative regulators of MAPKs (MAPK phosphatases, MKPs): dual specific phosphatase 6 and 14 (DUSP6/14) (Zeller et al. 2012), and sprouty homolog 2 (SPRY2) (Barbáchano et al. 2010). We hypothesized that E-cadherin expression or the lack of β-catenin signaling in $Cdh1^{fl/+}$ stomachs could lead to an increase in expression of a MAPK phosphatase that could cause a decrease in the phosphorylated state of ERK in these stomachs. Due to the large number of MKPs and the fact that the reported regulation by E-cadherin/β-catenin was at the transcriptional level, we began our examination of MKP expression in a panel of $Cdh1^{fl/fl}$ and $Cdh1^{fl/+}$ stomach RNAs by qPCR. I did not observe increased expression in the $Cdh1^{fl/+}$ RNAs of any of the 10 MAPK regulatory DUSPs (Kidger and Keyse 2016), 4 SPRYs, or 3 SPREDs (sprouty related EVH1 domain containing) (data not shown).

Third, in the context of a mouse model of lung carcinogenesis, it is has been shown that $Braf^{V600E}$ can drive oncogene-induced senescence (OIS) that is rescued by canonical WNT driven cMyc expression (Juan et al. 2014). I hypothesized that $Kras^{G12D}$ in $Cdh1^{fl/+}$ stomachs might similarly drive OIS that would result in an inhibition of MAPK activity. In $Cdh1^{fl/fl}$ stomachs, this could be rescued by cMyc upregulation as a result of E-cadherin loss-driven β-catenin signaling. This mechanism is not possible, as OIS is dependent on p53 activity and *Trp53* is knocked out in our model.

Fourth, E-cadherin is known to inhibit p120-Rac1 activity. This inhibition has been shown to be necessary for Raf/MEK activation (Soto et al. 2008). I hypothesized that loss of E-cadherin in *Cdh1*$^{fl/fl}$ stomachs led to loss of inhibition of p120-Rac and ultimate disinhibition of Raf/MEK (re: MAPK) activity. Unfortunately, there is no way to assess Rac1 activity in tissue sections.

E-cadherin does not down-regulate MAPK activity

Ultimately, the initial observation of a decrease in pERK expression in *Cdh1*$^{fl/+}$ stomachs compared to *Cdh1*$^{fl/fl}$ stomachs was not borne out upon examination of larger cohorts. By IF, there was no significant difference in pERK expression between the genotypes. However, by IHC there was a contrasting increase in pERK staining in *Cdh1*$^{fl/+}$ stomachs compared to *Cdh1*$^{fl/fl}$ stomachs (or decrease in pERK staining in *Cdh1*$^{fl/fl}$ stomachs compared to *Cdh1*$^{fl/+}$ stomachs). This difference is likely due to the lack of co-staining and subsequent controlling for YFP in the IHC analysis.

For IF analysis, I measured the area of pERK and YFP co-expression divided by total YFP^{+} area per microscopic field (averaged over multiple fields and tissue planes). This controlled for the relative abundance of Cre-transformed cells of interest by excluding cells untransformed cells and acellular areas. I analyzed the IHC data by measuring the total pERK stained area per slide divided by the total tissue area per slide (each slide containing several tissue planes). This IHC analysis did not account for the area of the tissue that was Cre transformed (i.e. YFP^{+}). This could be corrected by staining for YFP on a serial section and dividing the pERK stained area per slide by the

YFP^+ area per slide. Qualitatively, I did observe greater YFP positivity throughout $Cdh1^{fl/+}$ stomachs compared to $Cdh1^{fl/fl}$ stomachs that might explain this finding.

MAPK-independent Kras pathways may drive Kras signature in microarray data

Due to my initial observation of a decrease in pERK expression in $Cdh1^{fl/+}$ stomachs compared to $Cdh1^{fl/fl}$ stomach, I focused my work and analysis on the role of the MAPK pathway. However, revisiting the initial GSOA data suggests an alternative interpretation of the apparent effect of E-cadherin on Kras-regulated genes. The GSOA results not only suggested regulation of the MAPK pathway downstream of Kras, but also of the PI3K/Akt/mTOR, NF-κB, and PLCε/PKC/Ca^{2+} (i.e. NFAT) pathways. Our staining data suggest that E-cadherin does not negatively regulate the Ras/MAPK axis, but it may regulate one or more of these pathways. If yes, that regulation could explain the strong Kras-driven gene signature present in our $Cdh1^{fl/fl}$ over $Cdh1^{fl/+}$ stomach gene set. Further experiments are necessary to confirm or refute E-cadherin regulation of these pathways, I will discuss that further in the following conclusions and future directions chapter.

CHAPTER 6 CONCLUSIONS AND FUTURE DIRECTIONS

i. ACKPY Metastatic Model of Gastric Cancer

Conclusions

The ACKPY mouse model is a promising new model of metastatic gastric cancer. By combining genetic lesions that represent common pathways mutated in gastric cancer, we have generated a clinically relevant model of gastric cancer that mimics both the etiology of disease and the observed disease progression. Unlike most mouse models of gastric cancer, ours metastasizes widely, mirroring the common presentation of patients in the clinic with advanced disease. In contrast to other mouse models of gastric cancer, ours progresses quickly, allowing for timely analyses. I demonstrated the potential preclinical utility of our model by treating our mice with a MEK inhibitor. However, this model, as all models, is not without limitation and caveats.

First, though we set out to generate a model of diffuse gastric cancer, the phenotype we observe is that of mixed-type, containing both intestinal-type and diffuse-type lesions. This phenotype may be a disadvantage of the model, as it is the least common form of gastric cancer (Polkowski et al. 2016). Yet, this is the first mouse model of mixed-type gastric cancer and is therefore the only model available to study this hybrid form of the disease. Furthermore, it may have implications for understanding the differences, similarities, and distinct etiologies of intestinal- and diffuse-type cancers, as both types of lesions arise from the same genetic modifications in our model. The presence of both intestinal- and diffuse-type lesions in one model may also be an

advantage as treatments could be assessed as to their effect on each type of lesion in the same model.

The above presumes the prevailing narrative that intestinal- and diffuse-type gastric cancers represent distinct diseases with differing etiologies. Intestinal-type gastric cancer has traditionally been associated with the Correa pathway and is thought to be more related to environmental effects (Correa 1992; Muñoz and Asvall 1971). The histologic progression to diffuse-type is less well understood (Fox and Wang 2007), and the etiology is less associated with environmental effects (Muñoz and Asvall 1971) but is known to be related to loss of expression of E-cadherin (Graziano, Humar, and Guilford 2003). In these discussions the presence of mixed-type gastric cancer is always conveniently absent.

However, *H. pylori* infection is strongly associated with both forms of the disease (Fox and Wang 2007). Further, the recent molecular classification systems developed by the Cancer Genome Atlas (TCGA) and the Asian Cancer Research Group (ACRG) do not categorize intestinal- and diffuse-type disease perfectly within subsets. Though both groups find that their classification of Laurén types is statistically significant, a thorough review of the data reveals a more complex picture. Additionally, mixed-type gastric cancer is quite evenly distributed among subtypes (Table 6-1 & Table 6-2) (Bass et al. 2014; Cristescu et al. 2015). These data might suggest that our current classification scheme, based solely on histologic appearance as described by Laurén in the 1960s, does not actually define distinct diseases.

	TCGA Classification									
	Total		EBV		MSI		GS		CIN	
	n	%	n	%	n	%	n	%	n	%
Diffuse	69	23.4%	5	19.2%	6	9.4%	40	69.0%	18	12.2%
Intestinal	196	66.4%	15	57.7%	48	75.0%	15	25.9%	118	80.3%
Mixed	19	6.4%	3	11.5%	3	4.7%	3	5.2%	10	6.8%
Not Specified	11	3.7%	3	11.5%	7	10.9%	0	0.0%	1	0.7%

Table 6-1. Distribution of samples by Laurén classification within The Cancer Genome Atlas (TCGA) subtypes (Bass et al. 2014).

	ACRG Classification									
	Total		MSS/TP53$^-$		MSS/TP53$^+$		MSI		MSS/EMT	
	n	%	n	%	n	%	n	%	n	%
Diffuse	135	45.0%	42	39.3%	36	45.6%	20	29.4%	37	80.4%
Intestinal	146	48.7%	58	54.2%	38	48.1%	42	61.8%	8	17.4%
Mixed	17	5.7%	7	6.5%	4	5.1%	5	7.4%	1	2.2%
Not Specified	2	0.7%	0	0.0%	1	1.2%	1	1.0%	0	0.0%

Table 6-2. Distribution of samples by Laurén classification within The Asian Cancer Research Group (ACRG) subtypes (Cristescu et al. 2015).

Similarly, though the cell of origin of gastric cancer is still not well-defined, the data implicating Mist1$^+$ as the cell of origin demonstrates that both sub-types can originate from the same cell, albeit through different genetic manipulations (Hayakawa et al. 2015). This is in contrast to cancers of other sites, where sub-types have been shown to arise from distinct cells of origin either from similar or distinct genetic manipulations (Blanpain 2013). Taken together with our data showing that diffuse-type and intestinal-type lesions can arise from the same genetic background, this might suggest that these histologic classifications do not correlate with etiology of disease as well as was once thought. Our work on the cell of origin of gastric cancer deserves further investigation.

Another caveat is the relative rarity of the specific genetic lesions we used to generate our model. Kras mutations occur in only 9% of TCGA cases. However, as

discussed in Chapter 1, if one looks at all members of the Epidermal Growth Factor Receptor (EGFR)/Ras/Raf families, amplification or mutation occurs in >60% of cases (Bass et al. 2014; Cerami et al. 2012). This analysis omits other Receptor Tyrosine Kinases (RTKs) that can activate Kras. Likely the percentage of tumors with Kras activation would only increase if other RTKs were considered. In fact, many RTKs have been implicated in gastric carcinogenesis (Table 6-3). Because oncogenic Kras is a common effector of many of these RTKs, it allows the modeling of RTK amplification/mutation in general rather than that of one specific RTK. However, it does not model all of the potential downstream effectors of RTKs. Nonetheless, one of its favorable attributes is its common use and the wide array of literature on which one could draw on while interpreting results.

Receptor Tyrosine Kinases (RTKs)		**Reference**
PDGFR	Platelet Derived Growth Factor Receptor	(Chung and Antoniades 1992)
IGF-1R	Insulin-like Growth Factor-1 Receptor	
TGFαR	Transforming Growth Factor α Receptor	
EGFR	Epidermal Growth Factor Receptor	(Gong et al. 2010)
HER2 (ERBB2)	Human EGF Receptor 2	
FGFR1	Fibroblast Growth Factor Receptor 1	
FGFR2α	Fibroblast Growth Factor Receptor 2α	
Insulin R	Insulin Receptor	
EphA4	Erythropoietin-Producing Human Hepatocellular Receptor A4	
FGFR2	Fibroblast Growth Factor Receptor 2	(Deng et al. 2012)
EGFR	Epidermal Growth Factor Receptor	
HER2 (ERBB2)	Human EGF Receptor 2	
HGFR(MET)	Hepatocyte Growth Factor Receptor	

Table 6-3. Receptor Tyrosine Kinases (RTKs) implicated in gastric carcinogenesis.

Additionally, though mutations in *CDH1* are causal in hereditary diffuse gastric cancer and loss of E-cadherin is common in sporadic diffuse-type gastric cancer, it is rarely lost or mutated in intestinal-type gastric cancer (Liu et al. 2014). However, just as we looked at the entire RTK/RAS/RAF pathway to argue the relevance of the inclusion

of oncogenic Kras in our model, so should we do the same for E-cadherin related genes. In fact, in the TCGA data set, one or more components of the adherens junction are altered in 49% of gastric cancer cases (Figure 6-1) (Bass et al. 2014; Cerami et al. 2012).

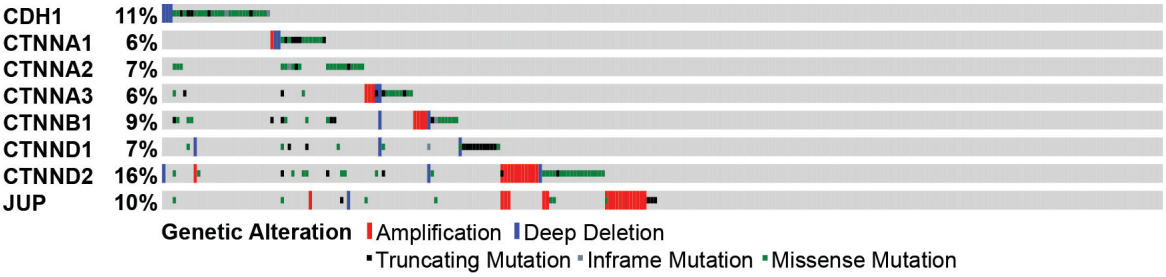

Figure 6-1. Genetic alterations in adherens junction components in The Cancer Genome Atlas (TCGA) gastric cancer cohort (Bass et al. 2014; Cerami et al. 2012).

Further, in the data available, from the cBioPortal, *CDH1* and *KRAS* mutations or other alterations rarely occur together in human gastric cancer (Bass et al. 2014; Cerami et al. 2012). However, this may be explained by the interaction I propose here. If, for example, a cell losses *CDH1* expression it will also lose inhibition of the *KRAS* downstream pathways, in effect activating these pathways. Thus there may not be evolutionary pressure to gain oncogenic mutations of *KRAS*. Further it is known that, at least in a pancreatic cancer model, oncogenic *Kras* inhibits E-cadherin (Rachagani et al. 2011). Thus, a cell that acquires a *KRAS* mutation may disinhibit itself by inhibiting E-cadherin, relieving the evolutionary pressure to mutate *CDH1*.

Finally, though our model metastasizes widely, it does not perfectly recapitulate the distribution of metastasis observed in gastric cancer patients. Clinically, one does see local lymph node involvement as we do in our model, but the most common sites of spread are to the peritoneum and liver, while lung metastases are more rare (Avital et al.

2015). That having been said, our model is the only clinically relevant model with significant metastasis.

Future Directions

The ACKPY model offers many avenues for future study, some of which I have addressed in the previous chapters. First, an exploration of the role of oncogenic Kras in the metastatic phenotype of our model is certainly pertinent. Whereas E-cadherin is typically considered an invasion suppressor gene (Birchmeier, Hülsken, and Behrens 1995) here we see it functioning as a primary tumor suppressor. It is the addition of oncogenic Kras to the *Trp53/Cdh1* double-conditional knockout that expands the metastatic range from rare micro-metastatic lesions of local lymph nodes (Shimada et al. 2012) to highly penetrant metastases to local lymph nodes, lungs, and mediastinal lymph nodes, as well as rarer micro-metastases to the liver. More detailed analysis of livers may reveal a higher frequency of metastases, as only 3 sections of tissue 200 μm apart were analyzed from each liver, leaving much of the tissue uninvestigated. Further, investigation of other tissues such as bone and the retroperitoneum might reveal other sites of metastasis.

Study of the mixed-type histology of the model may reveal insights into the differing etiology of intestinal- and diffuse-type lesions. This could be done through experiments that isolate and compare lesions of differing histology. For example, laser capture micro-dissection could be used followed by microarray, RNA-seq, or mass-spectrometric analyses.

Much work can be done to further investigate the cell of origin of gastric cancer. Initial experiments should seek to determine any overlap between Mist1^{+}, Lgr5^{+}, and Atp4b^{+} cell populations; this could be performed easily by lineage tracing, co-immunostaining, or flow cytometry. I hypothesize that Mist1^{+} or Lgr5^{+} stem cell-derived pre-parietal or parietal cells are the actual cell transformed in those models, and this hypothesis could also be tested using lineage tracing experiments.

Finally, there are a variety of topics that could be studied using this model. I performed a pilot experiment examining the involvement of the microbiome in the development of gastric cancer in our mice. In a different pilot experiment, I observed a correlation between number of circulating tumor cells and lung macrometastases. Both these findings lay promising groundwork for validation and further study.

ii. E-cadherin as Gatekeeper to Mutant Kras and p53 Loss-Driven Gastric Cancer

Conclusions

I present evidence that E-cadherin may act as a gatekeeper to oncogenic *Kras* and *Trp53* loss-driven gastric cancer. I show that the presence of a wild-type *Cdh1* allele in our model delays oncogenesis significantly. Further, when tumors do form, they often show loss of E-cadherin expression. While the preliminary data is intriguing, more experiments need to be performed to definitively prove this hypothesis. As discussed, this gatekeeper function is not without precedent, as the tumor suppressor *APC* acts similarly in a colorectal cancer model (Dow et al. 2015). Of note, the other targeted model of oncogenic Kras-driven gastric cancer also has deletion of *APC* (Hayakawa et al. 2015). APC and E-cadherin functionality overlap in their regulation of β-catenin (Mohammed et

al. 2016; Liu et al. 2014). One hypothesis that can be drawn from these data is that canonical WNT signaling is necessary for oncogenic *Kras* and *Trp53* loss-driven tumorigenesis in the gut.

The other finding that resulted from adding wild-type Cdh1 back to our model was the subcutaneous tumor phenotype. I initially assumed these lesions were metastases resulting from gastric tumors. However, the fact that we did not detect primary tumors of the stomach in the majority of the mice with subcutaneous tumors makes this interpretation unlikely. The sarcomatoid histology of the tumors might suggest they are not gastric in origin, but the gastric tumors that do rarely occur in these mice also have sarcomatoid features. One cannot rule out the possibility of small, sarcomatoid stomach lesions that metastasize early to the subcutaneous space.

I have come to favor the alternative explanation that these are sarcomas arising from off-target Cre activity in the subcutaneous space. I present several additional pieces of evidence that suggest this, including microarray data comparing these lesions to human gastric cancer and sarcoma samples as well as analysis of expression of stomach-specific genes. Additionally, the latency to formation of these tumors is similar to that of an oncogenic *Kras* and *Trp53* loss-induced model of sarcoma (Kirsch et al. 2007).

Future Directions

Further investigation of E-cadherin as gatekeeper to oncogenic *Kras* and *Trp53* loss-driven gastric cancer is certainly necessary. First, quantification of loss of E-cadherin in tumors arising in the $Cdh1^{fl/+}$ and/or $Cdh1^{+/+}$ must be performed. Second, the mechanism of loss should be investigated. Additionally, comparisons of tumor areas to

non-tumor areas by microarray or RNA-seq may implicate signaling pathways that are necessary for tumor formation. Comparison of tumor areas that have lost E-cadherin expression and tumor areas that retain E-cadherin to non-tumor areas may be similarly useful and reveal the changes, other than of E-cadherin loss, that allow tumor progression. Finally, generating an E-cadherin loss allele that could be restored could prove its gatekeeper status. One such model is a drug inducible shRNA knock-down as was used in the *APC/Kras/Trp53* colorectal cancer paper (Dow et al. 2015). Another option is an XTR *Cdh1* allele (Robles-Oteiza et al. 2015). Additionally, the hypothesis that canonical WNT signaling is necessary for oncogenic *Kras* and *Trp53* loss-driven tumorigenesis in the gut could be tested in our model and/or in the APC/Kras/p53 colorectal cancer model by breeding the conditional β-catenin allele (Brault et al. 2001) onto either model.

Finally, one could pursue definitive evidence on the origin of the subcutaneous tumors that arise in the $Cdh1^{fl/+}$ and $Cdh1^{+/+}$ models. Evidence that they are sarcomas could be derived from *Atp4b-Cre;*$Rosa26^{LSL\text{-}YFP/+}$ mice. Detailed examination of the skin by immunofluorescence for YFP expression and highly sensitive polymerase chain reaction (PCR) for the recombined $Rosa26^{LSL\text{-}YFP}$ allele could reveal a rare Cre expressing cell population in the subcutaneous space. Definitive proof of gastric origin (i.e. that they are metastases) would be more difficult and likely involve lineage tracing using a second marker of gastric or epithelial origin. Hypothetically, one could add a FLP recombinase allele (CK19-FLP) driven by the cytokeratin 19 promoter and a FRT-STOP-FRT red fluorescent protein (FSF-RFP) allele to the $Cdh1^{fl/+}$ model. If the cutaneous tumors are

epithelial in lineage, they will fluoresce from both the RFP and YFP alleles. If they are mesenchymal derived sarcomas, they should only fluoresce from the YFP allele.

iii. E-cadherin Loss Upregulates β-catenin Signaling in the ACKPY Mouse Model of Gastric Cancer

Conclusions

I present, to my knowledge, the first evidence that E-cadherin loss leads directly to the upregulation of β-catenin *in vivo* using microarray and qPCR for the upregulation of TCF/LEF and canonical WNT targets, respectively. Additionally, I demonstrate a loss of membranous β-catenin that correlates with loss of E-cadherin. I show that inhibition of this pathway prolongs survival of our ACKPY mice. Further, I present the hypothesis that this effect of E-cadherin loss is only possible in the context of oncogenic Kras suppression of the β-catenin destruction complex. This potential *in vivo* evidence of such crosstalk between oncogenic Kras and the canonical WNT pathway would itself be novel. However, each of these findings has limitations that bear addressing.

First, the comparisons via microarray and qPCR were performed on whole glandular stomach samples. These data leave open the possibility that the comparisons may have been skewed by differential content of recombined tissue. For example, if the $Cdh1^{fl/fl}$ stomachs are primarily composed of recombined tissue and the $Cdh1^{fl/+}$ stomachs have a lower content of recombined tissue, the comparison may be better characterized as $Cdh1^{fl/fl}$ tumor versus normal stomach. This is unlikely given the high burden of recombined tissue as observed by YFP staining (data not shown), but still a possibility. An ideal experiment would compare only Cre recombined (YFP^{+}) tissue from $Cdh1^{fl/fl}$

and *Cdh1*$^{fl/+}$ mice. Unfortunately, my attempts to select for recombined cell populations by fluorescence assisted cell sorting (FACS) for YFP^{+} cells did not yield high enough cell numbers to extract good quality RNA. Alternatively, YFP^{+} areas could be selected by laser capture micro-dissection. A less ideal but simpler possibility would be to include YFP expression in the qPCR experiment and normalize the results to YFP content.

Second, while I present loss of membranous β-catenin in *Cdh1*$^{fl/fl}$ and *Cdh1*$^{fl/+}$ tumors, I do not show a concomitant increase in cytoplasmic or nuclear β-catenin. This is a common technical difficulty with immunofluorescence (IF) staining for β-catenin. One solution might be to attempt to increase the sensitivity for β-catenin by adding a signal amplification step to the protocol. Further, the use of immunohistochemical (IHC) methods rather than IF might allow visualization of nuclear β-catenin. However, multiple staining by IHC is problematic and not possible beyond two targets, so co-staining for E-cadherin and YFP, as I do with IF, would not be possible. Staining of serial sections is a potential solution to this problem, though less elegant than co-staining.

Third, while I do show that administering a commonly used β-catenin/TCF inhibitor (PKF118-310) prolongs survival of the ACKPY mice, I do not show that its effects are on-target. This could be done by assaying for the expression of canonical WNT targets in treated and untreated mice. However, the effect size of treatment with PKF118-310 is so small that choosing an appropriate time point for such analysis could be impossible. One might suggest increasing the dose of the inhibitor to improve the effect size, however higher doses are not well-tolerated due to toxicity. As outlined in the

previous section, addition of the conditional β-catenin allele to the model would show dependence on β-catenin specifically.

Future Directions

In the previous section, I addressed several experimental improvements that would more definitively show β-catenin upregulation due to E-cadherin loss in the ACKPY model. There are several *in vitro* methods that would be of use if I were able to isolate cell lines from both $Cdh1^{fl/fl}$ and $Cdh1^{fl/+}$ stomach tissue. For example, expression analysis could be done in these cell lines, luciferase reporter technology could be used to show activity at β-catenin/TCF/LEF response elements, and nuclear localization of β-catenin could be shown by cell fractionation. However, we have been unable to isolate cell lines from $Cdh1^{fl/+}$ stomachs that are not fully transformed. One solution would be to re-express E-cadherin in $Cdh1^{fl/fl}$ cells; however, there is little novelty to that experiment as repression of β-catenin by E-cadherin expression is well-documented (Gottardi, Wong, and Gumbiner 2001). Breeding a β-catenin reporter allele onto the $Cdh1^{fl/fl}$ and $Cdh1^{fl/+}$ models could demonstrate direct regulation at the level of β-catenin/TCF response elements. Maretto and colleagues generated such a construct utilizing the β-galactosidase reporter (LacZ gene) under the control of β-catenin/TCF response elements (Maretto et al. 2003).

To test the role of oncogenic Kras in this process, I would perform several experiments. The first, and simplest, would utilize RNA already isolated from aged ACPY (original double conditional model) stomachs, which should contain tumors that lack oncogenic Kras but have E-cadherin knocked out. I would perform qPCR for

canonical WNT targets in these samples alongside the *Cdh1*$^{fl/fl}$ and *Cdh1*$^{fl/+}$ models. Though limited by the caveats described above, if upregulation is not evident in the ACPY stomachs then it would suggest a role for oncogenic Kras in the upregulation of canonical WNT targets. This would have to be confirmed in experiments that examine only at recombined (YFP^{+}) tissue. I would include ACPY stomachs in any of the other analyses listed above. Their inclusion in any of the studies that breed additional alleles onto the model would be simple, as they are always generated during breeding of the model. If my hypothesis that oncogenic Kras is necessary for upregulation of canonical WNT signaling due to E-cadherin loss is correct, one would expect ACPY tumor formation not to be dependent on β-catenin (in the conditional β-catenin allele experiments) and not to show β-catenin reporter activity (in the β-galactosidase reporter experiments). While *in vitro* methods would be of great use in testing this hypothesis, I have not yet been able to generate cell lines from ACPY tumors. The use of knock-downs (using shRNA technology) or knock-outs (using CRISPR technology) of oncogenic Kras in ACKPY cell lines is a potential solution for use *in vitro*.

iv. Loss of E-cadherin Correlates with Upregulation of Oncogenic Kras Target Genes in the ACKPY Mouse Model of Gastric Cancer

Conclusions

I present microarray data that shows that gene sets upregulated by Kras activity are overrepresented in the set of genes upregulated in *Cdh1*$^{fl/fl}$ over *Cdh1*$^{fl/+}$ stomachs. Further, gene sets upregulated by several of the major downstream effectors of Kras are also overrepresented. This is surprising given that both the *Cdh1*$^{fl/fl}$ and *Cdh1*$^{fl/+}$ models

express oncogenic Kras; one would expect similar Kras activity in these two models. One interpretation of these data is that E-cadherin inhibits oncogenic Kras or its effector pathways in the $Cdh1^{fl/+}$ model. This hypothesis is intriguing given our data suggesting that E-cadherin is a gatekeeper to oncogenesis in our model. While oncogenic *Kras* and loss of *Trp53* are sufficient to drive tumorigenesis in many other models, they are not so in ours. Perhaps E-cadherin inhibition of oncogenic Kras is the mechanism behind this gatekeeper function (Figure 6-2). Finally, given the data on APC in the Kras/Trp53 colorectal cancer model (Dow et al. 2015), the common regulation of β-catenin by APC and E-cadherin may mediate this inhibition throughout the gut.

These findings and hypotheses are not without caveats. As described in the previous section, the microarray data is limited by the use of whole glandular stomach samples. Further, the microarray data showed overrepresentation of MAPK upregulated gene sets in our set of genes upregulated in $Cdh1^{fl/fl}$ over $Cdh1^{fl/+}$ stomachs. However, these findings were not indicative of E-cadherin regulation of the MAPK pathway as assayed by pERK abundance.

One further caveat is the possibility that even though $Cdh1^{fl/+}$ stomachs appear to possess a high content of recombined cells, these cells may not be cycling as rapidly as those in the frank tumors of $Cdh1^{fl/fl}$ stomachs. Thus, Kras downstream signaling would be artifactually lower in $Cdh1^{fl/+}$ recombined cells compared to $Cdh1^{fl/fl}$ recombined cells. This difference would still be due to the presence or absence of a wild-type *Cdh1* allele. However, it may indicate a different mechanism of decreased tumor formation than the interaction between E-cadherin and Kras that I propose. Future experiments would,

ideally, also show equivalent proliferative activity of these cells either qualitatively by Ki67 staining, or quantitatively by BrdU incorporation. In an attempt to address this issue in the microarray I examined the expression of *Mki67* and *Pcna*. Notably, *Mki67* expression was not statistically significantly different between $Cdh1^{fl/+}$ and $Cdh1^{fl/fl}$ stomachs. Whereas *Pcna* was actually up by 63.6% in $Cdh1^{fl/+}$ over $Cdh1^{fl/fl}$ stomachs (q-value=1.48%).

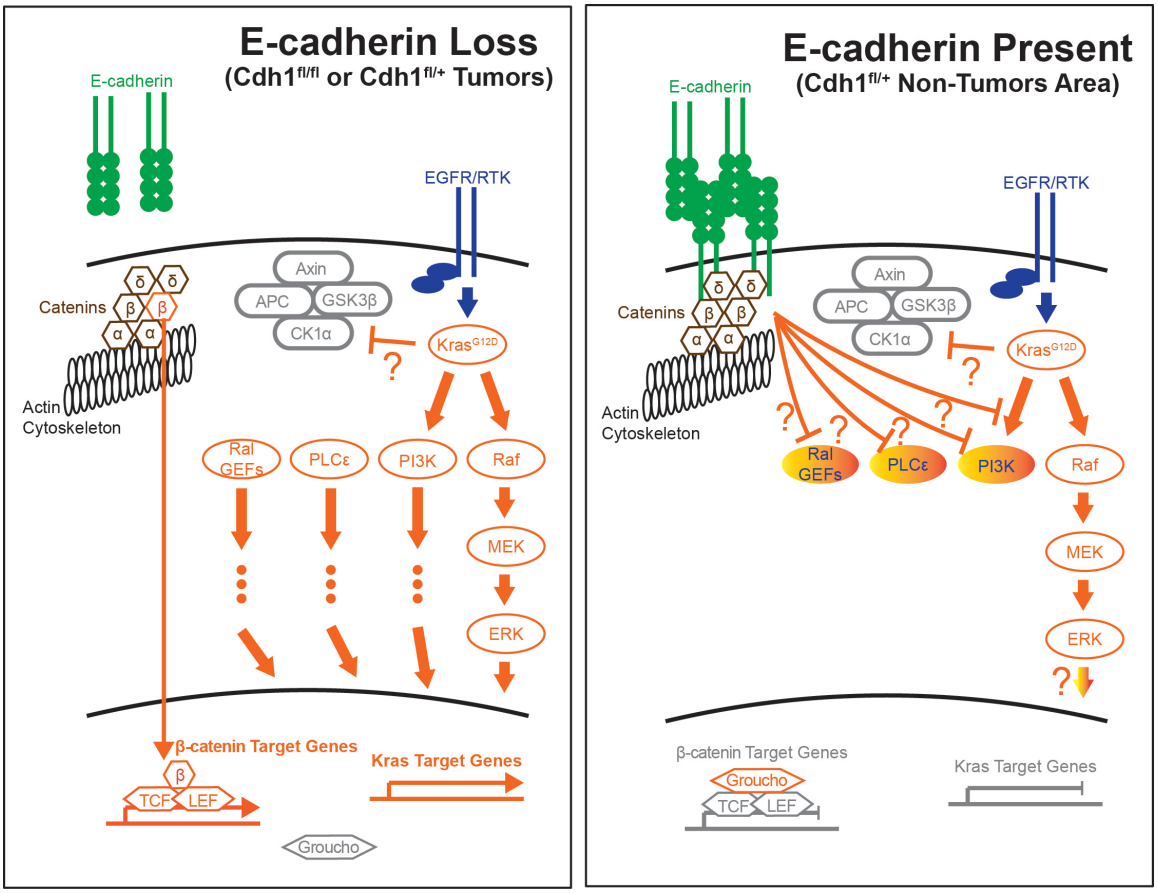

Figure 6-2. Hypotheses related to E-cadherin loss in the ACKPY model.

Future Directions

Though I observed no difference in ERK activation between the *Cdh1*$^{fl/fl}$ and *Cdh1*$^{fl/+}$ models, E-cadherin may still be regulating other pathways downstream of oncogenic Kras. The microarray data identified the PI3K, NF-κB, and NFAT pathways as other possible targets/mechanisms. Using IF or IHC, I would assay for the activation of the PI3K pathway via phopsho-AKT, for NF-κB nuclear versus cytoplasmic localization or phospho-p65 content, and for NFAT nuclear versus cytoplasmic localization in *Cdh1*$^{fl/fl}$ and *Cdh1*$^{fl/+}$ tissues. Additionally, it may be worth repeating the microarray experiment using RNA isolated only from YFP^{+} areas in the *Cdh1*$^{fl/fl}$ and *Cdh1*$^{fl/+}$ models (as discussed earlier, either by FACS or laser capture micro-dissection). Doing so would reduce background signal from non-parietal cell tissue. Further, I would ensure that all *Cdh1*$^{fl/+}$ tissue was derived from stomachs that lacked tumor by saving a portion of the stomach for histologic analysis.

APPENDIX 1 MATERIALS AND METHODS

i. Animals

The University of Pennsylvania Animal Care and Use Committee approved all animal studies. Parental mouse strains, background, source, genotyping, and primary reference are available in Table 0-1.

Allele	Background	Source	Genotyping	Reference
Atp4b-Cre	B6.FVB(N1)	Gordon Lab Washington University in St. Louis	5'-CAGCGGAGGGCAGATAGCAAGCAAG 5'-CCGGTTATTCAACTTGCACC 411 bp Transgene	(Syder et al. 2004)
Cdh1^{fl}	B6.129(N3)	The Jackson Laboratory (005319)	5'-GGGTCTCACCGTAGTCCTCA 5'-GATCTTTGGGAGAGCAGTCG 243 bp Wild-type/310 bp Mutant	(Boussadia et al. 2002)
Kras$^{LSL-G12D}$	B6.129(N10)	Tyler Jacks Laboratory Massachusetts Institute of Technology (backcrossed to C57BL/6 in the Ryeom Laboratory)	5'-GCAGGTCGAGGGACCTAATA 5'- TGTCTTTCCCCAGCACAGT 5'-CTGCATAGTACGCTATACCCTGT 250 bp Wild-type/100 bp Mutant	(Jackson et al. 2001)
Trp53^{fl}	B6.129(N10)	Tyler Jacks Laboratory Massachusetts Institute of Technology (backcrossed to C57BL/6 in the Ryeom Laboratory)	5'- GGTTAAACCCAGCTTGACCA 5'- GGAGGCAGAGACAGTTGGAG 270 bp Wild-type/390 bp Mutant	(Marino et al. 2000)
Rosa26$^{LSL-YFP}$	B6.129(N?)	Stanger Lab Perelman School of Medicine at the University of Pennsylvania	5'- AAAGTCGCTCTGAGTTGTTAT 5'- GGAGCGGGAGAAATGGATATG 5'-AAGACCGCGAAGAGTTTGTC 600 bp Wild-type/320 bp Transgene	(Srinivas et al. 2001)

Table 0-1. Mouse strains used to generate ACKPY mice.

ACKPY Breeding

Over the course of six generations I crossed these 5 alleles into two parental strains: ACPY (*Atp4b-Cre;Cdh1$^{fl/fl}$;Trp53$^{fl/fl}$;Rosa26$^{LSL-YFP/LSL-YFP}$*) and CKPY (*Kras$^{LSL-G12D/+}$;Cdh1$^{fl/fl}$;Trp53$^{fl/fl}$;Rosa26$^{LSL-YFP/LSL-YFP}$*). When interbred, these lines produced 3 useful genotypes: ¼ are the desired ACKPY; ¼ are the first breeder genotype, ACPY; and ¼ are the second breeder genotype, CKPY (Figure 0-1). Of note, the ACPY group is

the double conditional knockout of *Cdh1* and *Trp53*, from Shimada et al 2012, with the addition of conditional YFP expression.

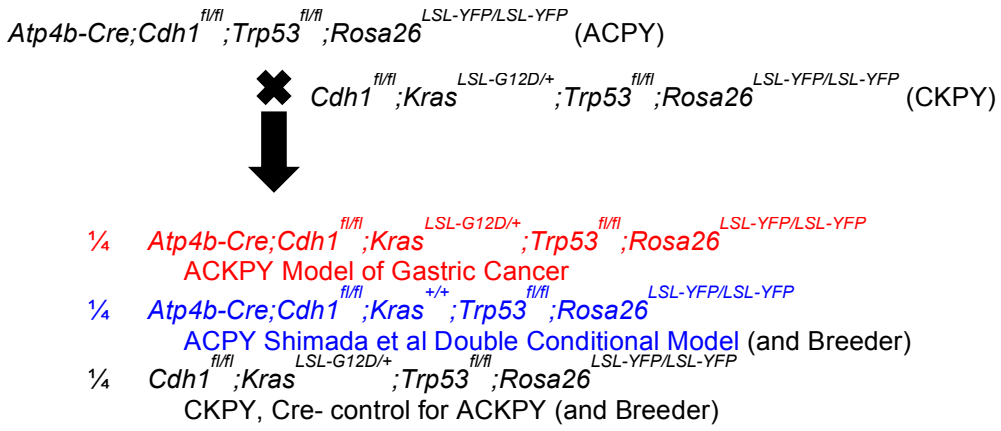

Figure 0-1. Breeding scheme to derive ACKPY mice and relevant controls.

Cdh1$^{fl/+}$ and *Cdh1*$^{+/+}$ Breeding

To investigate the dependence of our ACKPY model on *Cdh1* loss I bred one or two alleles of wild-type Cdh1 back onto the ACKPY mice. These *Cdh1*$^{fl/+}$ and *Cdh1*$^{+/+}$ mice were bred by crossing ACPY mice to KPY mice (*Kras*$^{LSL\text{-}G12D/+}$;*Trp53*$^{fl/fl}$;*Rosa26*$^{LSL\text{-}YFP/LSL\text{-}YFP}$) mice for one or more generations.

Survival Analysis

For ACKPY mice, end point was reached at natural death or humane euthanasia at loss of 20% maximum body weight. To account for the mixed background, ten independent breeding pairs were utilized, each contributing two sibling pairs of ACKPY and ACPY mice (excepting one breeding pair that only contributed one ACPY sibling).

For *Cdh1*$^{fl/+}$ and *Cdh1*$^{+/+}$ mice, end point was reached at natural death or humane euthanasia at loss of 20% maximum body weight. Animals that required humane

euthanasia for subcutaneous tumor burden > 2 cm^3 were censored in the analysis. To account for the mixed background, at least 10 independent breeding pairs were utilized in generating the cohorts.

Metastatic Analysis

Ten of the ACKPY mice from the survival cohort were analyzed for metastases. Epigastric fat, liver, lungs, and any abnormal lesions were dissected and analyzed (see Histology and Immunofluorescence).

Analysis of Disease Progression

Five ACKPY and five CKPY matched Cre negative control mice were sacrificed at 3, 6, and 9 weeks. To account for mixed background, five independent sets of ACKPY and CKPY negative control mice were used from five independent breeding pairs. Stomachs were dissected out and analyzed (see Histology and Immunofluorescence).

In vivo Drug Treatments

Drug treatments were initiated in 4-week-old mice ACKPY mice. MEK inhibitor (PD0325901, APExBIO) was administered *ad libitum* in the mouse chow (Purina 5010) at 7 mg/kg (incorporation by Research Diets Inc.). PKF118-310 (EMD Millipore) was administered 3x weekly as an IP injection of a 0.1 mg/mL solution in 0.1% DMSO at a dose of 1 mg/kg, control mice received volumetrically equivalent doses of 0.1% DMSO via IP injection. Mice were analyzed for survival (see Survival Analysis).

Intra-tracheal AdenoCre Inoculation

Viral precipitates were formed by mixing $2.5x10^7$ pfu of AdenoCre (University of Iowa Viral Vector Core Facility) and 0.6 μmoles $CaCl_2$ (Sigma) to a total volume of 60 μL in DMEM (Gibco) per mouse and incubating at room temperature for 10 minutes. Mice of the indicated genotypes were anesthetized, intubated with a 22 g angiocatheter, and inoculated with 60 μL of viral precipitates via the catheter.

v. Microbiome Study

Microbiome Depletion

Microbiome depletion was achieved by antibiotic administration via the drinking water *ad libitum* at 1 g/L ampicillin (Polyflex, Boehringer Ingelheim Vetmedica, Inc), 1 g/L neomycin (NeoMed 325, Bimeda Inc), 1 g/L metronidazole (Watson Pharma Inc.), 0.5 g/L vancomycin (vancomycin hydrochloride, Mylan Institutional LLC), and 4 g/L sucralose (Splenda, McNeil Nutritionals, LLC).

Quantification of Microbiome Depletion

At necropsy gastric contents and cecal contents were flash frozen. DNA was extracted from 50-300 mg of gastric or cecal contents using the QIAamp Fast DNA Stoool Mini Kit (QIAGEN) according to the manufacturers instructions. qPCR was performed on a ViiA 7 Real-Time PCR System (Thermo Fisher Scientific) using SYBR Green PCR Master Mix (Thermo Fisher Scientific) according to the manufacturers directions using 20 ng of stomach or cecal content DNA per 10 μL reaction. Amplifications were performed as technical triplicates and biological quadruplicates.

Generic 16S rRNA primers 5'-ACTCCTACGGGAGGCAGCAGT (UniF340) and 5'-ATTACCGCGGCTGCTGGC (UniR514) were used for amplification (Barman et al. 2008).

vi. Detect of Circulating Tumor Cells

Blood Collection and RBC Lysis

A 1 mL insulin syringe (BD #329412) was coated with 1 mg/mL heparin (Sigma #H3149-250KU) in PBS (Sigma #D5652-10X1L). As much blood as possible was collected by cardiac puncture and transferred to an EDTA coated tube (BD #367841). The remainder of the procedure was carried out in the dark. 100-200 ul of blood was RBC lysed by the addition of 5 volumes of RBC lysis buffer (G-Biosciences #786-650) and incubated at room temperate for 5 min with mixing. FACS buffer (PBS + 5% FBS + 2 mM EDTA) was added to the lysis reaction up to 3 mLs, mixed, and centrifuged at 2400 x g for 5 min. The supernatant was removed and the cell pellet resuspended in 100 ul FACS Buffer.

CD45 Staining and Flow Cytometric Analysis

1 ul of anti-CD45-APC (Biolegend #103112) was added to 100 ul of suspended cells, mixed and incubated in the darkat room temperature for 15 min. To wash, 500 ul of FACS buffer was added, the suspension mixed, centrifuged at 400 x g for 5 min, and the supernatant discarded. The cell pellet was resuspended in 300-500 ul FACS buffer. Immediately prior to flow cytometric analaysis 2 ul of 5 mg/mL DAPI (ThermoFisher Scientific #D1306) was added to the cell suspension and mixed for live/dead

discrimination. The samples were run on a BD FACSVerse flow cytometer and CTCs per sample were quantified (defined as DAPI-, CD45-, YFP+).

vii. Histology

Tissue Preparation

Tissues were dissected from indicated mice, fixed in 10% formalin in phosphate buffered saline (PBS), and dehydrated. Stomachs were opened along the greater curvature, washed of contents in PBS, the forestomach stomach was removed, and the glandular stomach cut into two or three levels to be embedded together. The Abramson Family Cancer Research Institute (AFCRI) histology core facility embedded the tissues in paraffin, sectioned them at 5 um, and provided me with unstained slides or stained them with hematoxylin and eosin (H&E).

Immunofluorescence

Unstained sections were warmed to 55 C, de-waxed in two xylene washes for 10 minute each, and rehydrated through an ethanol gradient (100%, 100%, 95%, 70%, 50%, 0%, 0%, 0%, 5 minutes each). Antigen retrieval was performed in a 2100 Retriever (Aptum Biologics Ltd.) using Antigen Unmasking Solution (Vector Labs). Samples were then washed three times in H_2O and equilibrated to phosphate buffered saline (PBS), 5 minutes each. They were then permeabilized in 0.2% Triton-X in PBS for 45 minutes. Sections were washed three times with PBS and treated with blocking solution (10% goat serum and 1% bovine serum albumin in PBS) for 1 hour. Hybridization of non- mouse

primary antibodies was performed overnight in blocking solution at 4 C (see Table 0-2 for antibody information and dilutions).

For mouse antibodies, sections were triple washed with PBS for 5 min each then blocked with Streptavidin/Biotin Blocking Kit (Vector Labs): sections were incubated with streptavidin solution for 15 minutes, washed twice with PBS for 5 min each, and the incubation and washes repeated with biotin solution. Hybridization of mouse primary antibody (see Table 0-2 for antibody information and dilutions) was done using the Mouse on Mouse (M.O.M.) Basic Kit (Vector Labs): sections were incubated for 1 hour in M.O.M. Mouse Ig Blocking Reagent, washed twice in PBS for 2 minutes each, equilibrated to M.O.M. Diluent for 5 minutes, treated with primary antibody in M.O.M. Diluent for 30 minutes at room temperature, washed twice in PBS for 2 minutes, and incubated with M.O.M. Biotinylated Anti-Mouse IgG Reagent in M.O.M. Diluent for 10 minutes.

For non-mouse antibodies or continuing after hybridization to mouse antibody, sections were triple washed with PBS for 5 min each and then incubated with secondary antibody diluted 1:1000 in 1% bovine serum albumin in PBS for 2 hours at room temperature. They were again triple washed with PBS for 5 min each and mounted with Fluor-Gel II with DAPI (Electron Microscopy Sciences).

Target	**Company**	**Catalog #**	**Dilution**	**Host**	**Secondary (Thermo Fisher Scientific Catalog #)**
YFP (anti-GFP)	Abcam	ab13970	1:1000	Chicken	anti-Chicken Alexa Fluor 488 (A-11039)
E-cadherin	BD	610181	1:1000	Mouse	AlexaFluor 555 conjugated Streptavidin (S-21381)
β-catenin	CST	8480	1:100	Rabbit	anti-Rabbit Alexa Fluor 594 (A-21207)
pERK	CST	4370	1:200	Rabbit	anti-Rabbit Alexa Fluor 594 (A-21207)

Table 0-2. Antibody information for immunofluorescence staining.

Immunohistochemistry

Unstained sections were warmed to 55 C, de-waxed in two xylene treatments for 10 minute each and rehydrated through an ethanol gradient (100%, 100%, 95%, 70%, 50%, 0%, 0%, 0%, 5 minutes each). Antigen retrieval was performed in a 2100 Retriever (Aptum Biologics Ltd.) using Antigen Unmasking Solution (Vector Labs). Samples were then washed three times in H_2O and further washed and permeabilized in Tris Buffered Saline (TBS, BioRad) + 0.25% Tween (BioRad), referred to as TBST, for two washes of 5 minutes each. Sections were treated with blocking solution (10% goat serum and 1% bovine serum albumin in TBST) for 1 hour. Hybridization of with primary antibody was performed overnight in blocking solution at 4 C (see Table 0-3 for antibody information and dilutions).

Sections were washed twice with TBST and once with TBS, 5 minutes each, and endogenous peroxidases oversaturated by incubation with 0.3% H_2O_2 in TBS. Samples were triple washed with TBST, 5 minutes each, and hybridized to secondary antibody (see Table 0-3) in blocking buffer for 1 hour at room temperature. Enzymatic detection was performed using the Vectastain ABC HRP Kit (Vector Labs) and DAB Peroxidase (HRP) Substrate Kit (Vector Labs). Sections were triple washed with TBST, double washed with TBS (5 minutes each) and hybridized to Vectastain ABC HRP reagent (prepared according to manufacturers instructions) for 30 minutes at room temperature. Slides were again washed twice with TBST and twice with TBS, 5 min each, and then incubated with DAB Substrate (prepared according to manufacturers instructions) for the time indicated in Table 0-3. Washing with H_2O stopped reaction. Samples were then

counterstained in Hematoxylin (50:50 solution in H_2O) for 3 minutes at room temperature and washed under running H_2O for 5 minutes. Slides were dehydrated through a series of ethanol solutions (80%, 95%, 100%. 100%) for 5 minutes each and two xylene washes of 20 minutes each. Sections were mounted using PROTOCOL SecureMount (Fisher) and coverslips.

Target	Company	Catalog#	Dilution	Host	Secondary Dilution (Company & Catalog #)	Time to Develop
pERK	CST	4370	1:200	Rabbit	Biotinylated Goat Anti-Rabbit IgG Antibody 1:200 (Vector Labs BA-1000)	190 sec
Isotype	CST	3900	1:2000	Rabbit		

Table 0-3. Antibodies for immunohistochemical staining.

Image Acquisition

Bright field and epifluorescence images were acquired on a Leica DMI6000B microscope and processed using the LAS-AF software or a Zeiss Axio Imager.M2 microscope and processed using the ZEN 2 software. Confocal images were acquired on a Leica TCS SP5 laser scanning confocal microscope and processed using the LAS-AF software.

viii. Cell Lines

Derivation

Indicated tissue was harvested from mice that had reached humane end-point. Tissues were minced and digested in collagenase II (2.5 mg/mL, Worthington) and DNase (0.5 mg/mL, Worthington) in HBSS (Gibco) at 37 C for 45 minutes. Alternatively, tissue and collagenase II/DNase solution were placed in a C tube (Miltenyi Biotec) and a single cell suspension was generated using a gentleMACS Octo Dissociator with Heaters program "37_m_TDK_1" (Miltenyi Biotec). Excess Fetal Bovine Serum (FBS, Hyclone) was added to quench enzymes and digested tissue was pelleted by centrifugation. Pellet was

resuspended and plated in normal growth medium: Advanced DMEM (Cellgro) + 10% FBS + Penicillin/Streptomycin (Lonza) + L-glutamine (Gibco). After 24 hours incubation at 37 C under 5% CO_2, adherent cells were washed three times with phosphate buffered saline (PBS, Sigma) and medium replaced.

Passaging of Cell Lines

Cell lines were maintained in Advanced DMEM (Cellgro) + 10% FBS + Penicillin/Streptomycin (Lonza) + L-glutamine (Gibco) on tissue culture treated plastic in 37 C incubators under 5% CO_2. Sub-cultivation was performed by washing adherent cells with PBS and incubating with 0.25% Trypsin-EDTA (Gibco) until detached. Trypsin was quenched by the addition of excess complete medium. Cells were re-plated at a sub-culture ratio of 1:5 or higher.

Flank Tumor Formation

Cell lines were sub-cultured for several passages prior to use. Cells were harvested with 0.25% Trypsin-EDTA, quenched with excess FBS, washed with PBS, and injected subcutaneously in the flank at $5x10^6$ cells per 0.1 cc PBS per mouse. Tumors were measured every 2-3 days using digital calipers (Fisher) and tumor volume calculated as $(0.5)*(width^2)*(length)$. For experimental model of metastasis, flank tumors were resected under sterile conditions when tumor volumes were approximately 500 mm^3. Mice were euthanized and lung tissue analyzed for metastasis three weeks post resection.

ix. Gene Expression Analysis

RNA isolation

Glandular stomachs were dissected from indicated mice, homogenized using a gentleMACS Dissociator with M tubes (Miltenyi Biotec) in QIAzol Lysis Reagent (Qiagen), and RNA isolation performed using the RNeasy Microarray Tissue Mini Kit with optional DNase treatment (Qiagen) according to the manufacturers protocols. Quantification of total RNA was performed on a NanoDrop (Thermo Fisher Scientific).

Microarray Target Preparation and Hybridization

The UPENN Molecular Profiling Facility provided microarray services, including quality control tests of the total RNA samples by Agilent Bioanalyzer and Nanodrop spectrophotometry. All protocols were conducted as described in the Affymetrix WT Plus Reagent Kit Manual and the Affymetrix GeneChip Expression Analysis Technical Manual. Briefly, 250ng of total RNA was converted to first-strand cDNA using reverse transcriptase primed by poly(T) and random oligomers that incorporated the T7 promoter sequence. Second-strand cDNA synthesis was followed by *in vitro* transcription with T7 RNA polymerase for linear amplification of each transcript, and the resulting cRNA was converted to cDNA, fragmented, assessed by Bioanalyzer, and biotinylated by terminal transferase end labeling. Five and a half micrograms of labeled cDNA were added to Affymetrix hybridization cocktails, heated at 99ºC for 5 min and hybridized for 16 h at 45ºC to Mouse Transcriptome 1.0 ST GeneChips (Affymetrix Inc., Santa Clara CA) using the GeneChip Hybridization oven 645. The microarrays were then washed at low (6X SSPE) and high (100mM MES, 0.1M NaCl) stringency and stained with

streptavidin-phycoerythrin. Fluorescence was amplified by adding biotinylated anti-streptavidin and an additional aliquot of streptavidin-phycoerythrin stain. A GeneChip 3000 7G scanner was used to collect fluorescence signal. Affymetrix Command Console and Expression Console were used to quantitate expression levels for targeted genes; default values provided by Affymetrix were applied to all analysis parameters.

Principle Component Analysis, Hierarchical Clustering, and Heat Maps

Principle Component Analysis was performed using Expression Console Software (Affymetrix). The Penn Genomic Analysis Core Bioinformatics group performed unsupervised hierarchical clustering of *Cdh1*$^{fl/fl}$ and *Cdh1*$^{fl/+}$ stomach tissue expression data using Partek Genomics Suite (Partek Inc). Hierarchical clustering and heat map production for *Cdh1*$^{fl/+}$ stomach and subcutaneous tumor expression data was performed using GenePattern 2.0 Software (Reich et al. 2006): HierarchicalClustering (Eisen et al. 1998), HierarchicalClusteringViewer, and HeatMapViewer modules.

Differential Gene Expression Analysis

Differentially expressed genes were determined using the Transcriptome Analysis Console (TAC) Software (Affymetrix) with a FDR q-value cut-off of 5% and a fold-change cut-off of 2.

Gene Set Overlap Analysis

Differentially expressed mouse genes were manually mapped to their human homologs using the HomoloGene database (http://www.ncbi.nlm.nih.gov/homologene) from the National Center for Biotechnology Information (NCBI) (Geer et al. 2010). Gene set

overlaps were computed for gene lists using the Investigate Gene Sets function (http://software.broadinstitute.org/gsea/msigdb/annotate.jsp) on the Gene Set Enrichment Analysis page of the Broad Institute (Subramanian et al. 2005).

Quantitative Real-Time Polymerase Chain Reaction (qPCR)

Complementary DNA (cDNA) was synthesized using the High Capacity cDNA Reverse Transcription Kit (Thermo Fisher Scientific) according to the manufacturers directions with 2 μg RNA per 10 μL reaction. qPCR was performed on a ViiA 7 Real-Time PCR System (Thermo Fisher Scientific) using SYBR Green PCR Master Mix (Thermo Fisher Scientific) according to the manufacturers directions using 0.5 μL cDNA per 10 μL reaction. Amplifications were performed as technical quadruplicates and biological sextuplicates. Values were normalized to HPRT expression. Mouse gene-specific primers (Table 0-4) were selected from PrimerBank (X. Wang and Seed 2003; Spandidos et al. 2008; Spandidos et al. 2010).

Gene	Forward Primer	Reverse Primer	Amplicon Size	PrimerBank ID
Hprt	5'-TCAGTCAACGGGGGACATAAA	5'-GGGGCTGTACTGCTTAACCAG	142 bp	7305155a1
Myc	5'-ATGCCCCTCAACGTGAACTTC	5'-CGCAACATAGGATGGAGAGCA	228 bp	27545183a1
Ccnd1	5'-GCGTACCCTGACACCAATCTC	5'-CTCCTCTTCGCACTTCTGCTC	183 bp	6680868a1
MMP7	5'-CTGCCACTGTCCCAGGAAG	5'-GGGAGAGTTTTCCAGTCATGG	175 bp	6754716a1
Axin2	5'-TGACTCTCCTTCCAGATCCCA	5'-TGCCCACACTAGGCTGACA	105 bp	31982733a1
Lef1	5'-TGTTTATCCCATCACGGGTGG	5'-CATGGAAGTGTCGCCTGACAG	67 bp	27735019a1
Cd44v1	5'-CACCATTGCCTCAACTGTGC	5'-TTGTGGGCTCCTGAGTCTGA	116 bp	6491804a1

Table 0-4. Quantitative Real-Time Polymerase Chain Reaction Primers.

x. Quantification and Statistics

Lung Tumor Area Quantification

Area quantification was performed using Fiji (Schneider, Rasband, and Eliceiri 2012; Schindelin et al. 2012; Schindelin et al. 2015) image analysis software using the Adjust

Threshold Color (Thresholding method: Default, Color space: HSB), Select, and Measure functions. Tumor area settings were Hue 205-231, Saturation 40-120, and Brightness 90-225. Total lung area settings were Hue 0-255, Saturation 0-255, and Brightness 0-184. Data is represented as tumor area divided by total lung area for one section containing at least 4 of 5 lung lobes.

pERK Immunofluorescence Quantification

Area quantification was performed using Fiji (Schneider, Rasband, and Eliceiri 2012; Schindelin et al. 2012; Schindelin et al. 2015) image analysis software using the Adjust Threshold Color, Select, and Measure functions. pERK and YFP overlap area settings for Adjust Color Threshold (Thresholding method: Default, Color space: HSB) were Hue 40-50, Saturation 0-225, and Brightness autoset by program (with "Dark background" radio button selected). YFP area settings for Adjust Color Threshold (Thresholding method: Default, Color space: Lab) were L* auto-set by program, a* 0-150, and b* 0-225 (with "Dark background" radio button selected). Data is represented as pERK and YFP overlap area divided by YFP area for 1-2 images per tissue level over 2-3 tissue levels per sample.

pERK Immunohistochemistry Quantification

Area quantification was performed using Fiji (Schneider, Rasband, and Eliceiri 2012; Schindelin et al. 2012; Schindelin et al. 2015) image analysis software using the Adjust Threshold Color (Thresholding method: Default, Color space: HSB), Select, and Measure functions. pERK staining area settings were Hue 0-40, Saturation 0-255, and Brightness 0-184. Total stomach tissue area settings were Hue 0-255, Saturation 0-255, and

Brightness 0-184. Data is represented as pERK staining area divided by total stomach tissue area for 2-3 tissue planes.

Statistics

Statistical analyses (other than those previously described for microarray analysis) were performed in Prism 5 (GraphPad Software). Survival analysis p-values were calculated using the Log-rank (Mantel-Cox) test. All other p-values were calculated using the student's t-test (unpaired, two-tailed).

BIBLIOGRAPHY

Adler, Douglas G., Francis A. Farraye, and James M. Crawford. 2015. "Gastrointestinal Tract Endoscopic and Tissue Processing Techniques and Normal Histology." In , edited by Robert D. Odze and John R. Goldblum, Third edit, 4–33e.3. Philadelphia: Saunders/Elsevier. https://www.clinicalkey.com/#!/content/book/3-s2.0-B9781455707478000017.

Andersson, Patrik, Jacqueline McGuire, Carlos Rubio, Katarina Gradin, Murray L Whitelaw, Sven Pettersson, Annika Hanberg, and Lorenz Poellinger. 2002. "A Constitutively Active Dioxin/aryl Hydrocarbon Receptor Induces Stomach Tumors." *Proceedings of the National Academy of Sciences of the United States of America* 99 (15). National Academy of Sciences: 9990–95. doi:10.1073/pnas.152706299.

Andl, Claudia D, and Anil K Rustgi. 2005. "No One-Way Street: Cross-Talk between E-Cadherin and Receptor Tyrosine Kinase (RTK) Signaling: A Mechanism to Regulate RTK Activity." *Cancer Biology & Therapy* 4 (1): 28–31. http://www.ncbi.nlm.nih.gov/pubmed/15662113.

Avital, Itzhak, Alexander Stojadinovic, Peter W. T. Pisters, David P. Kelsen, and Christopher G. Willett. 2015. "Cancer of the Stomach." In *DeVita, Hellman, and Rosenberg's Cancer: Principles & Practice of Oncology*, edited by Vincent T. Jr. DeVita, Theodore S. Lawrence, and Steven A. Rosenberg, 10th editi. Philadelphia, PA: Lippincott Williams & Wilkins.

Barbáchano, A, P Ordóñez-Morán, J M García, A Sánchez, F Pereira, M J Larriba, N Martínez, et al. 2010. "SPROUTY-2 and E-Cadherin Regulate Reciprocally and

Dictate Colon Cancer Cell Tumourigenicity." *Oncogene* 29 (34). Nature Publishing Group: 4800–4813. doi:10.1038/onc.2010.225.

Bardeesy, N., A. J. Aguirre, G. C. Chu, K.-h. Cheng, L. V. Lopez, A. F. Hezel, B. Feng, et al. 2006. "Both p16Ink4a and the p19Arf-p53 Pathway Constrain Progression of Pancreatic Adenocarcinoma in the Mouse." *Proceedings of the National Academy of Sciences* 103 (15). National Academy of Sciences: 5947–52. doi:10.1073/pnas.0601273103.

Barker, Nick, Meritxell Huch, Pekka Kujala, Marc van de Wetering, Hugo J. Snippert, Johan H. van Es, Toshiro Sato, et al. 2010. "Lgr5+ve Stem Cells Drive Self-Renewal in the Stomach and Build Long-Lived Gastric Units In Vitro." *Cell Stem Cell* 6 (1): 25–36. doi:10.1016/j.stem.2009.11.013.

Barman, Melissa, David Unold, Kathleen Shifley, Elad Amir, Kueichun Hung, Nicolaas Bos, and Nita Salzman. 2008. "Enteric Salmonellosis Disrupts the Microbial Ecology of the Murine Gastrointestinal Tract." *Infection and Immunity* 76 (3). American Society for Microbiology: 907–15. doi:10.1128/IAI.01432-07.

Bass, Adam J., Vesteinn Thorsson, Ilya Shmulevich, Sheila M. Reynolds, Michael Miller, Brady Bernard, Toshinori Hinoue, et al. 2014. "Comprehensive Molecular Characterization of Gastric Adenocarcinoma." *Nature* 513 (7517). Nature Publishing Group: 202–9. doi:10.1038/nature13480.

Birchmeier, W, J Hülsken, and J Behrens. 1995. "E-Cadherin as an Invasion Suppressor." *Ciba Foundation Symposium* 189: 124-36-41, 174–76. http://www.ncbi.nlm.nih.gov/pubmed/7587628.

Blanpain, Cédric. 2013. “Tracing the Cellular Origin of Cancer.” *Nature Cell Biology* 15 (2). Nature Research: 126–34. doi:10.1038/ncb2657.

Boussadia, Oréda, Stefanie Kutsch, Andreas Hierholzer, Véronique Delmas, and Rolf Kemler. 2002. “E-Cadherin Is a Survival Factor for the Lactating Mouse Mammary Gland.” *Mechanisms of Development* 115 (1): 53–62. doi:10.1016/S0925-4773(02)00090-4.

Brabletz, T, A Jung, S Dag, F Hlubek, and T Kirchner. 1999. “Beta-Catenin Regulates the Expression of the Matrix Metalloproteinase-7 in Human Colorectal Cancer.” *The American Journal of Pathology* 155 (4). American Society for Investigative Pathology: 1033–38. http://www.ncbi.nlm.nih.gov/pubmed/10514384.

Brault, V, R Moore, S Kutsch, M Ishibashi, D H Rowitch, A P McMahon, L Sommer, et al. 2001. “Inactivation of the Beta-Catenin Gene by Wnt1-Cre-Mediated Deletion Results in Dramatic Brain Malformation and Failure of Craniofacial Development.” *Development (Cambridge, England)* 128 (8). The Company of Biologists Ltd: 1253–64. doi:10.1074/jbc.271.3.1520.

Braun, Benjamin S, David A Tuveson, Namie Kong, Doan T Le, Scott C Kogan, Jacob Rozmus, Michelle M Le Beau, Tyler E Jacks, and Kevin M Shannon. 2004. “Somatic Activation of Oncogenic Kras in Hematopoietic Cells Initiates a Rapidly Fatal Myeloproliferative Disorder.” *Proceedings of the National Academy of Sciences of the United States of America* 101 (2). National Academy of Sciences: 597–602. doi:10.1073/pnas.0307203101.

Brembeck, Felix H, Franz S Schreiber, Therese B Deramaudt, Linden Craig, Ben

Rhoades, Gary Swain, Paul Grippo, Doris A Stoffers, Debra G Silberg, and Anil K Rustgi. 2003. “The Mutant K-Ras Oncogene Causes Pancreatic Periductal Lymphocytic Infiltration and Gastric Mucous Neck Cell Hyperplasia in Transgenic Mice.” *Cancer Research* 63 (9). American Association for Cancer Research: 2005–9. doi:10.1016/0092-8674(88)90571-5.

Caca, K, F T Kolligs, X Ji, M Hayes, J Qian, A Yahanda, D L Rimm, J Costa, and E R Fearon. 1999. “Beta- and Gamma-Catenin Mutations, but Not E-Cadherin Inactivation, Underlie T-Cell Factor/lymphoid Enhancer Factor Transcriptional Deregulation in Gastric and Pancreatic Cancer.” *Cell Growth & Differentiation : The Molecular Biology Journal of the American Association for Cancer Research* 10 (6). AACR: 369–76. http://www.ncbi.nlm.nih.gov/pubmed/10392898.

Cantorna, M T, and E Balish. 1990. “Inability of Human Clinical Strains of Helicobacter Pylori to Colonize the Alimentary Tract of Germfree Rodents.” *Canadian Journal of Microbiology* 36 (4): 237–41. http://www.ncbi.nlm.nih.gov/pubmed/2357642.

Caulin, Carlos, Thao Nguyen, Gene A. Lang, Thea M. Goepfert, Bill R. Brinkley, Wei-Wen Cai, Guillermina Lozano, et al. 2007. “An Inducible Mouse Model for Skin Cancer Reveals Distinct Roles for Gain- and Loss-of-Function p53 Mutations.” *Journal of Clinical Investigation* 117 (7). American Society for Clinical Investigation: 1893–1901. doi:10.1172/JCI31721.

Cerami, E., J. Gao, U. Dogrusoz, B. E. Gross, S. O. Sumer, B. A. Aksoy, A. Jacobsen, et al. 2012. “The cBio Cancer Genomics Portal: An Open Platform for Exploring Multidimensional Cancer Genomics Data.” *Cancer Discovery* 2 (5). American

Association for Cancer Research: 401–4. doi:10.1158/2159-8290.CD-12-0095.

Ceteci, Fatih, Semra Ceteci, Christiaan Karreman, Boris W. Kramer, Esther Asan, Rudolf Götz, and Ulf R. Rapp. 2007. "Disruption of Tumor Cell Adhesion Promotes Angiogenic Switch and Progression to Micrometastasis in RAF-Driven Murine Lung Cancer." *Cancer Cell* 12 (2): 145–59. doi:10.1016/j.ccr.2007.06.014.

Chan, Annie On On. 2006. "E-Cadherin in Gastric Cancer." *World Journal of Gastroenterology* 12 (2). Baishideng Publishing Group Inc: 199–203. http://www.ncbi.nlm.nih.gov/pubmed/16482618.

Chan, Iris T., Jeffery L. Kutok, Ifor R. Williams, Sarah Cohen, Lauren Kelly, Hirokazu Shigematsu, Leisa Johnson, et al. 2004. "Conditional Expression of Oncogenic K-Ras from Its Endogenous Promoter Induces a Myeloproliferative Disease." *Journal of Clinical Investigation* 113 (4). American Society for Clinical Investigation: 528–38. doi:10.1172/JCI20476.

Chibon, Frédéric, Pauline Lagarde, Sébastien Salas, Gaëlle Pérot, Véronique Brouste, Franck Tirode, Carlo Lucchesi, et al. 2010. "Validated Prediction of Clinical Outcome in Sarcomas and Multiple Types of Cancer on the Basis of a Gene Expression Signature Related to Genome Complexity." *Nature Medicine* 16 (7). Nature Research: 781–87. doi:10.1038/nm.2174.

Chiurillo, Miguel Angel. 2015. "Role of the Wnt/β-Catenin Pathway in Gastric Cancer: An in-Depth Literature Review." *World Journal of Experimental Medicine* 5 (2). Baishideng Publishing Group Inc: 84–102. doi:10.5493/wjem.v5.i2.84.

Chung, C K, and H N Antoniades. 1992. "Expression of c-Sis/platelet-Derived Growth

Factor B, Insulin-like Growth Factor I, and Transforming Growth Factor Alpha Messenger RNAs and Their Respective Receptor Messenger RNAs in Primary Human Gastric Carcinomas: In Vivo Studies with in Situ Hybridiz." *Cancer Research* 52 (12): 3453–59. http://www.ncbi.nlm.nih.gov/pubmed/1317752.

Correa, Pelayo. 1992. "Human Gastric Carcinogenesis: A Multistep and Multifactorial Process First American Cancer Society Award Lecture on Cancer Epidemiology and Prevention 1." *CANCER RESEARCH* 52: 6735–40.

Crawford, Howard C, Barbara M Fingleton, Laura A Rudolph-Owen, Kathleen J Heppner Goss, Bonnee Rubinfeld, Paul Polakis, and Lynn M Matrisian. 1999. "The Metalloproteinase Matrilysin Is a Target of β-Catenin Transactivation in Intestinal Tumors." *Oncogene* 18 (18). Nature Publishing Group: 2883–91. doi:10.1038/sj.onc.1202627.

Cristescu, Razvan, Jeeyun Lee, Michael Nebozhyn, Kyoung-Mee Kim, Jason C Ting, Swee Seong Wong, Jiangang Liu, et al. 2015. "Molecular Analysis of Gastric Cancer Identifies Subtypes Associated with Distinct Clinical Outcomes." *Nature Medicine* 21 (5). Nature Publishing Group: 449–56. doi:10.1038/nm.3850.

De Santis, G, S Miotti, M Mazzi, S Canevari, and A Tomassetti. 2009. "E-Cadherin Directly Contributes to PI3K/AKT Activation by Engaging the PI3K-p85 Regulatory Subunit to Adherens Junctions of Ovarian Carcinoma Cells." *Oncogene* 28 (9). Nature Publishing Group: 1206–17. doi:10.1038/onc.2008.470.

Deng, Niantao, Liang Kee Goh, Hannah Wang, Kakoli Das, Jiong Tao, Iain Beehuat Tan, Shenli Zhang, et al. 2012. "A Comprehensive Survey of Genomic Alterations in

Gastric Cancer Reveals Systematic Patterns of Molecular Exclusivity and Co-Occurrence among Distinct Therapeutic Targets." *Gut* 61 (5). BMJ Publishing Group Ltd and British Society of Gastroenterology: 673–84. doi:10.1136/gutjnl-2011-301839.

Dow, Lukas E., Kevin P. O'Rourke, Janelle Simon, Darjus F. Tschaharganeh, Johan H. van Es, Hans Clevers, and Scott W. Lowe. 2015. "Apc Restoration Promotes Cellular Differentiation and Reestablishes Crypt Homeostasis in Colorectal Cancer." *Cell* 161 (7): 1539–52. doi:10.1016/j.cell.2015.05.033.

Downward, Julian. 2003. "Targeting RAS Signalling Pathways in Cancer Therapy." *Nature Reviews Cancer* 3 (1). Nature Publishing Group: 11–22. doi:10.1038/nrc969.

Edgar, R., Michael Domrachev, and Alex E. Lash. 2002. "Gene Expression Omnibus: NCBI Gene Expression and Hybridization Array Data Repository." *Nucleic Acids Research* 30 (1). Oxford University Press: 207–10. doi:10.1093/nar/30.1.207.

Ehlers, S, M Warrelmann, and H Hahn. 1988. "In Search of an Animal Model for Experimental Campylobacter Pylori Infection: Administration of Campylobacter Pylori to Rodents." *Zentralblatt Für Bakteriologie, Mikrobiologie, Und Hygiene. Series A, Medical Microbiology, Infectious Diseases, Virology, Parasitology* 268 (3): 341–46. http://www.ncbi.nlm.nih.gov/pubmed/3261481.

Eisen, M B, P T Spellman, P O Brown, and D Botstein. 1998. "Cluster Analysis and Display of Genome-Wide Expression Patterns." *Proceedings of the National Academy of Sciences of the United States of America* 95 (25). National Academy of Sciences: 14863–68. http://www.ncbi.nlm.nih.gov/pubmed/9843981.

Ferlay, Jacques, Isabelle Soerjomataram, Rajesh Dikshit, Sultan Eser, Colin Mathers, Marise Rebelo, Donald Maxwell Parkin, David Forman, and Freddie Bray. 2015. "Cancer Incidence and Mortality Worldwide: Sources, Methods and Major Patterns in GLOBOCAN 2012." *International Journal of Cancer* 136 (5): E359–86. doi:10.1002/ijc.29210.

Ferlay, J, I Soerjomataram, M Ervik, R Dikshit, S Eser, C Mathers, M Rebelo, DM Parkin, D Forman, and F Bray. 2013. "GLOBOCAN 2012 v1.0." *Cancer Incidence and Mortality Worldwide: IARC CancerBase No. 11 [Internet]*. Lyon, France: International Agency for Research on Cancer; 2013. http://globocan.iarc.fr.

Filali, M., Ningli Cheng, Duane Abbott, Vladimir Leontiev, and John F. Engelhardt. 2002. "Wnt-3A/beta -Catenin Signaling Induces Transcription from the LEF-1 Promoter." *Journal of Biological Chemistry* 277 (36). American Society for Biochemistry and Molecular Biology: 33398–410. doi:10.1074/jbc.M107977200.

Fox, James G., and Timothy C. Wang. 2007. *Inflammation, Atrophy, and Gastric Cancer*. *Journal of Clinical Investigation*. Vol. 117. American Society for Clinical Investigation. doi:10.1172/JCI30111.

Fox, James G, Barbara J Sheppard, Charles A Dangler, Mark T Whary, Melanie Ihrig, and Timothy C Wang. 2002. "Germ-Line p53-Targeted Disruption Inhibits Helicobacter-Induced Premalignant Lesions and Invasive Gastric Carcinoma through down-Regulation of Th1 Proinflammatory Responses." *Cancer Research* 62 (3). American Association for Cancer Research: 696–702. doi:10.1016/s0092-8674(00)81871-1.

Geer, Lewis Y, Aron Marchler-Bauer, Renata C Geer, Lianyi Han, Jane He, Siqian He, Chunlei Liu, Wenyao Shi, and Stephen H Bryant. 2010. "The NCBI BioSystems Database." *Nucleic Acids Research* 38 (Database issue). Oxford University Press: D492-6. doi:10.1093/nar/gkp858.

Giraud, Andrew S., and Louise M. Judd. 2009. "Genetic Models of Gastric Cancer in the Mouse." In *The Biology of Gastric Cancers*, edited by Timothy C. Wang, James G. Fox, and Andrew S. Giraud, 483–512. New York: Springer.

Goldenring, James R., Gregory S. Ray, Robert J. Coffey, Paul C. Meunier, Patrick J. Haley, T.Bradford Barnes, and Bruce D. Car. 2000. "Reversible Drug–induced Oxyntic Atrophy in Rats." *Gastroenterology* 118 (6): 1080–93. doi:10.1016/S0016-5085(00)70361-1.

Gong, Jian, Asahiro Morishita, Kazutaka Kurokohchi, Joji Tani, Kiyohito Kato, Hisaaki Miyoshi, Hideyuki Inoue, et al. 2010. "Use of Protein Array to Investigate Receptor Tyrosine Kinases Activated in Gastric Cancer." *International Journal of Oncology* 36 (1). Spandidos Publications: 101–6.

Gottardi, C J, E Wong, and B M Gumbiner. 2001. "E-Cadherin Suppresses Cellular Transformation by Inhibiting Beta-Catenin Signaling in an Adhesion-Independent Manner." *The Journal of Cell Biology* 153 (5). Rockefeller University Press: 1049–60. doi:10.1083/jcb.153.5.1049.

Graziano, Frada, B. Humar, and P. Guilford. 2003. "The Role of the E-Cadherin Gene (CDH1) in Diffuse Gastric Cancer Susceptibility: From the Laboratory to Clinical Practice." *Annals of Oncology*. doi:10.1093/annonc/mdg486.

Guilford, Parry, Justin Hopkins, James Harraway, Maybelle McLeod, Ngahiraka McLeod, Pauline Harawira, Huriana Taite, Robin Scoular, Andrew Miller, and Anthony E. Reeve. 1998. "E-Cadherin Germline Mutations in Familial Gastric Cancer." *Nature* 392 (6674). Nature Publishing Group: 402–5. doi:10.1038/32918.

Guilford, Parry, Bostjan Humar, and Vanessa Blair. 2010. "Hereditary Diffuse Gastric Cancer: Translation of CDH1 Germline Mutations into Clinical Practice." *Gastric Cancer* 13 (1). Springer Japan: 1–10. doi:10.1007/s10120-009-0531-x.

Han, Sang-Uk, Young-Bae Kim, Hee-Jae Joo, Ki-Baik Hahm, Won-Heung Lee, Yong-Kwan Cho, Dae-Yong Kim, and Myung-Wook Kim. 2002. "Helicobacter Pylori Infection Promotes Gastric Carcinogenesis in a Mice Model." *Journal of Gastroenterology and Hepatology* 17 (3). Blackwell Science Pty: 253–61. doi:10.1046/j.1440-1746.2002.02684.x.

Hanahan, Douglas, and Robert A Weinberg. 2000. "The Hallmarks of Cancer." *Cell* 100 (1): 57–70. doi:10.1016/S0092-8674(00)81683-9.

Hanahan, Douglas, Robert A Weinberg, J.M. Adams, S. Cory, J.A. Aguirre-Ghiso, Z. Ahmed, R. Bicknell, et al. 2011. "Hallmarks of Cancer: The next Generation." *Cell* 144 (5). Elsevier: 646–74. doi:10.1016/j.cell.2011.02.013.

Hayakawa, Yoku, Hiroshi Ariyama, Jitka Stancikova, Kosuke Sakitani, Samuel Asfaha, Bernhard W. Renz, Zinaida A. Dubeykovskaya, et al. 2015. "Mist1 Expressing Gastric Stem Cells Maintain the Normal and Neoplastic Gastric Epithelium and Are Supported by a Perivascular Stem Cell Niche." *Cancer Cell* 28 (6): 800–814. doi:10.1016/j.ccell.2015.10.003.

Hayakawa, Yoku, James Fox, Tamas Gonda, Daniel Worthley, Sureshkumar Muthupalani, and Timothy Wang. 2013. “Mouse Models of Gastric Cancer.” *Cancers* 5 (1). Multidisciplinary Digital Publishing Institute: 92–130. doi:10.3390/cancers5010092.

He, T C, A B Sparks, C Rago, H Hermeking, L Zawel, L T da Costa, P J Morin, et al. 1998. “Identification of c-MYC as a Target of the APC Pathway.” *Science (New York, N.Y.)* 281 (5382). American Association for the Advancement of Science: 1509–12. doi:10.1126/science.281.5382.1509.

Heffner, Caleb S., C. Herbert Pratt, Randal P. Babiuk, Yashoda Sharma, Stephen F. Rockwood, Leah R. Donahue, Janan T. Eppig, and Stephen A. Murray. 2012. “Supporting Conditional Mouse Mutagenesis with a Comprehensive Cre Characterization Resource.” *Nature Communications* 3 (November). Nature Research: 1218. doi:10.1038/ncomms2186.

Herzig, M, F Savarese, M Novatchkova, H Semb, and G Christofori. 2007. “Tumor Progression Induced by the Loss of E-Cadherin Independent of β-catenin/Tcf-Mediated Wnt Signaling.” *Oncogene* 26 (16). Nature Publishing Group: 2290–98. doi:10.1038/sj.onc.1210029.

Hingorani, Sunil R., Emanuel F. Petricoin, Anirban Maitra, Vinodh Rajapakse, Catrina King, Michael A. Jacobetz, Sally Ross, et al. 2003. “Preinvasive and Invasive Ductal Pancreatic Cancer and Its Early Detection in the Mouse.” *Cancer Cell* 4 (6): 437–50. doi:10.1016/S1535-6108(03)00309-X.

Hingorani, Sunil R., Lifu Wang, Asha S. Multani, Chelsea Combs, Therese B.

Deramaudt, Ralph H. Hruban, Anil K. Rustgi, Sandy Chang, and David A. Tuveson. 2005. “Trp53R172H and KrasG12D Cooperate to Promote Chromosomal Instability and Widely Metastatic Pancreatic Ductal Adenocarcinoma in Mice.” *Cancer Cell* 7 (5): 469–83. doi:10.1016/j.ccr.2005.04.023.

Hovanes, Karine, Tony W.H. Li, Jesus E. Munguia, Trung Truong, Tatjana Milovanovic, J. Lawrence Marsh, Randall F. Holcombe, and Marian L. Waterman. 2001. “β-Catenin–sensitive Isoforms of Lymphoid Enhancer Factor-1 Are Selectively Expressed in Colon Cancer.” *Nature Genetics* 28 (1). Nature Publishing Group: 53–57. doi:10.1038/ng0501-53.

Howson, C P, T Hiyama, and E L Wynder. 1986. “The Decline in Gastric Cancer: Epidemiology of an Unplanned Triumph.” *Epidemiologic Reviews* 8 (6): 1–27. http://www.ncbi.nlm.nih.gov/pubmed/3533579.

Humar, Bostjan, Vanessa Blair, Amanda Charlton, Helen More, Iain Martin, and Parry Guilford. 2009. “E-Cadherin Deficiency Initiates Gastric Signet-Ring Cell Carcinoma in Mice and Man.” *Cancer Research* 69 (5). American Association for Cancer Research: 2050–56. doi:10.1158/0008-5472.CAN-08-2457.

Jackson, E L, Kenneth P Olive, David A Tuveson, Roderick Bronson, Denise Crowley, Michael Brown, and Tyler Jacks. 2005. “The Differential Effects of Mutant p53 Alleles on Advanced Murine Lung Cancer.” *Cancer Research* 65 (22). American Association for Cancer Research: 10280–88. doi:10.1158/0008-5472.CAN-05-2193.

Jackson, E L, N Willis, K Mercer, R T Bronson, D Crowley, R Montoya, T Jacks, and D A Tuveson. 2001. “Analysis of Lung Tumor Initiation and Progression Using

Conditional Expression of Oncogenic K-Ras." *Genes & Development* 15 (24). Cold Spring Harbor Laboratory Press: 3243–48. doi:10.1101/gad.943001.

Janssen, Klaus-Peter, Paola Alberici, Hafida Fsihi, Claudia Gaspar, Cor Breukel, Patrick Franken, Christophe Rosty, et al. 2006. "APC and Oncogenic KRAS Are Synergistic in Enhancing Wnt Signaling in Intestinal Tumor Formation and Progression." *Gastroenterology* 131 (4). Elsevier: 1096–1109. doi:10.1053/j.gastro.2006.08.011.

Jeanes, A, C J Gottardi, and A S Yap. 2008. "Cadherins and Cancer: How Does Cadherin Dysfunction Promote Tumor Progression?" *Oncogene* 27 (55). Nature Publishing Group: 6920–29. doi:10.1038/onc.2008.343.

Jho, Eek-hoon, Tong Zhang, Claire Domon, Choun-Ki Joo, Jean-Noel Freund, and Frank Costantini. 2002. "Wnt/beta-catenin/Tcf Signaling Induces the Transcription of Axin2, a Negative Regulator of the Signaling Pathway." *Molecular and Cellular Biology* 22 (4). American Society for Microbiology (ASM): 1172–83. http://www.ncbi.nlm.nih.gov/pubmed/11809808.

Johnson, Leisa, Kim Mercer, Doron Greenbaum, Roderick T. Bronson, Denise Crowley, David A. Tuveson, and Tyler Jacks. 2001. "Somatic Activation of the K-Ras Oncogene Causes Early Onset Lung Cancer in Mice." *Nature* 410 (6832). Nature Publishing Group: 1111–16. doi:10.1038/35074129.

Jones, EG. 1964. "Familial Gastric Cancer." *NZ Med J* 63: 287–96.

Juan, J., T. Muraguchi, G. Iezza, R. C. Sears, and M. McMahon. 2014. "Diminished WNT -> -Catenin -> c-MYC Signaling Is a Barrier for Malignant Progression

of BRAFV600E-Induced Lung Tumors." *Genes & Development* 28 (6). Cold Spring Harbor Laboratory Press: 561–75. doi:10.1101/gad.233627.113.

Kamangar, Farin, You-Lin Qiao, John T. Schiller, Sanford M. Dawsey, Thomas Fears, Xui-Di Sun, Christian C. Abnet, Ping Zhao, Philip R. Taylor, and Steven D. Mark. 2006. "Human Papillomavirus Serology and the Risk of Esophageal and Gastric Cancers: Results from a Cohort in a High-Risk Region in China." *International Journal of Cancer* 119 (3). Wiley Subscription Services, Inc., A Wiley Company: 579–84. doi:10.1002/ijc.21871.

Kaurah, Pardeep, Andrée MacMillan, Niki Boyd, Janine Senz, Alessandro De Luca, Nicki Chun, Gianpaolo Suriano, et al. 2007. "Founder and Recurrent CDH1 Mutations in Families With Hereditary Diffuse Gastric Cancer." *JAMA* 297 (21). American Medical Association: 2360. doi:10.1001/jama.297.21.2360.

Kidger, Andrew M., and Stephen M. Keyse. 2016. "The Regulation of Oncogenic Ras/ERK Signalling by Dual-Specificity Mitogen Activated Protein Kinase Phosphatases (MKPs)." *Seminars in Cell & Developmental Biology* 50: 125–32. doi:10.1016/j.semcdb.2016.01.009.

Kirsch, David G, Daniela M Dinulescu, John B Miller, Jan Grimm, Philip M Santiago, Nathan P Young, G Petur Nielsen, et al. 2007. "A Spatially and Temporally Restricted Mouse Model of Soft Tissue Sarcoma." *Nature Medicine* 13 (8): 992–97. doi:10.1038/nm1602.

Koike, Kazuhiko, Steven H Hinrichst, Kurt J Isselbachert, and Gilbert Jay. 1989. "Transgenic Mouse Model for Human Gastric Carcinoma." *Medical Sciences* 86:

5615–19.

Konda, Y, H Kamimura, H Yokota, N Hayashi, K Sugano, T Takeuchi, K. Araki, et al. 1999. “Gastrin Stimulates the Growth of Gastric Pit with Less-Differentiated Features.” *The American Journal of Physiology* 277 (4 Pt 1). American Physiological Society: G773-84. doi:10.1073/pnas.92.1.160.

La Vecchia, C, E Negri, B D’Avanzo, and S Franceschi. 1990. “Electric Refrigerator Use and Gastric Cancer Risk.” *British Journal of Cancer* 62 (1): 136–37. http://www.ncbi.nlm.nih.gov/pubmed/2390474.

Laprise, Patrick, Marie-Jos༎e Langlois, Marie-Jos༎e Boucher, Christian Jobin, and Nathalie Rivard. 2004. “Down-Regulation of MEK/ERK Signaling by E-Cadherin-Dependent PI3K/Akt Pathway in Differentiating Intestinal Epithelial Cells.” *Journal of Cellular Physiology* 199 (1). Wiley Subscription Services, Inc., A Wiley Company: 32–39. doi:10.1002/jcp.10432.

Lauren, P. 1965. “The Two Histological Main Types Of Gastric Carcinoma: Diffuse and So-Called Intestina-Type Carcinoma. An Attempt At A Histo-Clinical Classification.” *Acta Pathologica et Microbiologica Scandinavica* 64: 31–49. http://www.ncbi.nlm.nih.gov/pubmed/14320675.

Lauwers, Gregory Y. 2015. “Epithelial Neoplasms of the Stomach.” In *Gastrointestinal Tract Endoscopic and Tissue Processing Techniques and Normal Histology*, edited by Robert D. Odze and John R. Goldblum, Third edit, 707–721.e5. Philadelphia, PA: Saunders/Elsevier. https://www.clinicalkey.com/#!/content/book/3-s2.0-B978145570747800025X?scrollTo=%2523s0045.

Lee, A, M Chen, N Coltro, J O'Rourke, S Hazell, P Hu, and Y Li. 1993. "Long Term Infection of the Gastric Mucosa with Helicobacter Species Does Induce Atrophic Gastritis in an Animal Model of Helicobacter Pylori Infection." *Zentralblatt Für Bakteriologie : International Journal of Medical Microbiology* 280 (1–2): 38–50. http://www.ncbi.nlm.nih.gov/pubmed/8280955.

Lee, A, J G Fox, G Otto, and J Murphy. 1990. "A Small Animal Model of Human Helicobacter Pylori Active Chronic Gastritis." *Gastroenterology* 99 (5): 1315–23. http://www.ncbi.nlm.nih.gov/pubmed/2210240.

Lee, Adrian, Jani O 'rourke, Maria Corazon De Ungria, Bronwyn Robertson, George Daskalopoulos, and Michael F Dixon. 1997. "A Standardized Mouse Model of Helicobacter Pylori Infection: Introducing the Sydney Strain." *GASTROENTEROLOGY* 112: 1386–97.

Lefebvre, O, M P Chenard, R Masson, J Linares, A Dierich, M LeMeur, C Wendling, et al. 1996. "Gastric Mucosa Abnormalities and Tumorigenesis in Mice Lacking the pS2 Trefoil Protein." *Science (New York, N.Y.)* 274 (5285). American Association for the Advancement of Science: 259–62. doi:10.1126/science.274.5285.259.

Lemieux, E, S Cagnol, K Beaudry, J Carrier, and N Rivard. 2015. "Oncogenic KRAS Signalling Promotes the Wnt/β-Catenin Pathway through LRP6 in Colorectal Cancer." *Oncogene* 34 (38). Nature Publishing Group: 4914–27. doi:10.1038/onc.2014.416.

Li, Q., S. M. Karam, and J. I. Gordon. 1995. "Simian Virus 40 T Antigen-Induced Amplification of Pre-Parietal Cells in Transgenic Mice.: EFFECTS ON OTHER

GASTRIC EPITHELIAL CELL LINEAGES AND EVIDENCE FOR A p53-INDEPENDENT APOPTOTIC MECHANISM THAT OPERATES IN A COMMITTED PROGENITOR." *Journal of Biological Chemistry* 270 (26). American Society for Biochemistry and Molecular Biology: 15777–88. doi:10.1074/jbc.270.26.15777.

Li, Qiang, Zhiliang Jia, Li Wang, Xiangyu Kong, Qi Li, Kun Guo, Dongfeng Tan, et al. 2012. "Disruption of Klf4 in Villin-Positive Gastric Progenitor Cells Promotes Formation and Progression of Tumors of the Antrum in Mice." *Gastroenterology* 142 (3). NIH Public Access: 531–42. doi:10.1053/j.gastro.2011.11.034.

Li, Tony W-H, Ju-Hui T Ting, Noriko N Yokoyama, Alla Bernstein, Marc van de Wetering, and Marian L Waterman. 2006. "Wnt Activation and Alternative Promoter Repression of LEF1 in Colon Cancer." *Molecular and Cellular Biology* 26 (14). American Society for Microbiology (ASM): 5284–99. doi:10.1128/MCB.00105-06.

Li, XiuBin, Guan Yang, Liang Zhu, Yu-Ling Tang, Chong Zhang, Zhenyu Ju, Xiao Yang, and Yan Teng. 2016. "Gastric Lgr5+ Stem Cells Are the Cellular Origin of Invasive Intestinal-Type Gastric Cancer in Mice." *Cell Research* 26 (7). Nature Publishing Group: 838–49. doi:10.1038/cr.2016.47.

Liu, Xin, Kent-Man Chu, Xin Liu, and Kent-Man Chu. 2014. "E-Cadherin and Gastric Cancer: Cause, Consequence, and Applications." *BioMed Research International* 2014. Hindawi Publishing Corporation: 637308. doi:10.1155/2014/637308.

Lustig, Barbara, Boris Jerchow, Martin Sachs, Sigrid Weiler, Torsten Pietsch, Uwe

Karsten, Marc van de Wetering, et al. 2002. “Negative Feedback Loop of Wnt Signaling through Upregulation of conductin/axin2 in Colorectal and Liver Tumors.” *Molecular and Cellular Biology* 22 (4). American Society for Microbiology (ASM): 1184–93. http://www.ncbi.nlm.nih.gov/pubmed/11809809.

Maretto, S., M. Cordenonsi, S. Dupont, P. Braghetta, V. Broccoli, A. B. Hassan, D. Volpin, G. M. Bressan, and S. Piccolo. 2003. “Mapping Wnt/ -Catenin Signaling during Mouse Development and in Colorectal Tumors.” *Proceedings of the National Academy of Sciences* 100 (6). National Academy of Sciences: 3299–3304. doi:10.1073/pnas.0434590100.

Marino, Silvia, Marc Vooijs, Hanneke van der Gulden, Jos Jonkers, and Anton Berns. 2000. “Induction of Medulloblastomas in p53-Null Mutant Mice by Somatic Inactivation of Rb in the External Granular Layer Cells of the Cerebellum.” *Genes & Development* 14 (8). Cold Spring Harbor Laboratory Press: 994–1004. doi:10.1101/GAD.14.8.994.

Matkar, Smita S, Amy Durham, Angela Brice, Timothy C Wang, Anil K Rustgi, and Xianxin Hua. 2011. “Systemic Activation of K-Ras Rapidly Induces Gastric Hyperplasia and Metaplasia in Mice.” *American Journal of Cancer Research* 1 (4). e-Century Publishing Corporation: 432–45. http://www.ncbi.nlm.nih.gov/pubmed/21761008.

McCormick, Frank, and Osamu Tetsu. 1999. “|[beta]|-Catenin Regulates Expression of Cyclin D1 in Colon Carcinoma Cells.” *Nature* 398 (6726). Nature Publishing Group: 422–26. doi:10.1038/18884.

Mendoza, Michelle C, E Emrah Er, and John Blenis. 2011. "The Ras-ERK and PI3K-mTOR Pathways: Cross-Talk and Compensation." *Trends in Biochemical Sciences* 36 (6). NIH Public Access: 320–28. doi:10.1016/j.tibs.2011.03.006.

Mimata, Ayako, Hiroshi Fukamachi, Yoshinobu Eishi, and Yasuhito Yuasa. 2011. "Loss of E-Cadherin in Mouse Gastric Epithelial Cells Induces Signet Ring-like Cells, a Possible Precursor Lesion of Diffuse Gastric Cancer." *Cancer Science* 102 (5). Blackwell Publishing Ltd: 942–50. doi:10.1111/j.1349-7006.2011.01890.x.

Mito, Jeffrey K., Richard F. Riedel, Leslie Dodd, Guy Lahat, Alexander J. Lazar, Rebecca D. Dodd, Lars Stangenberg, et al. 2009. "Cross Species Genomic Analysis Identifies a Mouse Model as Undifferentiated Pleomorphic Sarcoma/Malignant Fibrous Histiocytoma." Edited by Syed A. Aziz. *PLoS ONE* 4 (11). Public Library of Science: e8075. doi:10.1371/journal.pone.0008075.

Mognol, G P, F R G Carneiro, B K Robbs, D V Faget, and J P B Viola. 2016. "Cell Cycle and Apoptosis Regulation by NFAT Transcription Factors: New Roles for an Old Player." *Cell Death and Disease* 7 (4). Nature Publishing Group: e2199. doi:10.1038/cddis.2016.97.

Mohammed, Maryam K, Connie Shao, Jing Wang, Qiang Wei, Xin Wang, Zachary Collier, Shengli Tang, et al. 2016. "Wnt/β-Catenin Signaling Plays an Ever-Expanding Role in Stem Cell Self-Renewal, Tumorigenesis and Cancer Chemoresistance." *Genes & Diseases* 3 (1). NIH Public Access: 11–40. doi:10.1016/j.gendis.2015.12.004.

Muñoz, N., and J. Asvall. 1971. "Time Trends of Intestinal and Diffuse Types of Gastric

Cancer in Norway." *International Journal of Cancer* 8 (1). Wiley Subscription Services, Inc., A Wiley Company: 144–57. doi:10.1002/ijc.2910080118.

Mutoh, Hiroyuki, Shinji Sakurai, Kiichi Satoh, Kiichi Tamada, Hiroto Kita, Hiroyuki Osawa, Takeshi Tomiyama, et al. 2004. "Development of Gastric Carcinoma from Intestinal Metaplasia in Cdx2-Transgenic Mice." *Cancer Research* 64 (21). American Association for Cancer Research: 7740–47. doi:10.1158/0008-5472.CAN-04-1617.

Nagy, Rebecca, Kevin Sweet, and Charis Eng. 2004. "Highly Penetrant Hereditary Cancer Syndromes." *Oncogene* 23 (38). Nature Publishing Group: 6445–70. doi:10.1038/sj.onc.1207714.

Nakagawa, H., Y. Hikiba, Y. Hirata, J. Font-Burgada, K. Sakamoto, Y. Hayakawa, K. Taniguchi, et al. 2014. "Loss of Liver E-Cadherin Induces Sclerosing Cholangitis and Promotes Carcinogenesis." *Proceedings of the National Academy of Sciences* 111 (3). National Academy of Sciences: 1090–95. doi:10.1073/pnas.1322731111.

Nam, Ki Taek, Hyuk–Joon Lee, Josane F. Sousa, Victoria G. Weis, Ryan L. O'Neal, Paul E. Finke, Judith Romero–Gallo, et al. 2010. "Mature Chief Cells Are Cryptic Progenitors for Metaplasia in the Stomach." *Gastroenterology* 139 (6): 2028–2037.e9. doi:10.1053/j.gastro.2010.09.005.

Nam, Ki Taek, Ryan O'Neal, Yeo Song Lee, Yong Chan Lee, Robert J Coffey, and James R Goldenring. 2012. "Gastric Tumor Development in Smad3-Deficient Mice Initiates from Forestomach/glandular Transition Zone along the Lesser Curvature." *Laboratory Investigation* 92 (6). Nature Publishing Group: 883–95.

doi:10.1038/labinvest.2012.47.

Neel, Nicole F, Timothy D Martin, Jeran K Stratford, Tanya P Zand, David J Reiner, and Channing J Der. 2011. "The RalGEF-Ral Effector Signaling Network: The Road Less Traveled for Anti-Ras Drug Discovery." *Genes & Cancer* 2 (3). Impact Journals, LLC: 275–87. doi:10.1177/1947601911407329.

Nomura, Sachiyo, Hirokazu Yamaguchi, Masako Ogawa, Timothy C Wang, Jeffrey R Lee, and James R Goldenring. 2005. "Alterations in Gastric Mucosal Lineages Induced by Acute Oxyntic Atrophy in Wild-Type and Gastrin-Deficient Mice." *American Journal of Physiology. Gastrointestinal and Liver Physiology* 288 (2). American Physiological Society: G362-75. doi:10.1152/ajpgi.00160.2004.

O'Dell, Michael R, Jing Li Huang, Christa L Whitney-Miller, Vikram Deshpande, Paul Rothberg, Valerie Grose, Randall M Rossi, et al. 2012. "Kras(G12D) and p53 Mutation Cause Primary Intrahepatic Cholangiocarcinoma." *Cancer Research* 72 (6). American Association for Cancer Research: 1557–67. doi:10.1158/0008-5472.CAN-11-3596.

Ohtani, Naoko. 2015. "Microbiome and Cancer." *Seminars in Immunopathology* 37 (1). Springer Berlin Heidelberg: 65–72. doi:10.1007/s00281-014-0457-1.

Okumura, Tomoyuki, Russell E Ericksen, Shigeo Takaishi, Sophie S W Wang, Zinaida Dubeykovskiy, Wataru Shibata, Kelly S Betz, et al. 2010. "K-Ras Mutation Targeted to Gastric Tissue Progenitor Cells Results in Chronic Inflammation, an Altered Microenvironment, and Progression to Intraepithelial Neoplasia." *Cancer Research* 70 (21). American Association for Cancer Research: 8435–45.

doi:10.1158/0008-5472.CAN-10-1506.

Ooi, Chia Huey, Tatiana Ivanova, Jeanie Wu, Minghui Lee, Iain Beehuat Tan, Jiong Tao, Lindsay Ward, et al. 2009. "Oncogenic Pathway Combinations Predict Clinical Prognosis in Gastric Cancer." Edited by Jason G. Mezey. *PLoS Genetics* 5 (10). Public Library of Science: e1000676. doi:10.1371/journal.pgen.1000676.

Oshima, Hiroko, Akihiro Matsunaga, Takashi Fujimura, Tetsuya Tsukamoto, Makoto M. Taketo, and Masanobu Oshima. 2006. "Carcinogenesis in Mouse Stomach by Simultaneous Activation of the Wnt Signaling and Prostaglandin E2 Pathway." *Gastroenterology* 131 (4): 1086–95. doi:10.1053/j.gastro.2006.07.014.

Pećina-Slaus, Nives. 2003. "Tumor Suppressor Gene E-Cadherin and Its Role in Normal and Malignant Cells." *Cancer Cell International* 3 (1). BioMed Central: 17. doi:10.1186/1475-2867-3-17.

Poh, Ashleigh R., Robert J.J. O'Donoghue, Matthias Ernst, and Tracy L. Putoczki. 2016. "Mouse Models for Gastric Cancer: Matching Models to Biological Questions." *Journal of Gastroenterology and Hepatology*, January, n/a-n/a. doi:10.1111/jgh.13297.

Polkowski, W, J W van Sandick, G J Offerhaus, F J ten Kate, J Mulder, H Obertop, and J J van Lanschot. 2016. "Prognostic Value of Laurén Classification and c-erbB-2 Oncogene Overexpression in Adenocarcinoma of the Esophagus and Gastroesophageal Junction." *Annals of Surgical Oncology* 6 (3): 290–97. Accessed August 8. http://www.ncbi.nlm.nih.gov/pubmed/10340889.

Pylayeva-Gupta, Yuliya, Elda Grabocka, and Dafna Bar-Sagi. 2011. "RAS Oncogenes:

Weaving a Tumorigenic Web." *Nature Reviews Cancer* 11 (11). Nature Publishing Group: 761–74. doi:10.1038/nrc3106.

Rachagani, S, S Senapati, S Chakraborty, M P Ponnusamy, S Kumar, L M Smith, M Jain, and S K Batra. 2011. "Activated KrasG^{12}D Is Associated with Invasion and Metastasis of Pancreatic Cancer Cells through Inhibition of E-Cadherin." *British Journal of Cancer* 104 (6). Nature Publishing Group: 1038–48. doi:10.1038/bjc.2011.31.

Ray, Kevin C., Kayla M. Bell, Jingbo Yan, Guoqiang Gu, Christine H. Chung, M. Kay Washington, and Anna L. Means. 2011. "Epithelial Tissues Have Varying Degrees of Susceptibility to KrasG12D-Initiated Tumorigenesis in a Mouse Model." Edited by Robert Oshima. *PLoS ONE* 6 (2). Public Library of Science: e16786. doi:10.1371/journal.pone.0016786.

Redman, Robert S., Varalakshmi Katuri, Yi Tang, Allan Dillner, Bibhuti Mishra, and Lopa Mishra. 2005. "Orofacial and Gastrointestinal Hyperplasia and Neoplasia in smad4+/- and Elf+/-/smad4+/- Mutant Mice." *Journal of Oral Pathology and Medicine* 34 (1). Munksgaard International Publishers: 23–29. doi:10.1111/j.1600-0714.2004.00246.x.

Reich, Michael, Ted Liefeld, Joshua Gould, Jim Lerner, Pablo Tamayo, and Jill P Mesirov. 2006. "GenePattern 2.0." *Nature Genetics* 38 (5). Nature Publishing Group: 500–501. doi:10.1038/ng0506-500.

Robles-Oteiza, Camila, Sarah Taylor, Travis Yates, Michelle Cicchini, Brian Lauderback, Christopher R. Cashman, Aurora A. Burds, Monte M. Winslow, Tyler

Jacks, and David M. Feldser. 2015. “Recombinase-Based Conditional and Reversible Gene Regulation via XTR Alleles.” *Nature Communications* 6 (November). Nature Research: 8783. doi:10.1038/ncomms9783.

Rogers, Arlin B, Nancy S Taylor, Mark T Whary, Erinn D Stefanich, Timothy C Wang, and James G Fox. 2005. “Helicobacter Pylori but Not High Salt Induces Gastric Intraepithelial Neoplasia in B6129 Mice.” *Cancer Research* 65 (23). American Association for Cancer Research: 10709–15. doi:10.1158/0008-5472.CAN-05-1846.

Sakagami, T, M Dixon, J O’Rourke, R Howlett, F Alderuccio, J Vella, T Shimoyama, and A Lee. 1996. “Atrophic Gastric Changes in Both Helicobacter Felis and Helicobacter Pylori Infected Mice Are Host Dependent and Separate from Antral Gastritis.” *Gut* 39 (5). BMJ Group: 639–48. http://www.ncbi.nlm.nih.gov/pubmed/9026476.

Sakamoto, Kei, Yohko Hikiba, Hayato Nakagawa, Yoku Hayakawa, Ayako Yanai, Masao Akanuma, Keiji Ogura, et al. 2010. “Inhibitor of κB Kinase Beta Regulates Gastric Carcinogenesis via Interleukin-1α Expression.” *Gastroenterology* 139 (1): 226–238.e6. doi:10.1053/j.gastro.2010.03.047.

Schindelin, Johannes, Ignacio Arganda-Carreras, Erwin Frise, Verena Kaynig, Mark Longair, Tobias Pietzsch, Stephan Preibisch, et al. 2012. “Fiji: An Open-Source Platform for Biological-Image Analysis.” *Nature Methods* 9 (7). Nature Research: 676–82. doi:10.1038/nmeth.2019.

Schindelin, Johannes, Curtis T. Rueden, Mark C. Hiner, and Kevin W. Eliceiri. 2015. “The ImageJ Ecosystem: An Open Platform for Biomedical Image Analysis.”

Molecular Reproduction and Development 82 (7–8): 518–29. doi:10.1002/mrd.22489.

Schneider, Caroline A, Wayne S Rasband, and Kevin W Eliceiri. 2012. "NIH Image to ImageJ: 25 Years of Image Analysis." *Nature Methods* 9 (7). Nature Research: 671–75. doi:10.1038/nmeth.2089.

Scudamore, Cheryl L. 2013. "Gastrointestinal System." In *A Practical Guide to the Histology of the Mouse*, 43–61. Chichester, UK: John Wiley & Sons, Ltd. doi:10.1002/9781118789568.ch3.

Searle, P. F., D. P. Thomas, K. B. Faulkner, and J. M. Tinsley. 1994. "Stomach Cancer in Transgenic Mice Expressing Human Papillomavirus Type 16 Early Region Genes From a Keratin Promoter." *Journal of General Virology* 75 (5). Microbiology Society: 1125–37. doi:10.1099/0022-1317-75-5-1125.

Shimada, Shu, Ayako Mimata, Masaki Sekine, Kaoru Mogushi, Yoshimitsu Akiyama, Hiroshi Fukamachi, Jos Jonkers, Hiroshi Tanaka, Yoshinobu Eishi, and Yasuhito Yuasa. 2012. "Synergistic Tumour Suppressor Activity of E-Cadherin and p53 in a Conditional Mouse Model for Metastatic Diffuse-Type Gastric Cancer." *Gut* 61 (3). BMJ Publishing Group Ltd and British Society of Gastroenterology: 344–53. doi:10.1136/gutjnl-2011-300050.

Shtutman, M, J Zhurinsky, I Simcha, C Albanese, M D'Amico, R Pestell, and A Ben-Ze'ev. 1999. "The Cyclin D1 Gene Is a Target of the Beta-catenin/LEF-1 Pathway." *Proceedings of the National Academy of Sciences of the United States of America* 96 (10). National Academy of Sciences: 5522–27.

http://www.ncbi.nlm.nih.gov/pubmed/10318916.

Siegel, Rebecca, Deepa Naishadham, and Ahmedin Jemal. 2012. "Cancer Statistics, 2012." *CA: A Cancer Journal for Clinicians* 62 (1). Wiley Subscription Services, Inc., A Wiley Company: 10–29. doi:10.3322/caac.20138.

Song, Xiaowen, Na Xin, Wei Wang, Chenghai Zhao, Xiaowen Song, Na Xin, Wei Wang, and Chenghai Zhao. 2015. "Wnt/β-Catenin, an Oncogenic Pathway Targeted by H. Pylori in Gastric Carcinogenesis." *Oncotarget* 6 (34). Impact Journals: 35579–88.

Soto, Edwin, Masahiro Yanagisawa, Laura A. Marlow, John A. Copland, Edith A. Perez, and Panos Z. Anastasiadis. 2008. "p120 Catenin Induces Opposing Effects on Tumor Cell Growth Depending on E-Cadherin Expression." *The Journal of Cell Biology* 183 (4). Rockefeller University Press: 737–49. doi:10.1083/jcb.200805113.

Spandidos, Athanasia, Xiaowei Wang, Huajun Wang, Stefan Dragnev, Tara Thurber, Brian Seed, SA Bustin, et al. 2008. "A Comprehensive Collection of Experimentally Validated Primers for Polymerase Chain Reaction Quantitation of Murine Transcript Abundance." *BMC Genomics* 9 (1). BioMed Central: 633. doi:10.1186/1471-2164-9-633.

Spandidos, Athanasia, Xiaowei Wang, Huajun Wang, and Brian Seed. 2010. "PrimerBank: A Resource of Human and Mouse PCR Primer Pairs for Gene Expression Detection and Quantification." *Nucleic Acids Research* 38 (Database issue). Oxford University Press: D792-9. doi:10.1093/nar/gkp1005.

Srinivas, S, T Watanabe, C S Lin, C M William, Y Tanabe, T M Jessell, and F Costantini. 2001. "Cre Reporter Strains Produced by Targeted Insertion of EYFP

and ECFP into the ROSA26 Locus." *BMC Developmental Biology* 1. BioMed Central: 4. http://www.ncbi.nlm.nih.gov/pubmed/11299042.

Stange, Daniel E., Bon-Kyoung Koo, Meritxell Huch, Greg Sibbel, Onur Basak, Anna Lyubimova, Pekka Kujala, et al. 2013. "Differentiated Troy+ Chief Cells Act as Reserve Stem Cells to Generate All Lineages of the Stomach Epithelium." *Cell* 155 (2): 357–68. doi:10.1016/j.cell.2013.09.008.

Subramanian, A., P. Tamayo, V. K. Mootha, S. Mukherjee, B. L. Ebert, M. A. Gillette, A. Paulovich, et al. 2005. "Gene Set Enrichment Analysis: A Knowledge-Based Approach for Interpreting Genome-Wide Expression Profiles." *Proceedings of the National Academy of Sciences* 102 (43). National Academy of Sciences: 15545–50. doi:10.1073/pnas.0506580102.

Surveillance Research Program, National Cancer Institute. n.d. "SEER*Explorer: An Interactive Website for SEER Cancer Statistics [Internet]."

Syder, Andrew J, Sherif M Karam, Jason C Mills, Joseph E Ippolito, Habib R Ansari, Vidya Farook, and Jeffrey I Gordon. 2004. "A Transgenic Mouse Model of Metastatic Carcinoma Involving Transdifferentiation of a Gastric Epithelial Lineage Progenitor to a Neuroendocrine Phenotype." *Proceedings of the National Academy of Sciences of the United States of America* 101 (13). National Academy of Sciences: 4471–76. doi:10.1073/pnas.0307983101.

Takasu, Shinji, Tetsuya Tsukamoto, Xue-Yuan Cao, Takeshi Toyoda, Akihiro Hirata, Hisayo Ban, Masami Yamamoto, et al. 2008. "Roles of Cyclooxygenase-2 and Microsomal Prostaglandin E Synthase-1 Expression and β-Catenin Activation in

Gastric Carcinogenesis in N-Methyl-N-Nitrosourea-Treated K19-C2mE Transgenic Mice." *Cancer Science* 99 (12). Blackwell Publishing Asia: 2356–64. doi:10.1111/j.1349-7006.2008.00983.x.

Tatematsu, M, K Ogawa, T Hoshiya, Y Shichino, T Kato, K Imaida, and N Ito. 1992. "Induction of Adenocarcinomas in the Glandular Stomach of BALB/c Mice Treated with N-Methyl-N-Nitrosourea." *Japanese Journal of Cancer Research : Gann* 83 (9): 915–18. http://www.ncbi.nlm.nih.gov/pubmed/1429199.

Tatematsu, M, M Yamamoto, H Iwata, H Fukami, H Yuasa, N Tezuka, T Masui, and H Nakanishi. 1993. "Induction of Glandular Stomach Cancers in C3H Mice Treated with N-Methyl-N-Nitrosourea in the Drinking Water." *Japanese Journal of Cancer Research : Gann* 84 (12): 1258–64. http://www.ncbi.nlm.nih.gov/pubmed/8294216.

Tebbutt, Niall C., Andrew S. Giraud, Melissa Inglese, Brendan Jenkins, Paul Waring, Fiona J. Clay, Sina Malki, et al. 2002. "Reciprocal Regulation of Gastrointestinal Homeostasis by SHP2 and STAT-Mediated Trefoil Gene Activation in gp130 Mutant Mice." *Nature Medicine* 8 (10). Nature Publishing Group: 1089–97. doi:10.1038/nm763.

"The Human Protein Atlas: ATP4B." n.d. http://www.proteinatlas.org/ENSG00000186009-ATP4B/tissue.

Thiem, Stefan, Moritz F Eissmann, Joachim Elzer, Anna Jonas, Tracy L Putoczki, Ashleigh Poh, Paul Nguyen, et al. 2016. "Stomach-Specific Activation of Oncogenic KRAS and STAT3-Dependent Inflammation Cooperatively Promote Gastric Tumorigenesis in a Preclinical Model." *Cancer Research* 76 (8). American

Association for Cancer Research: 2277–87. doi:10.1158/0008-5472.CAN-15-3089.

Thompson, John, Thomas Epting, Georg Schwarzkopf, Axel Singhofen, Anne-Marie Eades-Perner, Herman van der Putten, and Wolfgang Zimmermann. 2000. "A Transgenic Mouse Line That Develops Early-Onset Invasive Gastric Carcinoma Provides a Model for Carcinoembryonic Antigen-Targeted Tumor Therapy." *International Journal of Cancer* 86 (6). John Wiley & Sons, Inc.: 863–69. doi:10.1002/(SICI)1097-0215(20000615)86:6<863::AID-IJC16>3.0.CO;2-4.

Tomita, Hiroyuki, Shigeo Takaishi, Trevelyan R. Menheniott, Xiangdong Yang, Wataru Shibata, Guangchun Jin, Kelly S. Betz, et al. 2011. "Inhibition of Gastric Carcinogenesis by the Hormone Gastrin Is Mediated by Suppression of TFF1 Epigenetic Silencing." *Gastroenterology* 140 (3): 879–891.e18. doi:10.1053/j.gastro.2010.11.037.

Tsuchida, Nobuo, Avaniyapuram Kannan Murugan, Michele Grieco, Nobuo Tsuchida, Avaniyapuram Kannan Murugan, and Michele Grieco. 2016. "Kirsten Ras* Oncogene: Significance of Its Discovery in Human Cancer Research." *Oncotarget* 7 (29). Impact Journals: 46717–33.

Tsuzuki, T, A Egashira, H Igarashi, T Iwakuma, Y Nakatsuru, Y Tominaga, H Kawate, et al. 2001. "Spontaneous Tumorigenesis in Mice Defective in the MTH1 Gene Encoding 8-Oxo-dGTPase." *Proceedings of the National Academy of Sciences of the United States of America* 98 (20). National Academy of Sciences: 11456–61. doi:10.1073/pnas.191086798.

Uhlén, Mathias, Linn Fagerberg, Björn M. Hallström, Cecilia Lindskog, Per Oksvold,

Adil Mardinoglu, Åsa Sivertsson, et al. 2015. “Proteomics. Tissue-Based Map of the Human Proteome.” *Science (New York, N.Y.)* 347 (6220). American Association for the Advancement of Science: 1260419. doi:10.1126/science.1260419.

van de Wetering, M, N Barker, I C Harkes, M van der Heyden, N J Dijk, A Hollestelle, J G Klijn, H Clevers, and M Schutte. 2001. “Mutant E-Cadherin Breast Cancer Cells Do Not Display Constitutive Wnt Signaling.” *Cancer Research* 61 (1). American Association for Cancer Research: 278–84. doi:10.1016/s0959-437x(99)80068-9.

Waddell, T, M Verheij, W Allum, D Cunningham, A Cervantes, D Arnold, European Society for Medical Oncology (ESMO), European Society of Surgical Oncology (ESSO), and European Society of Radiotherapy and Oncology (ESTRO). 2013. “Gastric Cancer: ESMO-ESSO-ESTRO Clinical Practice Guidelines for Diagnosis, Treatment and Follow-Up.” *Annals of Oncology : Official Journal of the European Society for Medical Oncology / ESMO* 24 Suppl 6 (suppl 6). Oxford University Press: vi57-63. doi:10.1093/annonc/mdt344.

Wang, Timothy C., Charles A. Dangler, Duan Chen, James R. Goldenring, Theodore Koh, Raktima Raychowdhury, Robert J. Coffey, et al. 2000. “Synergistic Interaction between Hypergastrinemia and Helicobacter Infection in a Mouse Model of Gastric Cancer.” *Gastroenterology* 118 (1): 36–47. doi:10.1016/S0016-5085(00)70412-4.

Wang, X., and Brian Seed. 2003. “A PCR Primer Bank for Quantitative Gene Expression Analysis.” *Nucleic Acids Research* 31 (24). Oxford University Press: 154e–154. doi:10.1093/nar/gng154.

Wang, Xin, Roger Willin, Marie Svensson, Asa Ljungh, and Torkel Wadstrom. 2003.

"Two-Year Follow-up of Helicobacter Pylori Infection in C57BL/6 and Balb/cA Mice." *APMIS* 111 (4). Munksgaard International Publishers: 514–22. doi:10.1034/j.1600-0463.2003.1110410.x.

Washington, Kay. 2010. "7th Edition of the AJCC Cancer Staging Manual: Stomach." *Annals of Surgical Oncology* 17 (12). Springer-Verlag: 3077–79. doi:10.1245/s10434-010-1362-z.

Wielenga, V J, R Smits, V Korinek, L Smit, M Kielman, R Fodde, H Clevers, and S T Pals. 1999. "Expression of CD44 in Apc and Tcf Mutant Mice Implies Regulation by the WNT Pathway." *The American Journal of Pathology* 154 (2). American Society for Investigative Pathology: 515–23. doi:10.1016/S0002-9440(10)65297-2.

Xu, Xiaoling, Steven G Brodie, Xiao Yang, Young-Hyuck Im, W Tony Parks, Lin Chen, Yong-Xing Zhou, Michael Weinstein, Seong-Jin Kim, and Chu-Xia Deng. 2000. "Haploid Loss of the Tumor Suppressor Smad4/Dpc4 Initiates Gastric Polyposis and Cancer in Mice." *Oncogene* 19 (15). Nature Publishing Group: 1868–74. doi:10.1038/sj.onc.1203504.

Yamachika, T, H Nakanishi, K Inada, T Tsukamoto, N Shimizu, K Kobayashi, S Fukushima, and M Tatematsu. 1998. "N-Methyl-N-Nitrosourea Concentration-Dependent, rather than Total Intake-Dependent, Induction of Adenocarcinomas in the Glandular Stomach of BALB/c Mice." *Japanese Journal of Cancer Research : Gann* 89 (4): 385–91. http://www.ncbi.nlm.nih.gov/pubmed/9617343.

Yamamoto, M., Tetsuya Tsukamoto, Hiroki Sakai, Norimitsu Shirai, Hiroko Ohgaki, Chie Furihata, Lawrence A. Donehower, Kenji Yoshida, and Masae Tatematsu.

2000. “p53 Knockout Mice (-/-) Are More Susceptible than (+/-) or (+/+) Mice to N-Methyl-N-Nitrosourea Stomach Carcinogenesis.” *Carcinogenesis* 21 (10). Oxford University Press: 1891–97. doi:10.1093/carcin/21.10.1891.

Yan, D, M Wiesmann, M Rohan, V Chan, A B Jefferson, L Guo, D Sakamoto, et al. 2001. “Elevated Expression of axin2 and Hnkd mRNA Provides Evidence That Wnt/beta -Catenin Signaling Is Activated in Human Colon Tumors.” *Proceedings of the National Academy of Sciences of the United States of America* 98 (26). National Academy of Sciences: 14973–78. doi:10.1073/pnas.261574498.

Yu, Sungsook, Mijeong Yang, and Ki Taek Nam. 2014. “Mouse Models of Gastric Carcinogenesis.” *Journal of Gastric Cancer* 14 (2). Korean Gastric Cancer Association: 67–86. doi:10.5230/jgc.2014.14.2.67.

Zavros, Yana, Kathryn A Eaton, Weiqun Kang, Sivaprakash Rathinavelu, Vinay Katukuri, John Y Kao, Linda C Samuelson, and Juanita L Merchant. 2005. “Chronic Gastritis in the Hypochlorhydric Gastrin-Deficient Mouse Progresses to Adenocarcinoma.” *Oncogene* 24 (14). Nature Publishing Group: 2354–66. doi:10.1038/sj.onc.1208407.

Zeilstra, Jurrit, Sander P J Joosten, Maarten Dokter, Eugène Verwiel, Marcel Spaargaren, and Steven T Pals. 2008. “Deletion of the WNT Target and Cancer Stem Cell Marker CD44 in Apc(Min/+) Mice Attenuates Intestinal Tumorigenesis.” *Cancer Research* 68 (10). American Association for Cancer Research: 3655–61. doi:10.1158/0008-5472.CAN-07-2940.

Zeller, Eva, Katharina Hammer, Melissa Kirschnick, and Albert Braeuning. 2013.

"Mechanisms of RAS/β-Catenin Interactions." *Archives of Toxicology* 87 (4). Springer-Verlag: 611–32. doi:10.1007/s00204-013-1035-3.

Zeller, Eva, Katharina Mock, Moritz Horn, Sabine Colnot, Michael Schwarz, and Albert Braeuning. 2012. "Dual-Specificity Phosphatases Are Targets of the Wnt/β-Catenin Pathway and Candidate Mediators of β-catenin/Ras Signaling Interactions." *Biological Chemistry* 393 (10): 1183–91. doi:10.1515/hsz-2012-0130.

Zhang, Fuquan, and Jit Kong Cheong. 2016. "The Renewed Battle against RAS-Mutant Cancers." *Cellular and Molecular Life Sciences* 73 (9). Springer International Publishing: 1845–58. doi:10.1007/s00018-016-2155-8.

Zhang, Rui-Yan, Wen-Qi Du, Ying-Chun Zhang, Jun-Nian Zheng, and Dong-Sheng Pei. 2016. "PLCε Signaling in Cancer." *Journal of Cancer Research and Clinical Oncology* 142 (4). Springer Berlin Heidelberg: 715–22. doi:10.1007/s00432-015-1999-x.

Zhao, Z., J. Zuber, E. Diaz-Flores, L. Lintault, S. C. Kogan, K. Shannon, and S. W. Lowe. 2010. "p53 Loss Promotes Acute Myeloid Leukemia by Enabling Aberrant Self-Renewal." *Genes & Development* 24 (13). Cold Spring Harbor Laboratory Press: 1389–1402. doi:10.1101/gad.1940710.

Zhao, Zengming, Ning Hou, Yanxun Sun, Yan Teng, and Xiao Yang. 2010. "Atp4b Promoter Directs the Expression of Cre Recombinase in Gastric Parietal Cells of Transgenic Mice." *Journal of Genetics and Genomics*. Vol. 37. doi:10.1016/S1673-8527(09)60083-7.